THE UNIVERSITY OF CHICAGO

TISSUE STRESS AND POSTTRANSLATIONAL MODIFICATIONS OF GLUTEN DRIVE THE DEVELOPMENT OF TISSUE DESTRUCTION IN CELIAC DISEASE

A DISSERTATION SUBMITTED TO

THE FACULTY OF THE DIVISION OF THE BIOLOGICAL SCIENCES

AND THE PRITZKER SCHOOL OF MEDICINE

IN CANDIDACY FOR THE DEGREE OF

DOCTOR OF PHILOSOPHY

COMMITTEE ON IMMUNOLOGY

BY

SANGMAN MICHAEL KIM

CHICAGO, ILLINOIS

MARCH 2019

TABLE OF CONTENTS

LIST OF FIGURES

LIST OF TABLES

ACKNOWLEDGEMENTS

I would like to thank my thesis advisor Bana Jabri for her brilliance, for her guidance in the execution of the studies that are discussed here, and most of all for her unwavering dedication to my growth as a scientist and scholar. The work that I describe in my thesis is the culmination of the efforts of many people. In particular, the celiac mouse model project was started by Valerie Abadie, and she, Thomas Lejeune, and Jordan Ernest played an indispensable role in performing the experiments that are described in Chapter 2 and Chapter 3. Our collaboration with Chaitan Khosla and Brad Palanski allowed for the experiments that were performed in Chapter 3. As can be seen in the author lists of Chapter 2 and 3, many other people helped me with this work, and I sincerely thank all of them for their help and support.

Additionally, I would like to acknowledge the people in the Jabri lab that played a huge role in my life over the course of my Ph.D. I would like to thank Toufic Mayassi, Romain Bouziat, Reini Hinterleitner, Marlies Meisel, Matt Zurenski, Cezary Ciszewski, and Valentina Discepolo for their advice, encouragement, and support over the years. I would like to acknowledge the critical role of my classmates, and the University of Chicago Committee on Immunology in my scientific development. I would like to thank my family and friends for being my rock throughout this time. Finally, I would like to dedicate my thesis to the memory of my aunt, Hye-Ryeong Kim.

ABSTRACT

Celiac disease (CeD) is a dietary gluten-triggered autoimmune disorder that is characterized by $CD8^+$ T cell mediated killing of intestinal epithelial cells (IECs) ultimately resulting in small intestinal villous atrophy. The genetic and immunological determinants of disease have been relatively well characterized, with all patients having at least one copy of HLA-DQ2 or HLA-DQ8, and more than two-thirds of patients having high levels of proinflammatory cytokine interleukin 15 (IL-15) in their small intestinal mucosa. We used this knowledge to reverse-engineer a mouse model of disease that involves the overexpression of IL-15 in both the epithelium (villin-IL15 transgenic; denoted $IL\text{-}15^{IEC}$) and lamina propria (Dd-IL15 tg, denoted $IL\text{-}15^{LP}$) of the small intestine in mice that have the expression of human MHC class II molecule HLA-DQ8 on the surface of their antigen presenting cells (HLA-DQ8 tg). These DQ8-$IL\text{-}15^{LPxIEC}$ mice have the development of villous atrophy upon gluten feeding as well as CeD-associated cellular, serological, and transcriptional signatures.

The development and characterization of this model allowed us to investigate the cellular requirements for disease and importantly will be an indispensable tool for the validation of preclinical therapies. One important therapeutic target is transglutaminase 2 (TG2), an enzyme that is thought to be required for the pathogenesis of CeD, although this has never been demonstrated *in vivo*. We used the DQ8-$IL\text{-}15^{LPxIEC}$ mice to investigate how TG2 becomes enzymatically activated in the context of inflammation and gluten feeding, and used two different TG2 inhibitors to demonstrate the requirement for TG2 in tissue destruction and other CeD associated phenotypes.

CHAPTER 1. INTRODUCTION

1.1 The pathogenesis of celiac disease

1.1.1 Overview of celiac disease

Celiac disease (CeD) is a complex, polygenic inflammatory disorder with autoimmune-like features that currently occurs in 1% of the global population (Tack et al, 2010). In CeD, genetically susceptible individuals develop an inflammatory response to gluten, a class of proteins found in wheat, barley, rye, and related species. CeD patients develop small intestinal villous atrophy (destruction of the villi that line the small intestinal epithelium) along with crypt hyperplasia, and this intestinal pathology leads to gastrointestinal symptoms such as chronic diarrhea, malabsorption, abdominal pain, bloating, and failure to thrive, as well as extraintestinal symptoms such as anemia, osteoporosis, and neurological disorders (Tack et al, 2010).

Strict adherence to a gluten-free diet (GFD) can result in the resolution of symptoms and restoration of normal intestinal morphology, particularly in patients that are diagnosed during childhood (Rubio-Tapia et al., 2010). However, approximately 34% of adult CeD patients fail to completely heal on a GFD, and patients that are not responsive to a GFD have a poor prognosis, with significantly elevated risk of developing enteropathy-associated T cell lymphoma (Rubio-Tapia et al., 2010). The prevalence of individuals that do not recover on a GFD, and the burden of lifelong gluten avoidance highlight the need for non-dietary therapies. However, efforts to develop pharmacological treatments for CeD have been hindered by the gaps in our understanding of disease

pathogenesis, and particularly by the lack of a preclinical animal model of disease (Plugis & Khosla, 2015).

There appear to be two critical events that are required for the small intestinal tissue destruction that defines CeD: the induction of a gluten-specific pro-inflammatory T helper-1 (Th1) response and the targeted killing of intestinal epithelial cells (IEC) by hyper-activated intraepithelial lymphocytes (IELs) (Jabri and Sollid, 2009; Tjon et al., 2010). What we know about these two components of disease, and how they are triggered in the context of the celiac small intestine, as well as the gaps in knowledge that we attempt to address with our work, will be discussed in depth in the following sections.

1.1.2 The loss of oral tolerance to gluten

The development of CeD is strictly associated with major histocompatibility complex (MHC) class II haplotype HLA-DQ2 or HLA-DQ8, with approximately 90% of individuals with CeD having at least one copy of HLA-DQ2 and the remining patients expressing HLA-DQ8 (Karell et al., 2003). There is a gene dosage effect, with individuals that have two copies of HLA-DQ2 having a five-fold higher risk of disease than individuals that are heterozygous (Mearin et al., 1983). This suggests a central role for $CD4^+$ T cells in the pathogenesis of disease, and HLA-DQ2 and HLA-DQ8 restricted gluten-specific $CD4^+$ T cells have been isolated from the small intestinal biopsies of CeD patients (Lundin et al., 1993; Lundin et al., 1994).

Our intestinal immune system has evolved to not respond to innocuous food antigens or commensal bacteria in an active $CD4^+$ T cell-mediated process that is termed

"oral tolerance" (Rezende and Weiner et al, 2017). In response to high doses of orally administered antigens, $CD4^+$ T cells that are specific against that antigen are clonally deleted or become anergic (Friedman 1994, Chen et al., 1995). Intriguingly, low doses of oral antigen lead to the induction of forkhead box P3 $(Foxp3)^+$ regulatory $CD4^+$ T cells (Tregs), and in response to subsequent challenges with these antigens, even in extraintestinal sites, these Tregs suppress immunity by secreting anti-inflammatory cytokines IL-10 and transforming growth factor β (TGFβ) (Mucida et al., 2007; Curotto de Lafaille et al., 2008). Treg induction is mediated by $CD103^+$ dendritic cells (DCs), which take up oral antigens in the gut, and migrate to the mesenteric lymph nodes (mLNs) to activate naïve $CD4^+$ T cells. Upon activation, these Tregs upregulate gut homing molecules, and migrate to the gut lamina propria (LP) where they mediate tolerance. Both the polarization of naïve CD4 T cells to Tregs, and the upregulation of gut homing molecules are dependent on retinoic acid, which is a vitamin A metabolite, and the abundance of this molecule in the gut environment explains why this tolerance mechanism is gut specific (Iwata et al., 2004; Coombes et al., 2007; Sun et al., 2007).

Contrary to this paradigm, the $CD4^+$ T cells from CeD biopsies primarily secrete pro-inflammatory T helper 1 (Th1) cytokine interferon γ (IFNγ) upon restimulation with gluten (Nilsen et al., 1995), suggesting that during the course of CeD development, there is a loss of oral tolerance (LOT) to gluten protein. This is accompanied by a significant increase in the number of plasma cells that are found in the celiac lesion, and an unusually large percentage of these plasma cells are specific against gluten (and in particular, gluten sub-component gliadin), or the auto-antigen transglutaminase 2 (TG2; an enzyme

whose role in CeD is discussed in depth in **Section 1.2**) (Mesin et al., 2012). The development of the gluten- and TG2-specific B cell response is thought to depend on gluten-specific $CD4^+$ T cells (Mesin et al., 2012), although this hypothesis needs to be verified in animal models. The LOT to gluten, as proxied by high levels of serum antibodies specific to gliadin and TG2, is now the primary readout for CeD diagnosis (Mesin et al., 2012). How LOT to gluten protein develops in CeD has been a major topic of investigation for our lab and others.

While 20-30% of the Western European population is HLA-$DQ2^+$, only 1% of that population develops CeD (Tack et al., 2010), suggesting that there are additional genetic and environmental factors that contribute to disease pathogenesis and the LOT to gluten. This is further corroborated by studies using humanized HLA-$DQ2^+$ transgenic mice demonstrating that in the absence of additional factors, the default CD4 T cell response to oral gluten is tolerogenic (Du Pré et al., 2011). The high concordance rate between monozygotic twins (Greco et al., 2002) suggests the contribution of genetic factors, and the non-HLA genetic components of disease have been investigated using genome-wide association studies. The pathways associated with CeD include genes that code for chemokine receptor activity, cytokine binding, T cell activation, and lymphocyte differentiation, underscoring the importance of dysregulated immunity and particularly T cells in CeD (Abadie et al., 2011). The environmental component of disease is highlighted by epidemiological examples such as the normal frequency of CeD in Finnish Karelia (0.9%), compared to the low incidence in the adjacent Russian Karelia (0.2%); these two geographically adjacent regions harbor genetically similar populations with similar levels

of gluten consumption, but have very different economic and hygienic environments (Kondrashova et al., 2008).

Environmental factors that have been proposed to have an impact on LOT include dysbiosis of the microbiota and viral infections (Kim et al., 2015). The evidence supporting a role for the microbiota in the development of CeD include the fact that delivery by cesarean sections (Decker et al., 2010) and early antibiotic use (Canova et al., 2014) are positively correlated with disease risk. A mechanistic investigation into the effect of dysbiosis on the LOT in CeD remains to be performed.

The evidence for viral infections and the resultant production of type-1 IFNs playing a role in CeD stems from studies documenting dysregulated expression of IFN-α in CeD patients (Monteleone, 2001; Di Sabatino et al., 2007; Raki et al., 2013), and the fact that that treatment of hepatitis C patients with IFN-α leads to some patients developing CD (Cammarota et al., 2000). Type-1 IFNs can induce activation of DCs (Gallucci et al., 1999) and blocking IFN-α inhibits IFN-γ transcripts in ex vivo organ culture of CeD biopsies challenged with gluten (Sabatino et al., 2007). Research from our laboratory directly demonstrated that viral infection can lead to LOT. Infection with either reovirus strain T1L (Bouziat et al., 2017) or murine norovirus strain CW3 (Bouziat et al., 2018) at the time of oral antigen exposure can lead to the induction of antigen-specific Th1 immunity. Interestingly, infection with alternative strains from the same families of virus, reovirus T3D-RV, or murine norovirus strain CR6 did not have the same effect on tolerance, and infection with the LOT-inducing strains was associated with a pro-inflammatory

transcriptional signature that is dependent on interferon regulatory factor 1 (IRF1) (Bouziat et al., 2017; Bouziat et al., 2018).

Finally, we also demonstrated that pro-inflammatory cytokine IL-15 can alter DCs to induce Th1 responses, even in the presence of retinoic acid, and overexpression of IL-15 in the intestinal LP and mLN of mice is sufficient to cause the LOT to gluten (DePaolo et al., 2011), which is important because IL-15 levels are elevated in the small intestines of a large percentage of CeD patients (Mention et al., 2003; Setty et al., 2015; Abadie and Jabri 2014; Jabri and Abadie 2015). The role of IL-15 in the pathogenesis of celiac disease is discussed at length in **Section 1.1.5**.

1.1.3 The licensing of cytotoxic intraepithelial lymphocytes in celiac disease

In CeD, although the LOT to gluten is a defining feature of disease that occurs in every patient (as evidenced by the presence of serum anti-gliadin and anti-TG2 antibodies), this is not sufficient for the development of villous atrophy. This lack of sufficiency is evidenced by the aforementioned mouse models that demonstrate the LOT to gluten but maintain normal small intestinal architecture (DePaolo et al., 2011; Bouziat et al., 2017; Bouziat et al., 2018), and by a patient subpopulation that is referred to as potential CeD; these individuals have gliadin and TG2 specific serum antibodies, but do not yet have small intestinal villous atrophy (Setty et al., 2015).

The cell type that is thought to mediate IEC killing, and the resultant villous atrophy, are IELs that have become aberrantly activated during the course of disease pathogenesis (Jabri and Sollid, 2009; Tjon et al., 2010). IELs are a heterogenous group

of non-circulating tissue resident lymphocytes that can be defined by their surface receptor phenotype and developmental origin. Type A IELs are adaptively induced by microbial signals (Umesaki et al., 1993), and consist of T cell receptor (TCR)αβ$^+$ CD8αβ$^+$ and TCRαβ$^+$ CD4$^+$ populations in both human and mouse (Hayday et al., 2001; Mayassi and Jabri, 2018). Type B IELs seed the tissue early in life in a microbiota-independent manner, and consist of TCRγδ$^+$ cells as well as TCRαβ$^+$ CD8αα$^+$ cells, an autoreactive subset of thymically-derived IELs that is found in high abundance in the mouse gut, but is absent in humans (Hayday et al., 2001; McDonald et al., 2014; McDonald et al., 2015; Mayassi and Jabri, 2018). In the human small intestine, 80-90% of the IELs that are present during steady state conditions are TCRαβ$^+$ CD8αβ$^+$ (while these cells make up 30-50% of the mouse duodenal IELs) (Mayassi and Jabri, 2018), and it is these cells that are thought to cause tissue destruction in CeD (Jabri and Sollid, 2009; Tjon et al., 2010), although the participation of other subsets of IELs cannot be ruled out.

During steady state conditions, the TCRαβ$^+$ CD8αβ$^+$ IELs patrol the epithelial layer of the small intestine between IECs, and participate in tissue surveillance and the maintenance of barrier function (Mayassi and Jabri, 2018). Transcriptional profiling of *ex-vivo* TCRαβ$^+$ and TCRγδ$^+$ IELs from mice indicated that they are in an "activated yet resting state" (Shires et al., 2001), and although these cells are widely considered effector cells, they require additional signals to kill target cells. These additional signals come in the form of the cognate TCR recognition of foreign antigen presented by MHC class I, and the sensing of "altered self" through an array of natural killer receptors (NKRs) that can recognize ligands that are upregulated on the surface of IECs during times of infection

or tissue stress (Mayassi and Jabri, 2018). The antigen-specific activation of these cells can lead to the killing of infected or aberrant IECs via the secretion of granzymes, and the activation of immunity via the secretion of IFNγ (Mayassi and Jabri, 2018), and signaling through activating NKRs lowers the activation threshold for TCR-mediated killing (Roberts et al., 2001).

The number of both TCRαβ$^+$ and TCRγδ$^+$ IELs are greatly increased in the celiac lesion, and TCRαβ$^+$ numbers normalize with mucosal healing on a GFD, while TCRγδ$^+$ numbers remain increased, which is why it is believed that the TCRαβ$^+$ IELs are the cells that are responsible for tissue destruction (Kutlu et al., 1993). TCRαβ$^+$ CD8αβ$^+$ IELs from CeD biopsies have increased expression of activating NKRs, namely natural killer group 2D (NKG2D) and NKG2C/CD94, and the downregulation of inhibitory NKR, NKG2A/CD94 (Jabri et al., 2000; Meresse et al., 2004; Meresse et al., 2006). NKG2D recognizes infection or stress inducible molecules MICA/B (Groh et al., 1996; Groh et al., 1999; Bauer et al., 1999), while NKG2C/CD94 recognizes non-classical MHC class I molecule HLA-E, which can be upregulated by IFNγ (Braun et al., 1998; Meresse et al., 2006). The activating NKR bearing hyper-activated cytotoxic IELs isolated from the intestines of CeD patients (which will be referred to as intraepithelial cytoxic T lymphocytes, or IE-CTL henceforth) are transcriptionally reprogrammed to be more “NK-like” in nature, and in the absence of inhibitory receptors, these cells become “licensed to kill,” i.e. they have the ability to kill target cells independently of TCR ligand interaction (Meresse et al., 2004; Meresse et al., 2006), which is a critical finding because the IE-CTLs from CeD biopsies do not appear to be gluten-specific (Lundin et al., 1993, Sollid, 2002). The IECs in the

celiac lesion have upregulation of both MICA/B and HLA-E, which explains how they are specifically targeted for killing by licensed IE-CTL (Jabri and Sollid, 2009; Tjon et al., 2010). The mechanisms behind the upregulation of stress ligands on the surface of IECs is not fully known, although the fact HLA-E expression is regulated by IFNγ suggests that this could be one interface of crosstalk with the gluten specific Th1 response that defines CeD. How IE-CTLs undergo hyperactivation and NK-reprograming is an area of active investigation, and work from our lab and others has uncovered a key role for IL-15 that will be discussed in depth in **Section 1.1.5**.

1.1.4 IL-15 function during steady state conditions

IL-15 is a 15 kDa cytokine that can be expressed in a wide variety of tissues and cell types, including cells that are hematopoietic (including dendritic cells, monocytes and macrophages, mast cells, B and T cells) and non-hematopoietic (intestinal and respiratory epithelial cells, keratinocytes, fibroblasts, stromal cells) in origin (Grabstein et al., 1994; Fehniger and Caliguri, 2001, Jabri and Abadie, 2015). IL-15 is transcribed during times of innate immune activation, with NF-κB and IRF binding sites found in the promoter of both mouse and human IL-15, but the primary method of regulation is posttranscriptional (Waldman and Tagaya, 1999). IL-15 protein is post-transcriptionally regulated by multiple controlling elements that appear to have evolved to impede translation, including 12 start codons (AUGs) that are upstream of the 5′ UTR, 2 signal peptides that impede translation and intracellular trafficking, and an inhibitory cis-element in the coding sequence of the IL-15 mature protein C-terminus (Bamford et al., 1998). When all three of these controlling

elements were systemically removed, there was a 250-fold increase in IL-15 synthesis compared to endogenous IL-15 (Bamford et al., 1998), suggesting a complex and tight control of IL-15 production that might be indicative of the fact that high levels of IL-15 production could be dangerous to our tissues. Indeed, although IL-15 transcripts are detected in all of the previously mentioned tissues and cell types, during homeostasis, bioactive IL-15 is primarily found on the surface of DCs and monocytes (Waldmann, 2006).

IL-15 signaling primarily occurs in a cell-contact dependent manner, where IL-15 receptor α (IL-15Rα) on the surface of one cell presents IL-15 in trans to a second cell that expresses the heterodimeric receptor complex IL-2/15Rβ, and the common cytokine-receptor γ-chain (γc), thereby allowing signaling downstream of these receptors (Giri et al., 1995; Fehniger and Caliguri, 2001). Engagement of the IL-2/15Rβ and γc complex results in the activation of the janus kinase 1-signal transducer and activator of transcription 3 (JAK1-STAT3) and JAK3-STAT5 signaling pathways (Fehniger and Caliguri, 2001), and the resultant transcriptional consequences are target cell and context dependent (Jabri and Abadie, 2015). Of note, IL-2 signals through the same IL-2/15Rβ and γc complex and utilizes similar downstream signaling pathways, however IL-2 and its private receptor IL-2Rα are not nearly as broadly expressed as IL-15 and IL-15Rα, with the primary producer of IL-2 being activated T cells, and unlike IL-15, IL-2 is secreted (Waldmann, 2006). Although the *in vitro* consequences of IL-2 and IL-15 stimulation are similar (Grabstein et al., 1994), due to their distinct signaling properties and large differences in cellular and tissue distribution, IL-2 and IL-15 signaling have distinct and at times contrasting roles *in vivo* (Waldmann, 2006), and the lack of redundancy between

these two molecules is evidenced by the large abnormalities that are seen in mice that are deficient in either IL-2 or IL-15 signaling components (Fehniger and Caliguri, 2001).

IL-15 plays a key role in the differentiation, maintenance, and proliferation of NK cells, NK T cells, $CD8^+$ T cells, $TCR\alpha\beta^+$ $CD8\alpha\alpha^+$ IELs, and $TCR\gamma\delta^+$ IELs as evidenced by the fact that mice that are deficient in IL-15 or IL-15Rα have a marked reduction in these populations (Kennedy et al., 2000; Lodolce et al., 1998; Lodolce et al., 2001; Schluns et al. 2004). In particular, trans-presentation of IL-15 from innate immune or nonhematopoietic cells leads to the potent activation and proliferation of $CD8^+$ T cells (Zhang et al., 1998; Lodolce et al., 2001). The fact that IL-15 mRNA is present in a wide range of cells and tissues in a translationally inactive form, that can be translated upon microbial triggers (Zhou et al., 2007; Colpitts et al., 2012), or during cellular distress (Abadie and Jabri, 2014), suggests that IL-15 may function as a danger signal that converts neighboring T and NK cells into activated killer cells that might provide an effective host response to ongoing infection or during times of sterile inflammation (Waldman and Tagaya, 1999; Jabri and Abadie, 2015).

1.1.5 IL-15 in celiac disease

Increased or dysregulated IL-15 expression is associated with a number of autoimmune and inflammatory disorders, including rheumatoid arthritis, inflammatory bowel disease (IBD), alopecia areata, sarcoidosis, and multiple sclerosis (MS), and the role that IL-15 plays in the activation and maintenance of innate and adaptive immune cell subsets, and in particular its effects on T cells may explain why its dysregulation is

associated with these disorders (Fehniger and Caliguri, 2001; Waldmann, 2006; Abadie and Jabri 2014; Jabri and Abadie 2015).

IL-15 is greatly upregulated in both the small intestinal LP and epithelium of CeD patients (Mention et al., 2003; Setty et al., 2015), and appears to play a role in both the LOT to gluten and the licensing of IE-CTL that are required for the development of disease. As previously mentioned, our laboratory has demonstrated that the expression of transgenic IL-15 in the LP and mLN of mice can signal directly on DCs, and together with retinoic acid cause the induction of inflammatory cytokine IL-12p70 (DePaolo et al., 2011). In humanized HLA-DQ8 transgenic mice, naïve $CD4^+$ T cells that are primed by these inflammatory DCs became Th1 polarized and secrete IFNγ upon restimulation with gliadin (DePaolo et al., 2011). In this model we also saw the production of CeD associated anti-gliadin and anti-TG2 antibodies (DePaolo et al., 2011), and altogether, this suggests that elevated LP IL-15 can be a driver of LOT in CeD.

IL-15 can also signal directly on IELs via trans-presentation by IECs, and this signaling is required for the development of specific IEL subsets in mice (Schluns et al. 2004, Ma et al., 2009). The effects of IL-15 signaling on $TCR\alpha\beta^+$ $CD8\alpha\beta^+$ IELs was demonstrated *in vitro*, where IL15 treatment caused the upregulation of activating NKRs, CD94 (Jabri et al., 2000) and NKG2D (Roberts et al., 2001; Meresse et al., 2004), and IL-15 treatment can drive NKG2D-mediated *in vitro* killing of target cells in a TCR-independent manner (Meresse et al., 2004). In concordance with results seen in human, the treatment of $TCR\alpha\beta^+$ $CD8\alpha\alpha^+$ IELs from mouse led to an upregulation of NKG2D *in vitro*, and NKG2D blockade prevented killing of Rae-1 (the mouse homologue for MICA/B)

bearing IECs *in vitro* and *in vivo* (Zhou et al., 2007). This suggests that elevated epithelial IL-15 may be one of the signals that drive the licensing of TCRαβ^{+} CD8αβ^{+} IELs to kill IECs and cause villous atrophy during the progression of CeD.

1.2 The enzymatic activity of transglutaminase 2 in CeD

1.2.1 Transglutaminase 2 is a multifunctional protein

TG2 is a 79 kDa protein that belongs to a family of calcium-dependent enzymes that are known to catalyze various post-translational reactions (Lorand and Graham, 2003). Unlike the other eight members of the transglutaminase family, TG2 is ubiquitously expressed in virtually all tissues, and has widespread subcellular localization (Thomázy and Fésüs, 1989; Lorand and Graham, 2003). TG2 can perform several biochemical functions, the most well-characterized being its transamidation and deamidation activity. TG2 can crosslink proteins by facilitating isopeptide bond formation between a glutamine residue on one protein and a lysine residue on another, in a process called transamidation (**Fig. 1.1**; Klock et al., 2012). Alternatively, in the absence of lysine acceptor residues, and in low pH environments, it can cause the conversion of glutamine residues to glutamic acid in a process called deamidation, and when I refer to the enzymatic activity of TG2 going forward, I will be referring specially to its ability to deamidate its target proteins (**Fig. 1.1**; Klock et al., 2012). TG2 has also been reported to function as a G protein, a protein disulfide isomerase, and a serine/threonine kinase, and

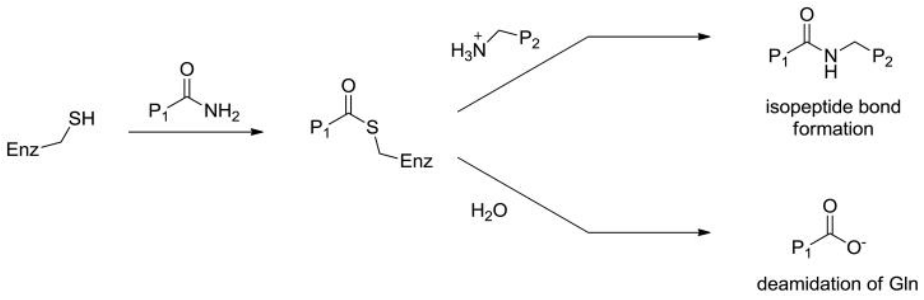

Figure 1.1. Enzymatic activity of TG2.
Cys in the active site of TG2 catalyzes the formation of an isopeptide bond between Gln residue in protein 1 (P1) and a Lys residue in protein 2 (P2). Alternatively, hydrolysis of the acyl-enzyme intermediate can result in the conversion of Gln to negatively charged Glu. (From Klock et al., 2012)

these activities are regulated by several cellular factors including calcium, nucleotides, and redox potential (Park et al., 2010). The concentration of these various factors is variable across different subcellular compartments, and therefore the subcellular localization of TG2 dictates the roles that it can play (Park et al., 2010). The known functions of TG2 and the regulation of those functions are summarized in **Table 1.1**.

Table 1.1. Functions and regulation of TG2.

	Transamidation/Deamidation	G protein	Protein Disulfide Isomerase	Kinase
Substrates/Partners	Gluten, many others	Receives signal from α1-adrenergic receptor and activates PLC	RNase A	IGFBP-3, Rb
Subcellular Localization	Extracellular	Plasma Membrane	ER	Cytosol
Function	Crosslinking of proteins; conversion of Gln to Glu	Signal transduction: cell survival	Catalysis of proper protein folding	Signal transduction: cell cycle progression and proliferation
Calcium	+	–	–	–
GTP	–	+	ns	nd
ATP	ns	+	ns	+
Phosphorylation	–	nd	nd	+
Reducing Agents	+	nd	–	nd
Transamidation Inhibitors	–	ns	ns	–

Columns denote known biochemical functions of TG2, rows 1-3 describe these functions; rows 4-9 are molecules /processes that positively or negatively regulate these functions. Positive regulation is denoted by a +, negative regulation is denoted by a -. *ns* no significant effect, *nd* not determined. (Park et al., 2010; Klock et al., 2012; Lorand and Graham, 2003)

1.2.2 The subcellular localization and activation of transglutaminase 2

Under normal physiological conditions, the majority of TG2 is intracellular and enzymatically inactive (Belkin, 2011). However, 1-20% can be present on the plasma membrane or in the extracellular matrix (ECM) depending on cell type (Belkin, 2011). Although TG2 has been shown to dynamically translocate intracellularly through the action of nuclear transport proteins or in response to intracellular calcium concentrations,

it is unclear what causes the extracellular export of TG2, as it lacks a leader sequence or the post-translational modifications that would facilitate its export (Lorand and Graham 2003; Park et al., 2010). When TG2 is released into the extracellular environment, the high concentration of calcium and low concentration of GTP lead to a large conformational change that exposes its catalytic triad, and allows it to be enzymatically active (Liu et al., 2002; Pinkas et al., 2007). This active form can then be reversibly inhibited by the formation of a disulfide bond between vicinal cysteine residues in the open conformation of the protein, and the majority of extracellular TG2 appears to be in this "open but inactive" form under steady-state conditions (**Fig. 1.2**; Stamnaes et al., 2010; Siegel et al., 2008). Understanding the factors that can lead to the extracellular release of TG2, as well as those that can cause disulfide bond reduction to drive its TG2 to be in an open and active state will have important implications for TG2 biology, and particularly for the prevention and treatment of CeD.

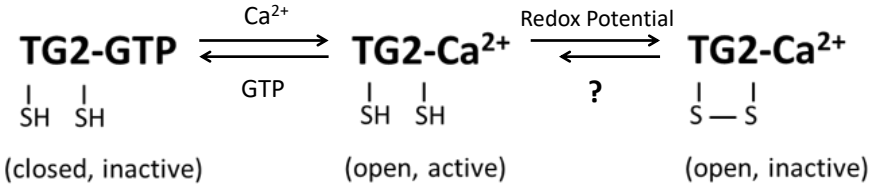

Figure 1.2. Three possible states of TG2 activity.
TG2 activity appears to be regulated by local concentration of Ca^{2+} and GTP (which is determined by subcellular localization) and by redox potential. (adapted from Jin et al., 2011)

1.2.3 Transglutaminase 2 increases the immunogenicity of gluten

The observation that CeD is triggered by gluten, and that removal of gluten from the diet can lead to the reversal of disease phenotypes was first discovered and described by Dutch pediatrician Willem Karel Dicke in the 1940s and 1950s (van Berge-

Henegouwen and Mulder, 1993). Since this discovery, there has been an intense research focus on the properties that make gluten immunogenic. Some groups have suggested that gluten itself has innate immune stimulatory properties that might aid in the activation of antigen presenting cells (APCs) as well as cause increases in intestinal permeability, although these properties were later assigned not to gluten, but to amylase-trypsin inhibitors that are also present in wheat (Jabri and Sollid et al., 2009; Schuppan et al., 2015).

The amino acid composition of gluten is unique in that it contains a high percentage of prolines and glutamines. The cyclic structure of proline gives it exceptional conformational rigidity and renders it resistant to digestion by gastric, pancreatic, and intestinal brush-border membrane proteases (Shan et al., 2002). Therefore, gluten makes it to the small intestinal duodenum in peptide fragments that are 10-50 residues long, making them suitable for presentation by MHC class II (Shan et al., 2002). Meanwhile, the glutamine residues present in gluten make it an exceptionally good substrate for TG2 and its enzymatic activity. TG2 has been shown to bind to gluten and deamidate its glutamine residues to negatively charged glutamic acids *in vitro* (**Fig. 1**; Molberg et al., 1998). This process is specific, as it has been shown that glutamine residues in the sequence glutamine-X-proline (where X can be any amino acid) are preferentially deamidated (Vader et al., 2002).

The reason that deamidation of gluten affects its immunogenicity is because HLA-DQ2 and HLA-DQ8 molecules have a preference to binding peptides that are negatively charged due to positive charges in their MHC binding grooves (Lee et al., 2001; Kim et

al., 2004; Henderson et al., 2007). Specifically, HLA-DQ2 prefers glutamates at its P4, P6, and P7 pockets, while HLA-DQ8 prefers glutamates at positions P1 and P9 (Lee et al., 2001; Kim et al., 2004; Henderson et al., 2007). HLA-DQ2 has the additional ability to facilitate a proline at position P1, and the biochemical properties of these two MHC binding grooves may explain why CeD exclusively occurs in HLA-DQ2$^+$ and HLA-DQ8$^+$ individuals, and why HLA-DQ2$^+$ individuals have higher disease risk (Qiao et al., 2005).

There is debate as to whether TG2 activity is required for gluten peptide recognition by CD4$^+$ T cells, or whether it solely plays a role in the amplification of the response. Regardless, there is ample evidence that TG2 activity causes the activation of more CD4$^+$ T cells, and causes a stronger response against gluten (Jabri and Sollid, 2009). This is in line with the threshold model of CeD, where it is posited that the development of full-blown CeD is the culmination of a series of events that may include the presence of non-HLA CeD genes, enteroviral infections, dysbiosis of the commensal bacteria, the innate immune stimulatory effects of gluten, and the TG2-mediated amplification of the CD4$^+$ T cell response (Jabri and Sollid, 2009; Tjon et al., 2010).

1.2.4 The activation of transglutaminase 2 during celiac disease pathogenesis

TG2 was first discovered by its ability to incorporate small molecule amines into proteins (Sarkar et al., 1957), and amine incorporation is the primary method for the assessment of *in vivo* TG2 enzymatic activity. 5-biotinamidopentylamine (5-BP) is a biotin containing small molecule amine that can be dosed into animals, and “open and active” TG2 causes its crosslinking to lysine-containing substrate proteins (Slaughter et al., 1992).

This allows for the utilization of the biotin-streptavidin interaction to approximate the magnitude and localization of TG2 enzymatic activity via immunohistochemical analysis. This has facilitated the assessment of factors that can cause the *in vivo* activation of TG2.

Toll-like receptor 3 (TLR3) ligand polyI:C, which is a double stranded RNA analog, was shown to cause the activation of TG2 when injected intraperitoneally (i.p.) in mice (Siegel et al., 2008). PolyI:C injection, as well as injection of other pure TLR ligands, is known to cause necrosis in small intestinal IECs (Gunther et al., 2015), and the TG2 activation seen in these models is likely due to the liberation of intracellular TG2 upon excessive amounts of tissue destruction, as opposed to the consequence of physiological levels of innate immune stimulation (Siegel et al., 2008). That said, this is a demonstration that in an environment of small intestinal injury, TG2 can become extracellular and activated, at least for a transient period of time.

It was next demonstrated that Th1-cytokine IFNγ can activate TG2, and that this activation may be mediated through IFNγ-induced release of thioredoxin (Trx), a redox protein that is able to reduce the inhibitory disulfide bond of TG2 in vitro, and can cause the activation of small intestinal TG2 when injected intravenously (i.v.) into mice (Jin et al., 2011; DiRaimondo et al., 2012; Plugis et al., 2015). IFNγ-induced activation of TG2 could be a plausible mechanism for the activation of TG2 in the context of CeD pathogenesis, although if TG2 deamdiation activity is required for the initiation of gluten-specific Th1 induction, then this order of events would not make sense. It is also possible that TG2 is initially activated by a yet unknown mechanism, causes the deamidation of gluten, and the subsequent induction of Th1 immunity, as well as tissue destruction and

the liberation of intracellular TG2, causes amplified TG2 activation, and this leads to larger amounts of deamdiated gluten, and a progressively amplified Th1 response.

Finally, as previously discussed, we demonstrated that infection with reovirus serotype T1L can cause the LOT to oral antigens if infection and antigen feeding occur at the same time (Bouziat et al., 2017). Infection with T1L also caused the activation of TG2 in the small intestine of mice 18 hours post infection (**Fig. 1.3**), and this virus mediated activation occurs in the absence of tissue injury or destruction (Bouziat et al., 2017). How infection with reovirus causes the activation of TG2 remains to be elucidated, and I will discuss the plausible mechanisms and future studies aimed at investigating this question in **Chapter 5**.

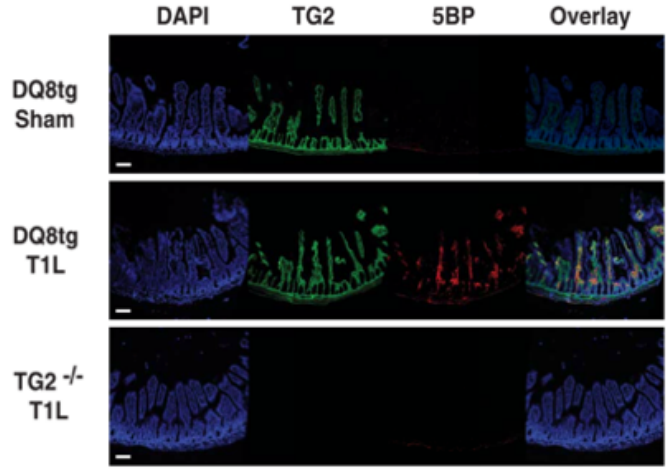

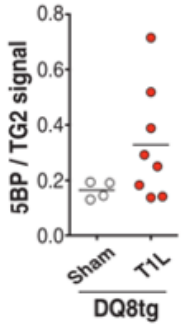

Figure 1.3. Reovirus T1L infection causes activation of TG2. DQ8tg mice were inoculated perorally with 10^{10} PFU of T1L (n = 8 mice) or PBS (sham, *n = 4 mice*). $TG2^{-/-}$ mice were inoculated perorally with 10^{10} PFU of T1L (*n = 2 mice*) and used as a negative control. Mice were euthanized at 18 hours after infection, and small intestines were collected and frozen in optimal cutting temperature compound. Representative images from stained frozen sections of the proximal small intestines are shown. Scale bars, 100 μm. Staining with 4′,6-diamidino-2-phenylindole (DAPI) is shown in blue, TG2 protein is shown in green and TG2 enzymatic activity as assessed by means of 5BP crosslinking is shown in red. TG2 enzymatic activity normalized to TG2 protein levels was quantified for each villus. The mean enzymatic activity in the proximal small intestine per mouse is shown. (From Bouziat et al., 2017)

1.3 Animal models of celiac disease

1.3.1 Existing animal models of celiac disease

Investigating the contribution and requirement for specific cell types and components of disease requires CeD animal models, however to date, considerable efforts have been hindered by the complexity of the disease, and a model that fully recapitulates all aspects of CeD pathology has not been developed (Korneychuk et al., 2015; Costes et al., 2015). We know that celiac lesion contains gluten-specific $CD4^+$ T cells that secrete the pro-inflammatory T helper 1 (Th1) cytokine IFNγ (Nilsen et al., 1995). However, modeling this gluten-specific $CD4^+$ Th1 response using humanized HLA-$DQ2^+$ or HLA-$DQ8^+$ mice does not lead to the development of villous atrophy (**Table 1.1**; Black et al., 2002; Verdu et al. 2008; de Kauwe et al., 2009; Galipeau et al., 2011; Du Pré et al., 2011; DePaolo et al., 2011; Laparra et al., 2012; Bouziat et al., 2017). In several of these models of LOT, there is an increase in the number of IELs in the small intestinal epithelium (**Table 1.1**), suggesting that the Th1 environment may contribute to the recruitment, proliferation, or survival of IEL, and pointing to crosstalk between gluten specific Th1 immunity and the epithelial component of disease. However, Th1 immunity is not sufficient to drive tissue destruction, and this is likely due to the fact that these models lack the second component of CeD, the licensing of IE-CTL, and the upregulation of stress ligands on the surface of IECs.

The events that lead to the licensing of IE-CTL and stress ligand upregulation on IECs are not fully understood. IL-15 has been shown to directly signal on IE-CTLs to induce the expression of NKG2D and enhance their cytotoxicity (Meresse et al., 2004),

and this knowledge led to the creation of a mouse model that has human IL-15 overexpression in the epithelium, under the control of the IEC specific T3b promoter (Ohta et al., 2002). These mice have significantly increased numbers of IELs, with a slightly increased percentage of NKG2D$^+$ IEL, and develop reduced villous length in their small intestines starting around 3-4 months of age (Ohta et al., 2002; Yokoyama et al., 2008). However, this model lacks the adaptive immune component of disease, which may explain why the percentage of NKG2D$^+$ IEL is $< 6\%$ of all TCRαβ$^+$ CD8 αβ$^+$IEL (while in active CeD biopsies, the vast majority of IELs are NKG2D$^+$) and why small intestinal tissue destruction is only partial in these mice (Ohta et al., 2002; Yokoyama et al., 2008).

This points to the requirement for a model that incorporates anti-gluten adaptive immunity as well as the epithelial stress components of disease, and this was first attempted in a model that utilizes the T3b-IL-15tg mice described above crossed with OT-II TCRtg mice that have CD4$^+$ T cells specific for ovalbumin (OVA), a model antigen that is found in chicken egg whites (Korneychuk et al., 2014). When these mice were fed with OVA for 3 months, they had the development of villous atrophy (Korneychuk et al., 2014). However, the OT-II CD4$^+$ T cells in these mice actually become Tregs after OVA feeding and seed the LP, mLN, and spleen of these mice (Korneychuk et al., 2014). The tissue destruction seen in these mice is likely due to the fact that enteropathy spontaneously occurs in T3b-IL-15tg mice (Ohta et al., 2002). The design, phenotypes, and limitations of the rodent models discussed in this section are summarized in depth in **Table 1.2**.

Table 1.2. Animal models of celiac disease.

Animal strain used	Treatment	CD4 T cells	Antibodies	IEL	Villous Atrophy	Limitations	Reference
Wistar rats	i.p. injection with IFNγ + gluten feeding	Increased numbers	n.d.	Increased numbers	Decreased villous height, but not statstically significant	HLA-independent, non-specific activation of immunity.	Laparra et al., 2012
Rag1 KO mice	Transfer of $CD4^+$ $CD45RB^{lo}$ $CD25^-$ T cells that are presensitized to gluten + gluten feeding	Th1/Th17	Anti-gliadin IgA and IgG2c	n.d.	Crypt hyperplasia and VA	HLA-independent, CD4 T cells are activated *in vitro*.	Freitag et al., 2009
DQ8tg / MHC class II KO mice	Mice are immunized with gluten/CFA + 3 weeks of gluten gavage	CD4 proliferation upon gluten restimulation; T cells secrete IL-10, IL-6, TGFβ	Anti-gliadin IgG	Increased numbers	None	No VA, requires immunization, CD4 T cell response appears to be tolerogenic in nature.	Black et al., 2002; Verdu et al., 2008
NOD / DQ8tg / MHC class II KO mice	Weekly gliadin/cholera toxin gavage.	n.d.	Anti-gliadin IgG (4/11 mice) and anti-TG2 IgA (3/11 mice)	Increased numbers	None	No VA, requires immunization, antibody response is very weak.	Galipeau et al., 2011
DR3-DQ2 / MHC class II KO / human CD4 tg mice	Mice are immunized with gluten/pertussis toxin/CFA + fed gluten diet for 18 weeks	n.d.	Low levels of anti-gliadin IgA and anti-TG2 IgA	n.d.	None	No VA, requires immunization, antibody response is very weak.	de Kauwe et al., 2009
	DQ2 restricted α2-gliadin specific T cells are transferred, and mice are immunized with α2-gliadin/CFA	T cell secrete Th1 cytokines upon restimulation with gliadin and concanavalin A	n.d.	n.d.	n.d.	Utilizes Th1 polarized immunization.	
DQ2.5 / MHC class II KO	Injected with DQ2 restricted γ-gliadin-gliadin specific T cells + fed with 75-100mg of deamidated gliadin	Induction of gliadin specific $Foxp3^-$ IL10-secreting reguatory T cells (Tr1)	n.d.	n.d.	None	No VA, no LOT	Du Pre et al., 2011
T3b promoter (IEC specific)-soluble human IL15tg mice	None	Increased numbers	Plasmacytosis	Increased numbers	Reduced villus length by 3-4 mo of age	No adaptive immune component (CD4 T cells / antibodies). Histology was qualitative and not quantitative, no dietary component.	Ohta et al., 2002; Yokoyama et al., 2008; Yokoyama et al., 2011
T3b promoter (IEC specific)-soluble human IL15tg mice / OT-II tg mice	chronic OVA diet	Increase in Tregs	n.d.	Increase in % of granzyme B^+ IEL, increased MFI granzyme B in IEL	VA in the duodenum by 3 months (7/11 mice)	Gluten independent. VA only occurs in old mice. No LOT. No antibodies. Rae1 seen in all conditions.	Korneychuck et al., 2014

1.3.2 Gluten specific adaptive immunity and epithelial tissue stress synergize to drive tissue destruction in celiac disease

The generation of a true mouse model of CeD would require the two essential components for the development of tissue destruction in CeD: the LOT to gluten, and the licensing of IE-CTL, which I discussed in **Section 1.1**. Additionally, in order to have the amplification of the Th1 response and the development of TG2 specific antibodies, a mouse model would require CeD predisposing MHC class II molecules HLA-DQ2 or HLA-DQ8 and the activation of TG2 enzymatic activity as discussed in **Section 1.2**.

We utilized our knowledge that IL-15 overexpression in the LP is sufficient to drive the LOT to gluten in HLA-DQ8 transgenic mice (DePaolo et al., 2011) and the fact that trans-presentation of IL-15 by IECs can cause the upregulation of activating NKRs (**Section 1.1.5**) to test the hypothesis that the combination of gluten-specific adaptive immunity and IL-15 driven epithelial stress is required for the activation of IE-CTLs and subsequent tissue destruction in CeD. The cell-contact dependent nature of IL-15 signaling required its overexpression in the LP to polarize the gluten specific adaptive immune response, and in the intestinal epithelium signal on IELs. The resultant DQ8-IL-15^{LPxIEC} mouse model is characterized in depth in **Chapter 2**, and gluten feeding of these mice leads to the development of gluten-specific Th1 immunity, the licensing of IE-CTL, and the development of villous atrophy that is DQ8, IL-15, and gluten dependent. In **Chapter 3**, we determined whether there was TG2 activation in DQ8-IL-15^{LPxIEC} mice, and tested the hypothesis that the TG2-mediated amplification of the gluten specific Th1 response is required for the development of villous atrophy by using two different TG2

inhibitors over the course of gluten feeding. In **Chapter 4**, I discuss implications of our work in the understanding of CeD pathogenesis as well the pathogenesis of other complex organ-specific autoimmune disorders. I detail ongoing work and future directions for this project in **Chapter 5**.

CHAPTER 2. THE INTERPLAY BETWEEN IL-15, GLUTEN AND HLA-DQ8 DRIVES THE DEVELOPMENT OF COELIAC DISEASE IN MICE

Authors: Sangman M. Kim†[1,2], Thomas Lejeune†[6,7], Jordan D. Ernest[1,2], Olivier Tastet[7], Valentina Discepolo[2], Eric V. Marietta[8,9,10], Brad A. Palanski[11], Cezary Ciszewski[1,2], Romain Bouziat[1,2], Irina Horwath[8], Matthew A. Zurenski[2], Ian Lawrence[2], Anne Dumaine[14], Vania Yotova[14], Jean-Christophe Grenier[14], Joseph A. Murray[8], Chaitan Khosla[11,12,13], Luis B. Barreiro[14,15], Valérie Abadie*‡[6,7], and Bana Jabri*[1,2,3,4,5]

Affiliations:

[1]Committee on Immunology, [2]Department of Medicine, [3]Department of Pathology, [4]University of Chicago Celiac Disease Center, [5]Section of Gastroenterology, Hepatology and Nutrition, Department of Pediatrics, University of Chicago, Chicago, Illinois, USA.

[6]Department of Microbiology, Infectiology, and Immunology, University of Montreal, [7]Sainte-Justine Hospital Research Centre, Montreal, Quebec, Canada

[8]Division of Gastroenterology and Hepatology, [9]Department of Immunology, [10]Department of Dermatology, Mayo Clinic, Rochester, MN, USA.

[11]Department of Chemistry, [12]Department of Chemical Engineering, [13]Stanford ChEM-H; Stanford University, Stanford, CA, USA.

[14]Department of Genetics, Sainte-Justine Hospital Research Centre, [15]Department of Pediatrics Faculty of Medicine; University of Montreal, Montreal, Quebec, Canada.

‡ Current address: Department of Medicine, Section of Gastroenterology, Hepatology and Nutrition, University of Chicago, Chicago, Illinois, USA.

†These authors contributed equally to this work.

*Co-senior and corresponding authors: bjabri@bsd.uchicago.edu (B.J.); vabadie@medicine.bsd.uchicago.edu (V.A.)

2.1 Abstract

Coeliac disease (CeD) is a complex, polygenic inflammatory enteropathy with autoimmune features caused by exposure to dietary gluten that occurs in a subset of genetically susceptible HLA-DQ8 and HLA-DQ2 individuals (Abadie et al., 2011; Green and Cellier 2007; Tjon et al., 2010). Attempts to develop a pathophysiologically relevant animal model that develops villous atrophy (VA) have failed. The need to develop non-dietary treatments for this common disorder is now widely recognized, but it is hampered by the lack of a preclinical model. Furthermore, while human studies have led to major advances in our understanding of CeD pathogenesis, direct demonstration of the respective roles of disease-predisposing HLA molecules, and adaptive and innate immunity in the development of tissue damage is missing. To address these unmet needs, we engineered a mouse model that reproduces the dual overexpression of IL-15 in the gut epithelium and the lamina propria (Lp) characteristic of active CeD, expresses the predisposing HLA-DQ8 molecule, and develops VA upon gluten ingestion. We show that overexpression of IL-15 in both the epithelium and Lp is required for development of VA, demonstrating the location-dependent central role of IL-15 in CeD pathogenesis. Furthermore, our study reveals the critical role played by both $CD4^+$ and cytotoxic $CD8^+$ T cells in VA development. Finally, it establishes that HLA-DQ8 is central for tissue destruction, but dispensable for loss of oral tolerance to gluten. This mouse model, by reflecting the complex interplay between gluten, genetics and the IL-15-driven tissue inflammation found in CeD, represents a powerful preclinical model to test new therapeutics and study disease pathogenesis.

2.2 Introduction

CeD currently affects 1% of the global population. Full-blown active CeD is characterized by the presence of small intestinal pathology associated with destruction of the gut epithelium, crypt hyperplasia, and a substantial infiltration of intraepithelial lymphocytes (IELs). As a consequence, patients classically present with gastrointestinal symptoms such as chronic diarrhea, malabsorption, abdominal pain, bloating, and failure to thrive, as well as extraintestinal manifestations such as anemia, osteoporosis, and neurological disorders (Husby et al., 2012). CeD patients produce highly disease-specific autoantibodies directed against tissue transglutaminase 2 (TG2) and anti-deamidated anti-gluten (DGP) antibodies that are used in the diagnostic work-up of CeD. Strict adherence to a lifelong gluten-free diet (GFD) typically results in resolution of symptoms and restoration of normal intestinal morphology (Rubio-Tapia et al., 2010). However, around 30-40% of individuals fail to completely heal on a GFD (Rubio-Tapia et al., 2010), and some develop major complications, such as refractory CeD, which is characterized by persistent VA on a GFD and a heightened risk for cryptic intraepithelial lymphoma (Rubio-Tapia and Murray, 2010). Furthermore, adherence to a GFD has negative impacts on the lifestyle and quality of life, explaining why compliance is often low (Leffler et al., 2008). This has led to the realization that alternative therapeutic options need to be developed (Plugis and Khosla, 2015).

The observation that CeD only develops in HLA-DQ2 or HLA-DQ8 individuals combined with the identification of HLA-DQ2 and HLA-DQ8 restricted gluten-specific T cells producing IFN-γ in the Lp of CeD patients suggests that a gluten-specific

proinflammatory T helper 1 (T_H1) response plays a critical role in the pathogenesis of CeD (Jabri and Sollid, 2009). However, two lines of evidence imply that anti-gluten CD4 T cell immunity is not sufficient for tissue destruction in CeD. First, despite the presence of adaptive anti-gluten immunity, a subset of individuals referred to as potential CeD patients lack tissue destruction (Setty et al., 2015). Second, humanized HLA-DQ2 or HLA-DQ8 animal models with inflammatory anti-gluten CD4 T cell immune responses induced upon activation with adjuvants failed to develop VA, even in the presence of high numbers of gluten-specific transgenic T cells (de Kauwe et al., 2009; Du Pré et al., 2011; Marrietta et al., 2004). These findings suggest that a second factor drives potential CeD patients to progress to overt CeD with VA (Ferguson et al., 1993). Observations in humans have shown that IELs expanded in active CeD patients express activating natural killer (NK) receptors that are activated by IL-15 expressed on intestinal epithelial cells (IECs) (Jabri et al., 2000). We proposed more specifically that $CD8^+$ cytotoxic intraepithelial T cells (IE-CTLs) are the key effector cell type that mediate tissue destruction based on recognition of IECs stress signals (Green and Jabri, 2003). This role of IE-CTLs in CeD was supported by ensuing human studies demonstrating the cytolytic capacities of IE-CTLs in CeD (Hue et al., 2004; Mention et al., 2003; Meresse et al., 2004; Meresse et al., 2006). Based on these observations, we hypothesized that a combination of adaptive anti-gluten immunity and epithelial distress characterized by IL-15 upregulation were both required for the development of VA (Green and Jabri, 2003; Jabri and Sollid, 2006). This hypothesis was later reinforced by human studies reporting that patients with potential CeD, who lack atrophy, lacked IL-15 overexpression in IECs and IE-CTLs with a killer

phenotype (Setty et al., 2015), and in mice showing that transfer of ovalbumin-specific CD4 T cells caused VA in mice overexpressing IL-15 in the intestinal epithelium (Korneychuk et al., 2014). However, this latter mouse model had levels of IL-15 overexpression leading to the development of spontaneous VA at 6 months of age, and the use of transgenic T cells expressing a TCR specific for ovalbumin bypassed the need for regulating the frequency of dietary antigen-specific T cells (Korneychuk et al., 2014). This may explain why VA developed in a gluten-independent manner and did not require the CeD-predisposing HLA molecules DQ2 and DQ8.

2.3 Results

Thus, despite all the advances in the field of CeD pathogenesis, a pathophysiological relevant mouse model of CeD with VA is still lacking (Korneychuk et al., 2014; Costes et al., 2015). Furthermore, we still need to elucidate the respective roles and interplay of IL-15, HLA molecules, CD4 and CD8 T cells in CeD pathogenesis. To address this gap, we generated a DQ8-IL-15^{LPxIEC} mouse expressing the CeD-predisposing molecule HLA-DQ8, and overexpressing IL-15 in both IECs and the Lp, mimicking what is seen in active CeD (Setty et al., 2015). These mice were generated by crossing immune competent IL-15^{LP}, IL-15^{IEC} with HLA-DQ8 mice on the C57BL/6 background (DePaolo et al., 2011; Meisel et al., 2017). These mice have levels of IL-15 overexpression that were insufficient by themselves to induce VA (as defined by a villous to crypt ratio of 2 and below). While HLA-DQ8 mice failed to develop VA, approximately 75% of DQ8-IL-15^{LPxIEC} mice developed small intestinal tissue destruction upon 30 days of gluten feeding (**Extended data Fig. 2.1A**). Importantly, the villous architecture was restored upon gluten exclusion (**Fig. 2.1A, B**). Furthermore, as in CeD patients, gluten-fed DQ8-IL-15^{LPxIEC} mice developed plasmacytosis in the Lp (**Fig. 2.1C and Extended data Fig. 2.1B**). The presence of IgG antibodies against deamidated gliadin peptides (DGP) and anti-TG2 IgG and IgA antibodies are hallmarks of active CeD that are used for diagnosis of patients, the former being increasingly acknowledged as a more accurate serological marker for the diagnosis of CeD in children and IgA-deficient individuals (Husby et al., 2012; Mozo et al., 2012; Mesin et al., 2012; Dieterich et al., 1997). TG2 deamidates specific glutamine residues in gliadin peptides, thereby increasing their affinity for HLA-DQ2 or HLA-DQ8

and rendering them more potent T cell epitopes (van de Wal et al., 1998; Molberg et al., 1998). We readily identified circulating anti-DGP IgG antibodies (**Fig. 2.1D and Extended data Fig. 2.1C**). As in humans, anti-DGP antibodies were an indicator of disease development (Husby et al., 2012), with the highest antibody titers being associated with the most severe intestinal lesions (**Extended data Fig. 2.2A**). However, despite our ability to detect IgA and TG2 colocalization in the small intestine, (**Extended data Fig. 2.2B**) we could not consistently detect anti-TG2 antibodies in the serum (**Extended data Fig. 2.2C**). This may reflect the absence of a VH5-51 mouse homolog that recognizes in its germline configuration TG2 (Di Niro et al., 2012). Furthermore, as anticipated, we also detected native gliadin-specific IgG (**Extended data Fig. 2.2D**) and IgA (**Extended data Fig. 2.2E**) antibodies. The presence of circulating anti-gluten IgG2c antibodies (**Fig. 2.1E**) was indicative of gliadin-specific B cell activation by T_H1 anti-gluten T cells. In accordance, IFNγ, the predominant cytokine associated with CeD in humans (Nilsen et al., 1998), was up-regulated in the Lp of gluten-fed DQ8-IL-15^{LPxIEC} mice (**Fig. 2.1F**).

IELs expansion is a hallmark of CeD that is also used for the diagnosis of the disease (Husby et al., 2012; Järvinen et al., 2003). Classically, IE-CTLs in the coeliac lesion express high levels of granzyme B and perforin (Setty et al., 2015; Oberhuber et al., 1996; Ciccocioppo et al., 2000), and abnormally high surface expression of activating NK receptors NKG2D and NKG2C/CD94, while lacking the inhibitory NKG2A/CD94 (Meresse et al., 2004; Meresse et al., 2006). The functional consequence of this surface NK receptor phenotype is the enhanced ability to kill cells bearing the stress-induced MICA/B molecules and the non-classical MHC class I molecule HLA-E, which are the main ligands

for NKG2D and CD94/NKG2C, respectively (Hue et al., 2004; Meresse et al., 2004; Meresse et al., 2006). DQ8-IL-15^{LPxIEC} mice displayed a gluten- and IL-15 dependent expansion of IELs (**Fig. 2.1G and Extended data Fig. 2.1D**), of which ten to thirty percent expressed IE-CTLs-associated cytotoxic molecules granzyme B (**Fig. 2.1H, Extended data Fig. 2.1E-G and Extended data Fig. 2.2F-H)** and perforin (**Fig. 2.1I**), and bear activating NKG2D receptor (**Fig. 2.1J and Extended data Fig. 2.1H, I**), denoting their cytolytic potential. The acquisition of cytotoxic features by IELs was accompanied by the upregulation in the epithelium of the mouse NKG2D ligand, Rae-1 (**Fig. 2.1K**) as well as the non-classical MHC class I molecule Qa-1 (**Fig. 2.1L**), which is recognized by NKG2C/CD94. Importantly, as in CeD patients and in accordance with mice restoring normal histology after 4-weeks of GFD (**Fig. 2.1B**), adaptive immune activation in DQ8-IL-15^{LPxIEC} mice occurs in a manner that is reversible after gluten withdrawal (**Fig. 2.1B-L and Extended data Fig. 2.2B, D, E and F-H**). Taken together, DQ8-IL-15^{LPxIEC} mice develop adaptive anti-gluten immunity, expansion of IE-CTLs with a killer phenotype, and tissue destruction in a gluten-dependent manner.

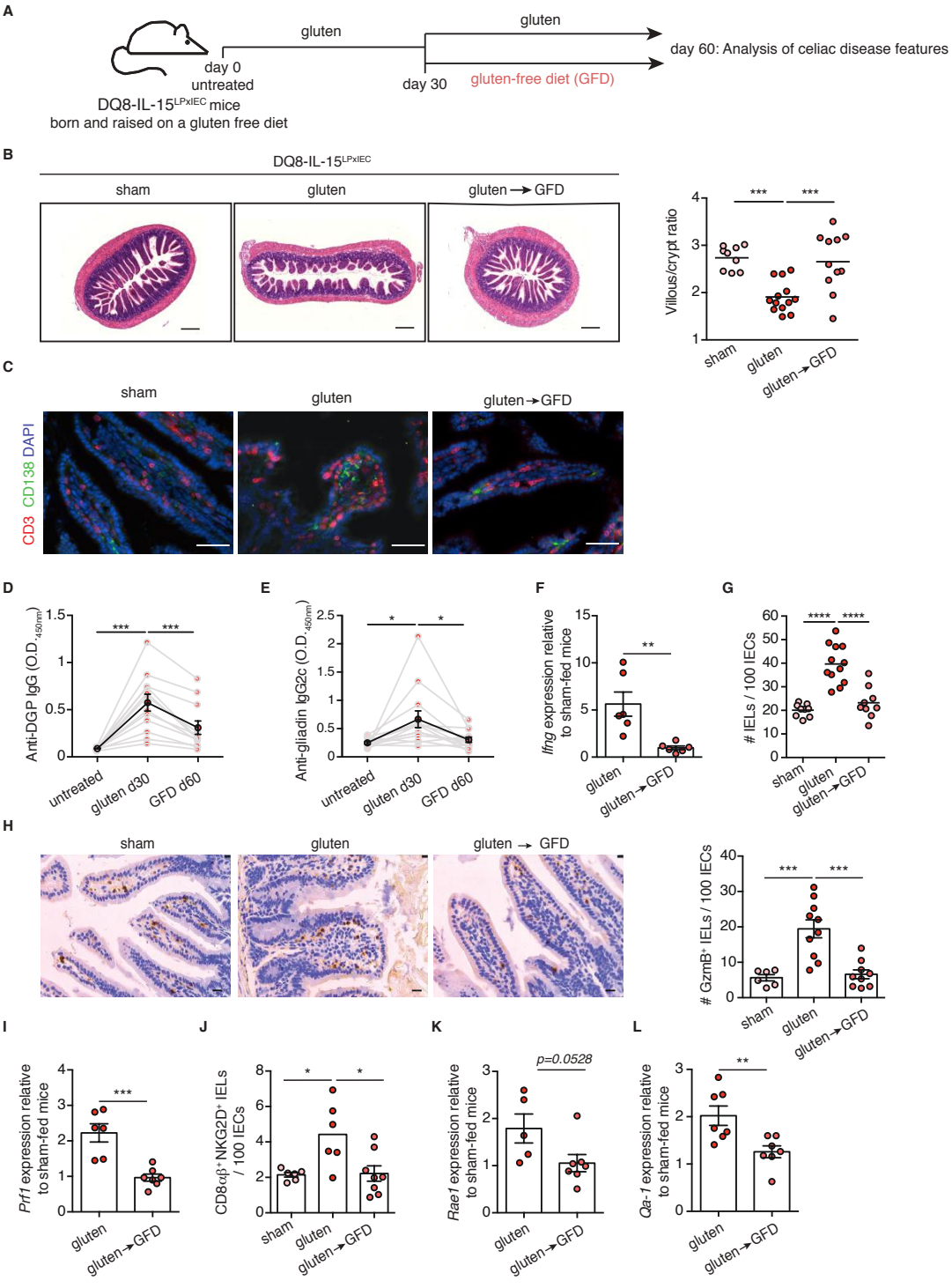

Figure 2.1. DQ8-IL-15^{LPxIEC} mice develop the hallmarks of CeD upon gluten feeding and recover on a GFD.

(**A-L**) Ten-week old DQ8-IL-15^{LPxIEC} mice that were raised on a gluten-free diet (GFD) were maintained on a GFD (denoted "sham"), fed with gluten for 60 days ("gluten"), or fed with gluten for 30 days and then reverted to a GFD ("gluten→GFD") for 30 days.

Figure 2.1., continued.
(**A**) Experimental timeline.
(**B**) Hematoxylin and eosin (H&E) staining of paraffin-embedded ileum sections. Scale bar, 200 μm. The graph depicts the ratio of the morphometric assessment of villous height to crypt depth.
(**C**) CD3ε$^+$ T cells (red) and CD138$^+$ plasma cells (green) were distinguished by immunohistochemistry (IHC) staining of frozen ileum sections. Scale bar, 50 μm.
(**D**) Serum anti-deamidated gliadin peptides (DGP) IgG levels were measured by ELISA. Sera were collected sequentially in the same mice before gluten feeding (untreated), thirty days after gluten feeding (gluten d30), and thirty days after reversion to a GFD (GFD d60). The black line represents the average for each of the groups.
(**E**) Serum anti-gliadin IgG2c levels were measured by ELISA as in (D).
(**F**) Expression of *IFN-γ* in the Lp was measured by qPCR. Relative expression levels in gluten and gluten→GFD groups were normalized against the expression levels observed in sham-fed DQ8-IL-15^{LPxIEC} mice.
(**G**) Quantification of intraepithelial lymphocytes (IELs) among intraepithelial cells (IECs) was performed on H&E stained ileum sections.
(**H**) Granzyme B staining by IHC on paraffin-embedded ileum sections. Scale bar, 20 μm. The graph depicts the average number of granzyme B$^+$ IELs / 100 IECs per mouse.
(**I**) Expression of *Prf1* in the intestinal epithelium was measured by qPCR. Analysis was performed as in (F).
(J) The intestinal epithelium was isolated and analyzed by flow cytometry. IELs were identified as TCRβ$^+$ CD4$^-$ CD8αβ$^+$ cells. In parallel, IELs were quantified among IECs on H&E stained ileum sections. NKG2D$^+$ NKG2$^-$ IELs are indicated by absolute number / 100 IECs.
(**K, L**) Expression of *Rae1* (K) *and Qa-1* (L*)* in the intestinal epithelium as measured by qPCR. Analysis was performed as in (F).
Data are representative of at least two independent experiments. Error bars, SEM. *P < 0.05, **P < 0.01, ***P < 0.001, ****P < 0.0001; One-way analysis of variance (ANOVA) / Tukey's multiple comparison [(B), (G), (H), (J)], RM One-way ANOVA / Tukey's multiple comparison [(D) and (E)], and unpaired Student's *t*-test [(F), (I), (K), (L)].

Studies in humans have suggested that the combination of adaptive anti-gluten immunity and IL-15 overexpression in IECs is required for IE-CTLs to acquire a fully activated killer phenotype (defined by the expression of activating NK receptors NKG2D and CD94 in the absence of the inhibitory NKG2A receptor, and high levels of granzyme and perforin) (Setty et al., 2015). As previously shown (DePaolo et al., 2011), DQ8-IL-15^{LP} mice failed to exhibit intestinal tissue damage upon gluten ingestion (**Extended data Fig. 2.3A**), despite mounting an adaptive anti-gluten immune response as assessed by the presence of anti-DGP antibodies (**Extended data Fig. 2.3B**). Furthermore, in

accordance with the observation that a subset of family members of CeD patients (first degree relatives of CeD patients who do not have any of the characteristic features of CeD despite the presence of IL-15 overexpression in the gut epithelium) do not have VA (Setty et al., 2015), DQ8-IL-15^{IEC} mice maintained a normal intestinal histology upon gluten introduction (**Extended data Fig. 2.3A**). Development of VA in DQ8-IL-15^{LPxIEC} mice was correlated with an expansion of IE-CTLs expressing a fully activated phenotype (**Fig. 2.2A-G and Extended data Fig. 2.3C-H**). Of note, expansion of IE-CTLs lacking an activated NK phenotype in DQ8-IL-15^{LP} mice reproduced the IE-CTLs phenotype seen in potential CeD, indicating that adaptive anti-gluten immunity has the capacity to expand IELs but not to induce a killer phenotype in IE-CTLs. Conversely, similar to family members of CeD patients (Setty et al., 2015), DQ8-IL-15^{IEC} mice failed to develop adaptive anti-gluten immunity (**Extended data Fig. 2.3B),** but expanded IE-CTLs with a partial activated NK phenotype (**Fig. 2.2A-D and Extended data Fig. 2.3D-H**). Finally, upregulation of Rae-1 (mouse homolog of MICA) (**Extended data Fig. 2.3I**) and Qa-1 (mouse ligand for CD94/NKG2 receptors) (**Extended data Fig. 2.3J**) was dependent on gluten and IL-15 overexpression in IECs. Taken together these data demonstrate that gluten feeding and IL-15 overexpression in IECs and the Lp need to synergize to observe concomitant upregulation of non-classical MHC class I molecules (**Extended data Fig. 2.3I, J)**, expansion of IE-CTLs with a fully activated phenotype (**Fig. 2.2A-D** and **Extended data Fig. 2.3E-H)** and VA (**Extended data Fig. 2.3A**). These observations support the hypothesis that IE-CTLs play a critical role in IECs destruction. In accordance, depletion of CD8^{+} IE-CTLs in gluten-fed DQ8-IL-15^{LPxIEC} mice using anti-CD8 monoclonal

antibody treatment throughout gluten feeding, led to a significant protection of the villous to crypt ratio (**Fig. 2.2H and Extended data Fig. 2.4A-C**). As expected, IEL depletion did not have an impact on the adaptive gluten-specific B cell response (**Extended data Fig. 2.4D**); however, while not affecting the expression of Qa-1 (**Extended data Fig. 2.4E)**, it did lead to a significant reduction in Rae-1 expression (**Extended data Fig. 2.4F**), suggesting a possible participation of IE-CTLs in the upregulation of specific tissue stress molecules. These data provide a mechanistic basis as to why potential CeD patients with adaptive anti-gluten immunity and family members with IL-15 overexpression in IECs do not develop VA.

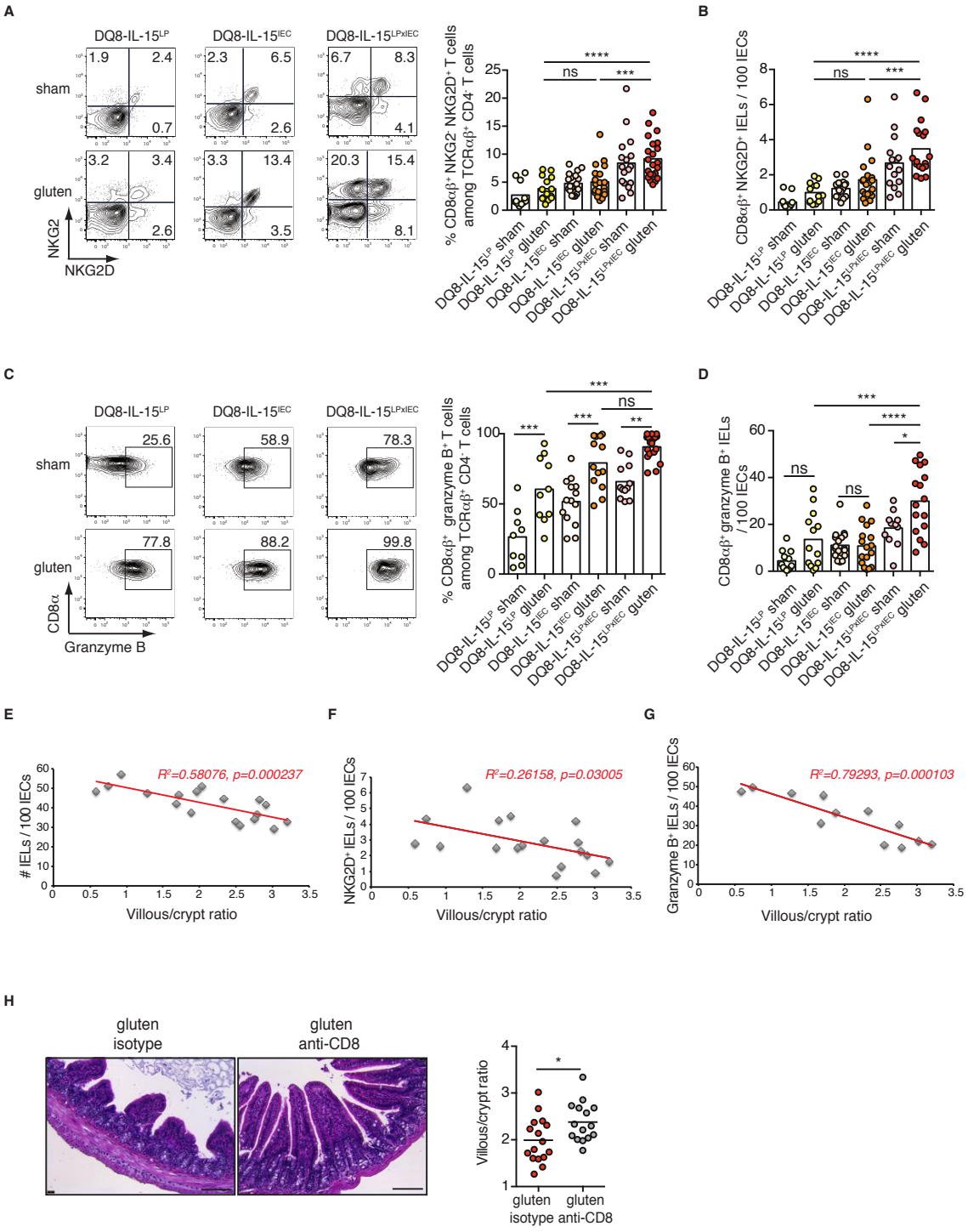

Figure 2.2. IL-15 expression in both the Lp and epithelium confers IELs with a cytotoxic phenotype and the ability to kill epithelial cells.

(**A-D**) Ten-week old DQ8-IL-15^{LP}, DQ8-IL-15^{IEC}, and DQ8-IL-15^{LPxIEC} mice that were raised on a GFD were maintained on a GFD (sham) or fed with gluten for 30 days (gluten).

(**A-D**) The intestinal epithelium was isolated and analyzed by flow cytometry. IELs were identified as TCRβ^{+} CD4^{-} CD8αβ^{+} cells. In parallel, IELs were quantified among IECs on H&E stained ileum

Figure 2.2., continued.
sections. NKG2D^{+} NKG2^{-} IELs are indicated by (A) percentage and (B) absolute number / 100 IECs. Intracellular granzyme B^{+} IELs are indicated by (C) percentage and (D) absolute number / 100 IECs.
(**E-G**) Correlations between the extent of villous atrophy determined by the analysis of the villous/crypt ratio and (E) the amount of IELs / 100 IECs, (F) the amount of IELs expressing NKG2D / 100 IECs, and (G) the amount of IELs expressing granzyme B / 100 IECs sham and gluten-fed DQ8-IL-15^{LPxIEC} mice.
(**H**) H&E staining of ileum sections of ten-week old DQ8-IL-15^{LPxIEC} mice that were raised on a GFD were fed with gluten for 30 days and concurrently treated with an anti-CD8 antibody or isotype control (treatment regimen and efficacy summarized in Extended data figure 2.4). Scale bar 100 μm. The graph depicts the ratio of the morphometric assessment of villous height and crypt depth.
[(A) to (D), and (H)] Data represent four independent experiments. [(E-G)] data represent three independent experiments. *P < 0.05, **P < 0.01, ***P < 0.001, ****P < 0.0001; One-way ANOVA / Tukey's multiple comparison [(A) to (D)], and unpaired Student's *t*-test [(H)].

CeD only occurs in individuals expressing HLA-DQ2 or HLA-DQ8 molecules, suggesting that, even though they are not sufficient, CD4^{+} T cells are required for the destruction of IECs. To demonstrate that CD4^{+} T cells are not only required for adaptive anti-gluten immunity but also VA, we depleted CD4^{+} T cells during the course of gluten feeding (**Extended data Fig. 2.5A-C**). As anticipated, CD4^{+} T cell depletion led to a loss of anti-DGP and anti-gluten antibodies (**Fig. 2.3A, B and Extended data Fig. 2.5D, E**). More importantly, CD4^{+} T cell depletion prevented development of VA (**Fig. 2.3C**), indicating that CD4^{+} T cells are required for tissue destruction in CeD. To better understand the underlying mechanisms, we analyzed the impact of CD4^{+} T cell depletion on IE-CTLs and IECs. CD4^{+} T cells were critical for the expansion of IE-CTLs with a fully activated killer phenotype (**Fig. 2.3D-G**), but not for the upregulation of Rae-1 (**Fig. 2.3H**) or Qa-1 (**Fig. 2.3I**). These results, combined with the observation that CD8^{+} T cell depletion prevents development of VA, indicate that CD4^{+} T cells play a key role for VA development in gluten-fed DQ8-IL-15^{LPxIEC} mice by modulating IE-CTLs but not IECs stress.

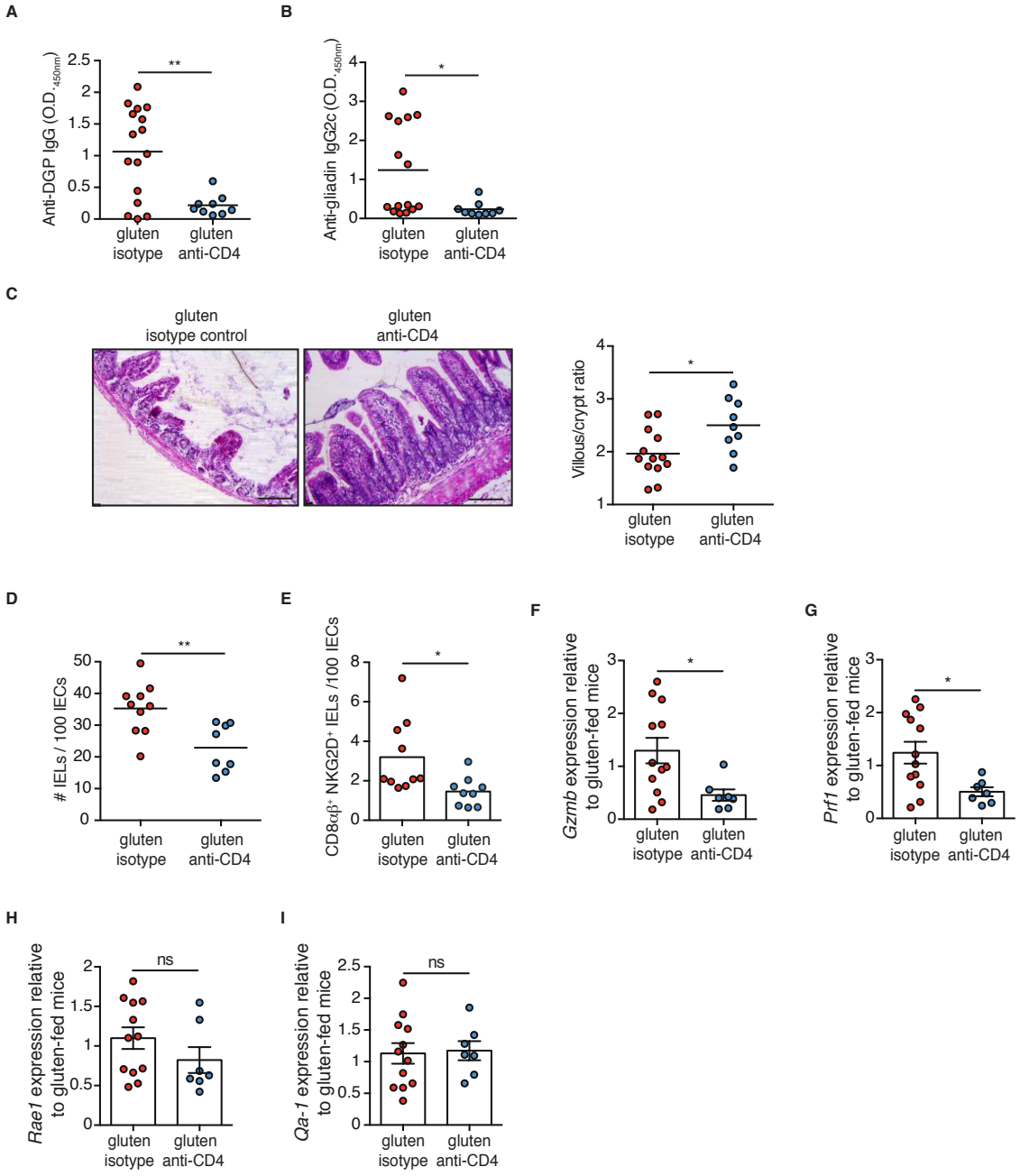

Figure 2.3. CD4 T cells are required for the licensing of IE-CTLs.

(**A-I**) Ten-week old DQ8-IL-15^{LPxIEC} mice that were raised on a GFD were fed with gluten for 30 days and concurrently treated with an anti-CD4 antibody or isotype control (treatment regimen and efficacy summarized in Extended data figure 2.6).

(**A**) Serum anti-DGP IgG levels were measured by ELISA. Sera were collected thirty days after gluten feeding.

(**B**) Serum anti-gliadin IgG2c levels were measured by ELISA. Sera were collected thirty days after gluten feeding.

Figure 2.3., continued.
(**C**) H&E staining of paraffin-embedded ileum sections. The graph depicts the ratio of the morphometric assessment of villous height to crypt depth. Scale bar, 100 μm.
(**D**) Quantification of intraepithelial lymphocytes (IELs) among intraepithelial cells (IECs) performed on H&E stained ileum sections.
(**E**) The intestinal epithelium was isolated and analyzed by flow cytometry. IELs were identified as TCRβ$^+$ CD4$^-$ CD8αβ$^+$ cells. NKG2D$^+$ NKG2$^-$ IELs are indicated by absolute number / 100 IECs.
(**F-I**) Expression of (F) *GzmB,* (G) *Prf1*, (H) *Rae1*, and *Qa-1* (I) in the intestinal epithelium as measured by qPCR. Relative expression levels were normalized against the expression levels observed in gluten-fed DQ8-IL-15^{LPxIEC} mice.
Data are representative of four independent experiments. Error bars, SEM. *P < 0.05, **P < 0.01, unpaired Student's *t*-test.

We next determined whether HLA-DQ8 was specifically required for tissue destruction in mice overexpressing IL-15 in IECs and the Lp. To address this question, DQ8-IL-15^{LPxIEC} and IL-15^{LPxIEC} mice were fed gluten for 30 days. Importantly, both mouse strains express the MHC class II Molecules I-A^b and only differ by the presence or absence of the CeD-predisposing HLA-DQ8 molecule (**Extended data Fig. 2.6A**). In contrast to DQ8-IL-15^{LPxIEC} mice, IL-15^{LPxIEC} mice failed to develop VA (**Fig. 2.4A**). Nevertheless, in line with previous studies (DePaolo et al., 2011), HLA-DQ8 was not required for the development of serum IgG antibodies against DGP (**Fig. 2.4B**) (levels of antibodies were even slightly higher in IL-15^{LPxIEC} as compared to DQ8-IL-15^{LPxIEC} mice) and a T_H1 inflammatory immune response in the Lp (**Fig. 2.4C**). Interestingly, and in line with the finding that CD4$^+$ T cells are critical for the expansion of IELs with a cytolytic phenotype (**Fig. 2.3D-H**), the number of IELs and IE-CTLs expressing NKG2D (**Fig. 2.4D, E**) and granzyme B (**Fig. 2.4F**) was significantly lower in IL-15^{LPxIEC} than in DQ8-IL-15^{LPxIEC} mice. Furthermore, levels of granzyme B expression were also decreased, albeit not to a significant level (**Fig. 2.4G**). In contrast, perforin, Qa-1 and Rae-1 expression were comparable (**Extended data Fig. 2.6B-D)**. Together, these results indicate that while HLA-DQ8 is dispensable for loss of tolerance to gluten, it is essential for the

requisite increase in cytolytic IE-CTLs to mediate tissue destruction. Comparative transcriptional analysis of total cells isolated from the epithelium of gluten-fed- DQ8, IL-15^{LPxIEC}, and DQ8-IL-15^{LPxIEC} mice revealed that a large number of pathways related to lymphocyte activation and antigen presentation were significantly more enriched in gluten-fed DQ8-IL-15^{LPxIEC} mice as compared to DQ8 and IL-15^{LPxIEC} mice in both the Lp and the epithelium (**Fig. 2.4H**). This suggests that the interplay between IL-15 and HLA-DQ8 contributes to optimal lymphocyte activation. In contrast, gluten was able to induce pathways involved in metabolic processes in all three mice strains (**Fig. 2.4H).** Closer analysis of the differentially expressed genes revealed that many CeD risk variants (Dubois et al., 2010), such as genes involved in antigen presentation (*Ciita*), T and B cell activation (*Ctla4, Icos, Rgs1*) and cytotoxic function (*Klra7*), T_H1 cell polarization (*Tbx21*) and inflammation (*Il18r1*) were most significantly upregulated in DQ8-IL-15^{LPxIEC} mice fed gluten (**Fig. 2.4I and Extended data Fig. 2.6E**). IL-15 overexpression alone was sufficient to promote an increase in the expression of most of these genes as compared to DQ8 mice (**Fig. 2.4I and Extended data Fig. 2.6E**). Of note, while gluten feeding frequently contributed to the upregulation of immune-related genes in mice overexpressing IL-15 both in IECs and the Lp, in the absence of IL-15 it generally failed to do so, with an exception for *Rgs1* (**Fig. 2.4I**). Taken together, these results suggest that the CeD-predisposing HLA-DQ8 molecule critically contributes to the increase in IE-CTLs with a cytolytic phenotype and the development of VA by cooperating with gluten and IL-15 to enhance the expression of intestinal immune pathways, including several genetic risk factors for CeD.

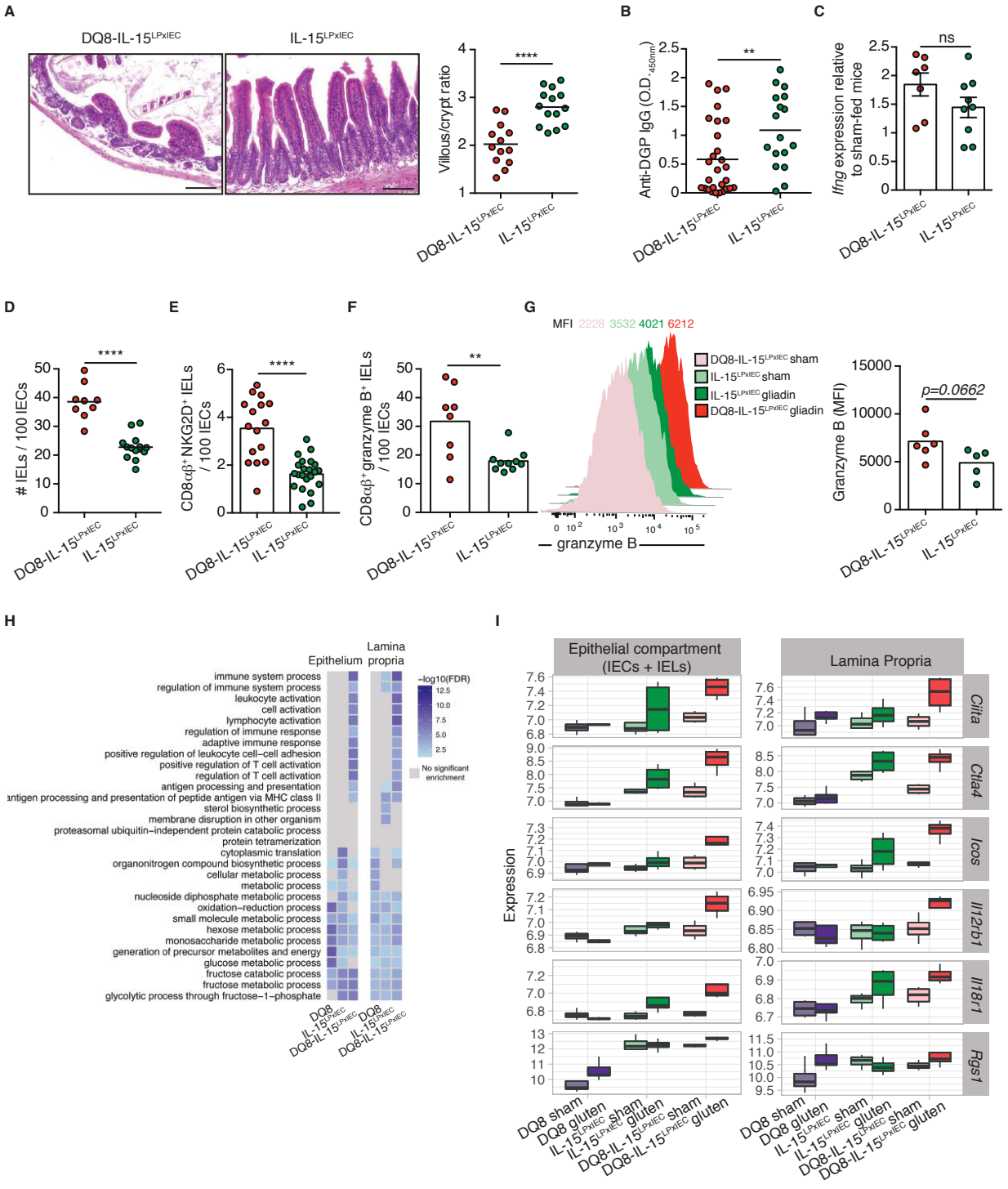

Figure 2.4. HLA-DQ8 is required to amplify gluten-specific adaptive immunity to the threshold required for tissue destruction.

(**A-I**) Ten-week old DQ8-IL-15^{LPxIEC}, IL-15^{LPxIEC}, and DQ8 mice that were raised on a GFD were maintained on a GFD (sham) or fed with gluten for 30 days (gluten).

(**A**) H&E staining of paraffin-embedded ileum sections. The graph depicts the ratio of the morphometric assessment of villous height to crypt depth. Scale bar, 100 μm.

Figure 2.4., continued.
(**B**) Anti-DGP IgG levels were measured by ELISA. Sera were collected thirty days after gluten feeding.
(**C**) Expression of *IFN-*γ in the LP was measured by qPCR. Relative expression levels in gluten groups were normalized against the expression levels observed in sham-fed DQ8-IL-15^{LPxIEC} mice.
(**D**) Quantification of intraepithelial lymphocytes (IELs) among intraepithelial cells (IECs) was performed on H&E stained ileum sections.
(**E, F**) The intestinal epithelium was isolated and analyzed by flow cytometry. IELs were identified as TCRβ^+ CD4$^-$ CD8$\alpha\beta^+$ cells. (E) NKG2D$^+$ NKG2$^-$ IELs are indicated by absolute number / 100 IECs. (F) Granzyme B$^+$ IEL are indicated by absolute number / 100 IECs.
(G) Intracellular granzyme B mean fluorescence intensity (MFI) was measured.
(**H**) Gene ontology terms significantly enriched among genes differently expressed in response to gluten challenge in DQ8, IL-15^{LPxIEC,} and DQ8-IL-15^{LPxIEC} mice.
(**I**) Examples of genes that are significantly upregulated in response to gluten uniquely in DQ8-IL-15^{LPxIEC} mice.
Data represent are representative of two [(C), (F)] or four [(A), (B), (D), (E), (G)] independent experiments. *P < 0.05, **P < 0.01, ****P < 0.0001; unpaired Student's *t*-test.

To further evaluate the relevance of DQ8-IL-15^{LPxIEC} mice as a model for CeD, we sought to directly compare the gluten dependent transcriptional changes in the small intestines of DQ8-IL-15^{LPxIEC} mice with those observed in active CeD patients. We collected RNA-sequencing data from duodenal biopsies obtained from 51 CeD patients and 45 healthy controls. Strikingly, we found that the differences in gene expression between gluten fed-DQ8, and DQ8-IL-15^{LPxIEC} mice were strongly correlated to the changes in gene expression observed between active CeD patients and healthy controls (**Fig. 2.5A**, $p< 1x10^{-5}$ for both the epithelium and the LP). The most strongly enriched gene ontology terms among genes up-regulated in both gluten fed-DQ8-IL-15^{LPxIEC} and active CeD patients as compared to gluten fed-DQ8 mice and healthy controls, respectively, belonged to immune pathways related to T cell activation (FDR=$2.0x10^{-4}$), and the regulation of antigen presentation (FDR=$1.1x10^{-4}$) (**Fig. 2.5B**), in accordance with the critical role of adaptive immunity in CeD pathogenesis. Moreover, we found a strong concordance between the gene ontology terms enriched among genes induced by gluten

challenge on DQ8-IL-15^{LPxIEC} mice and genes that were differently expressed between active CeD patients and healthy controls (**Extended data Fig. 2.7A, B),** suggesting that similar gene regulatory mechanisms underlie the development of CeD in humans and the DQ8-IL-15^{LPxIEC} mouse model.

Neutralizing monoclonal anti-IL15 antibody is currently being tested for its efficacy in refractory CeD patients. To demonstrate the preclinical potential of the DQ8-IL-15^{LPxIEC} model, we tested the IL-15 neutralizing monoclonal antibody M96 (DePaolo et al., 2011; Lebrec et al., 2013) as a treatment using a clinically relevant protocol. More specifically, DQ8-IL-15^{LPxIEC} mice exposed to gluten for 3-4 weeks (a duration sufficient to induce VA) (**Extended data Fig. 2.1A**) were placed on a GFD, and then re-challenged with gluten with or without anti-IL15 treatment (**Fig. 2.5C**). This regimen mimics clinical trials in patients with established CeD, who are on a GFD, and are challenged with gluten to test the hypothesis that anti-IL-15 can act in a therapeutic manner. Anti-IL15 treated mice were protected from development of VA compared to mice that received an isotype control (**Fig. 2.5D**), despite having developed adaptive anti-gluten immunity (**Fig. 2.5E, F**). All the mice maintained high levels of anti-DGP antibodies (**Fig. 2.5E**), suggesting that the antibody response in mice that have an anti-gluten CD4$^+$ T cell memory response does not require IL-15. There was, however, a reduction in the development of anti-gliadin IgG2c antibodies (**Fig. 2.5F**) and a reduction in Lp IFNγ transcript levels (**Fig. 2.5G**), indicating that anti-IL15 treatment led to a reduction in T_H1 immunity. In line with the decreased tissue damage, there was also a reduction in the number of IE-CTLs (**Fig. 2.5H-J**) as well as a decrease in granzyme B (**Extended data Fig. 2.8A**), perforin (**Fig.**

2.5K), and Rae1 transcript levels (**Fig. 2.5L**). In contrast, anti-IL15 treatment did not affect the levels of Qa-1 transcripts (**and Extended data Fig. 2.8B**). Together these results further demonstrate the central role played by IL-15 in CeD pathogenesis even after establishment of active disease, suggesting that anti-IL-15 treatment could be an effective treatment to prevent or ameliorate tissue destruction in established CeD. They also provide evidence that DQ8-IL-15^{LPxIEC} mice represent a powerful preclinical model of CeD.

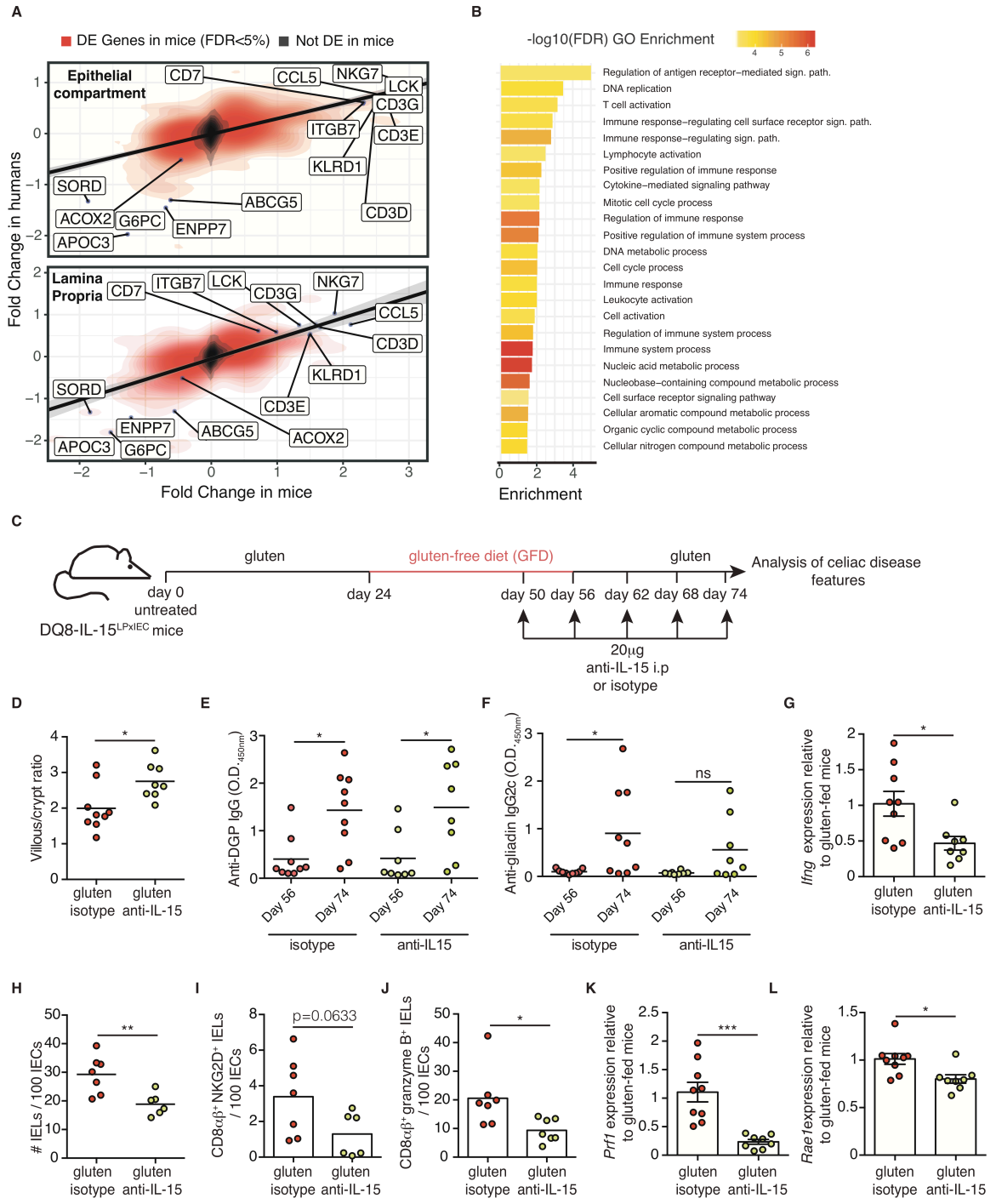

Figure 2.5. DQ8-IL-15^{LPxIEC} mice as a preclinical model for coeliac disease

(**A, B**) Transcriptional comparison of the intestinal epithelium and LP of gluten-fed DQ8-IL-15^{LPxIEC} mice and active CeD patients.

(**A**) Correlation between the log2 fold-changes in gene expression between gluten fed-DQ8 and DQ8-IL-15^{LPxIEC} mice (x-axis) in the epithelial compartment that encompass IELs and IECs (top panel) and the Lp (bottom panel) and the log2 fold-changes in gene expression observed between active CeD patients and healthy controls.

Figure 2.5., continued.
(**B**) Most strongly enriched gene ontology terms (FDR<0.1%) among genes up-regulated when comparing *both* gluten fed-DQ8 vs gluten fed-DQ8-IL-15^{LPxIEC} and active CeD patients vs healthy controls (defined as genes showing an FDR<0.01 in either the human or mice comparison & a nominal p-value < 0.05 in the other contrast). The x-axis depicts the fold-enrichment level observed and the color of the bars the statistical support for the observed enrichments (depicted in the form of –log10 FDR).
(**C-L**) Ten-week old DQ8-IL-15^{LPxIEC} mice that were raised on a GFD were fed with gluten for three weeks, returned to a GFD for 30 days, and then rechallenged with gluten and concurrently treated with an anti-IL-15 antibody or isotype control for an additional three weeks. All readouts were taken at the endpoint of the experiment unless otherwise indicated.
(**C**) Experimental timeline.
(**D**) H&E staining of paraffin-embedded ileum sections was performed. The graph depicts the ratio of the morphometric assessment of villous height to crypt depth.
(**E**) Serum anti-DGP IgG levels were measured by ELISA. Sera were collected on day 56 (immediately preceding gluten rechallenge) and day 74 (at the end of gluten rechallenge with anti-IL-15 or isotype treatment).
(**F**) Serum anti-gliadin IgG2c levels were measured by ELISA as in (E).
(**G**) Expression of *IFN-*γ in the lamina propria was measured by qPCR. Relative expression levels were normalized to the gluten-fed group for each independent experiment.
(**H**) Quantification of intraepithelial lymphocytes (IELs) among intraepithelial cells (IECs) was performed on H&E stained ileum sections.
(**I-J**) The intestinal epithelium was isolated and analyzed by flow cytometry. IELs were identified as TCRβ^+ CD4$^-$ CD8$\alpha\beta^+$ cells. NKG2D$^+$ NKG2$^-$ IELs (I) and granzyme B$^+$ IELs (J) are indicated by absolute number / 100 IECs.
(**K-L**) Expression of (K) *Prf1* and (L) *Rae1* in the intestinal epithelium was measured by qPCR. Relative expression levels were normalized against the expression levels observed in gluten-fed DQ8-IL-15^{LPxIEC} mice.
[(D) to (L)] Data represent three independent experiments. Error bars, SEM. *P < 0.05, **P < 0.01, ***P < 0.001, unpaired Student's *t*-test.

2.4 Discussion

Our study presents the first pathophysiological mouse model of CeD in which the ingestion of gluten in an immunocompetent host, in the absence of immunization with an adjuvant, promotes small intestinal VA in a gluten- and HLA-DQ8- dependent manner as seen in active CeD patients.

CeD provides a unique opportunity to study the pathogenesis of human autoimmune disorders, because the disease-predisposing HLA and the antigen are known, the antigen delivery can be controlled, and the tissue targeted by the immune processes is relatively easy to access. Studies in human and mice prompted us several years ago to propose a model of pathogenesis (Jabri and Sollid, 2006; Jabri and Sollid, 2017) in which IL-15 played a critical role (Jabri and Abadie et al., 2015; Meresse et al., 2012). The present study unambiguously confirms the role played by IL-15 in CeD pathogenesis, and demonstrates that IL-15 overexpression needs to take place in both the IECs and the Lp, where it activates distinct innate and adaptive immune pathways, in order for VA to develop. In addition, our study establishes that IL-15 also plays a role in the reactivation of the inflammatory anti-gluten immune response and the destruction of IECs upon gluten challenge, suggesting that it could be a therapeutic target in patients with established CeD and IL-15 overexpression. Furthermore, our findings demonstrate that $CD8^+$ CTLs are the critical effector cell type mediating small intestinal IECs destruction, but have no role in adaptive anti-gluten $CD4^+$ immunity.

HLA-DQ2 or HLA-DQ8-restricted gluten-reactive $CD4^+$ T cells are found in the intestinal mucosa of CeD patients but not healthy controls (Molberg et al., 1997). However,

studies both in humans and mice indicate that $CD4^+$ T cell immune responses are not sufficient to promote tissue destruction in CeD (Setty et al., 2015; de Kauwe et al., 2009; Marrieta et al., 2004; DePaolo et al., 2011). Our study provides a mechanistic basis for this observation by demonstrating that adaptive anti-gluten T cell immunity is critical for the expansion of IE-CTLs with a fully activated killer phenotype and development of VA. In addition, anti-DGP and more generally anti-gluten antibody responses are abrogated in the absence of $CD4^+$ T cells, supporting the view that the generation of these antibodies requires T cell help (Spencer and Sollid, 2016).

Interestingly, VA developed in most (around 75%), but not all, gluten-fed DQ8-IL-15^{LPxIEC} mice, and only when gluten, HLA-DQ8 and IL-15 were all present and work in concert. These observations are in line with the notion emerging from genome wide association studies (Withoff et al., 2016), that complex immune disorders like CeD do not develop from the functional defect of a single gene, but rather from the cumulative effect of small changes in gene expression across many immune-relevant genes. The finding that HLA-DQ8 is dispensable for loss of oral tolerance to gluten but not for VA emphasizes the concept that coeliac susceptible HLA molecules may be implicated in the development of VA through its role in the amplification of gluten-induced inflammatory immunity (Hovhannisyan et al., 2008; Sollid et al., 2012). This is in keeping with the concept that the magnitude of the immune response plays a role in CeD pathogenesis, as attested by the gene dosage effect observed for HLA allotypes in CeD (Ploski et al., 1993; Karell et al., 1993). Differences in the transcriptional signatures between gluten-fed DQ8, IL-15^{LPxIEC} and DQ8-IL-15^{LPxIEC} mice also indicate that gluten, HLA-DQ8 and IL-15

cooperate to enhance pathways associated with T cell immunity and adaptive immune responses. Altogether, our study suggests that IL-15 in the Lp, IL-15 in IECs, $CD4^+$ T cells, CTLs, HLA-DQ8, and gluten all regulate particular aspects of CeD immunopathology and epithelial distress that work in partnership to promote VA (**Extended data Fig. 2.9**). This reflects the complexity of the disease and underlines how CeD develops as a result of an interdependent interplay between multiple immune pathways that culminates in tissue destruction. It also may explain the wide spectrum of intestinal damage that CeD can present with (Marsh, 1992).

In summary, the DQ8-IL-15^{LPxIEC} mouse model recapitulates the key immunological and transcriptional aspects of CeD and therefore offers a unique opportunity for preclinical validation of novel therapeutic strategies. Specifically, because the development of VA in mice is HLA-DQ8 and gluten dependent, it will open the door for testing therapeutic strategies targeting not only the adaptive anti-gluten immune response but also other components vital to the tissue injury. This model will also allow to functionally assess the role of TG2 (Klöck et al., 2012) and B cells (Sollid and Jabri, 2013) in CeD pathogenesis and to determine whether they are valuable therapeutic targets. Ultimately, this preclinical mouse model of CeD provides a unique and vital tool for the development and implementation of new therapeutic strategies for CeD.

2.5 Methods

2.5.1 Mice

Mice used in these studies are on the C57BL/6 background. Mice were maintained under specific pathogen-free conditions at the University of Chicago and at the Sainte-Justine University Hospital Research Center. Importantly, no differences in the outcome of the experiments were observed between the two institutions, enabling to pool the data. HLA-DQ8 transgenic mice (DQ8) and DQ8-D^d-IL-15tg mice expressing IL-15 under the minimal MHC class I D^d promoter (named DQ8-IL-15^{LP} in the present study) were previously described (DePaolo et al., 2011). Villin-IL-15^{IEL} mice expressing IL-15 under the intestine-specific villin promoter of IECs (Meisel et al., 2017) were crossed to HLA-DQ8 mice. IL-15^{LP} mice were then crossed onto DQ8-IL-15^{IEC} mice to obtain the first generation DQ8-IL-15^{LPxIEC} mice. Next generations were obtained by backcrossing DQ8-IL-15^{LPxIEC} mice with DQ8-villin-IL-15^{IEL} mice. Finally, DQ8-IL-15^{LPxIEC} mice were crossed to IL-15^{LP} or IL-15^{IEC} mice to obtain IL-15^{LPxIEC} mice. All mice expressing HLA-DQ8 also express I-A^b MHC class II molecules. All strains were maintained on a gluten-free chow (AIN76A, Envigo). For all experiments, mice were used at 10 weeks of age. All experiments were performed in accordance with the Institutional Biosafety Committee and the Institutional Care and Use Committee of the University of Chicago, and with the Canadian Council on Animal Care guidelines and the Institutional Committee for Animal Care in Research of the Sainte-Justine University Hospital Research Center.

2.5.2 Antibodies and flow cytometry

The following conjugated antibodies were purchased from eBioscience: TCRβ APC (H57-597), CD8α APC-eFluor 780 (53-6.7), CD8β PE-Cy5 (eBioH35-17.2), CD314 (NKG2D) PE (CX5), NKG2AB6 PE (16a11), CD94 FITC (18d3). The following antibodies were purchased from BD Biosciences: CD4 PE-Cy7 (GK1.5), CD103 APC (M290), NKG2A/C/E FITC (20d5), CD3 FITC (17A2) CD16/CD32 (Fc Block) (2.4G2). HLA-DQ8 PE (HLADQ81), and CD11c BV421 (N418) were purchased from Biolegend. Granzyme B PE (GB12), I-A^b FITC (M5/114.15.2), and LIVE/DEAD™ Fixable Violet Dead Cell Stain Kit were purchased from Thermo Fisher Scientific. Flow cytometry was performed with a BD LSRFortessa II cell analyzer (BD Biosciences) and data were analyzed using FlowJo software (Treestar).

2.5.3 Epithelial, lamina propria, and mesenteric lymph nodes cells isolation

Epithelial cells including IELs and LP cells were isolated as previously described (Lefrançois and Lycke, 2001) using EDTA containing calcium-free media and collagenase VIII, respectively. For the analysis of the NK receptors by flow cytometry, cytotoxic molecules on IELs by flow cytometry and qPCR, and for the analysis of IFN-□ on LP cells, a cell purification step using a 40% Percoll (GE Healthcare) was used to enrich lymphocyte cell populations. Briefly, 1X PBS-washed epithelial and LP cells were resuspended in 10ml 40% Percoll solution then centrifuged for 30 minutes at 3000 x g. After removal of the supernatant, cells were washed in 1X PBS and counted. Mesenteric

lymph nodes were dissected, and made into a single cell suspension by mechanical disruption and passed through a 70μm nylon cell strainer (Corning).

2.5.4 Gluten feeding and depletions

To study the response to dietary gluten, mice were transferred from a GFD to a standard rodent chow at the beginning of each experiment and allowed to consume the gluten-containing chow *ad libitum*. Additionally, supplemental gluten (20mg crude gliadin (Sigma-Aldrich) or 100μg peptic-tryptic digests of gliadin) was administered via intragastric gavage, every other day for thirty or sixty days, using a 22-gauge round-tipped needle (Cadence Science). To study the impact of reversion to a GFD, mice were fed with gluten for thirty days, then placed on a GFD for thirty days.

In some experiments, DQ8-IL-15^{LPxIEC} mice were injected i.p. before initiation of gluten feeding and every 4-5 days at the time of feeding and continuing until termination with 200μg or 400μg of anti-CD4 (GK1.5, rat IgG2b), or 200μg anti-CD8α (2.43.1, rat IgG2b) or isotype controls obtained from the Antibody Technology Core Facility at the University of Chicago. IL-15 treatment was performed with 20μg of anti-mouse IL-15 antibody (M96, Amgen, mouse IgG2a) administered i.p. once a week before and during feeding.

2.5.5 Preparation of chymotrypsin-digested gliadin (CT-gliadin), peptic-tryptic digests of gliadin (PT-gliadin) and deamidated gliadin peptides (DGP)

CT-gliadin was prepared as previously described (Bouziat et al., 2017). To obtain DGP, CT-gliadin was dissolved in a 10mM $CaCl_2$ solution containing Guinea pig

liver transglutaminase (Zedira) and incubated overnight at 37°C with continuous shaking. Concentration of DGP was calculated based on the concentration of the CT-glia and the volume added during deamidation. To obtain PT-gliadin, gliadin was digested in 0.2 N HCl (pH 1.8) with pepsin (Sigma) for 2h at 37°C. Once the pH adjusted to 8.0, the digest was incubated with purified trypsin for 4h at 37°C, and thereafter with cotazym (lipase from porcine pancreas Type II, Sigma) for 2h under constant stirring. Concentration of PT-gliadin was determined using a BCA assay (Pierce).

2.5.6 Anti-TG2, anti-gluten and anti DGP ELISA

Serum was harvested thirty or sixty days after mice received the first gliadin feeding. For anti-gluten IgG2c, IgG and IgA ELISA, high-binding ELISA 96-well plates (Nunc, Thermo-Scientific) were coated with 50 µl of 100 µg/ml CT-gliadin in 100 mM Na_2HPO_4 overnight at 4 °C. Plates were washed three times with PBS containing 0.05% Tween-20 (PBS-T) and blocked with 200 µl of 2% BSA in PBS-T for 2 hours at room temperature. Serum was assessed in duplicate and at two dilutions, typically 1/50 and 1/200. Sera were incubated overnight at 4 °C and plates were washed three times with PBS-T. Specific anti-mouse Ig-horseradish peroxidase (HRP) (Southern Biotech) in blocking buffer was added to plates and incubated for 1 hour at room temperature. Plates were washed five times with PBS-T. 50 µl HRP substrate TMB (Thermo-Scientific) was added and the reaction stopped by the addition of 50 µl 2N H_2SO_4 (Fluka Analytical). Absorbance was read at 450 nm on Molecular Devices Versamax tunable microplate reader. For anti-DGP IgG ELISA, deamidated PTD gliadin was coated onto Immulon-2

HB ELISA plates (Thermo Scientific) at a concentration of 100μg/ml in 0.1M Na2HPO4 (Sigma Aldrich) and incubated overnight at 4C. Blocking buffer of 4% BSA/0.05% tween/1X PBS was used, and sera diluted at 1/200 with diluent of 0.1%BSA/0.05%tween/1XPBS. Biotinylated anti-mouse IgG and streptavidin-HRP (Both Jackson Immunoresearch) were used as the detection reagents. TMB (Sigma Aldrich) was used as the substrate. Plates were then read at 450nm. Levels of anti-DGP IgG and anti-gliadin IgG, IgG2c, IgA were expressed in OD values.

2.5.7 Histology

Hematoxylin & Eosin staining was performed on 5μM thick sections of 10% formalin-fixed paraffin-embedded ileum. Slides were analyzed using a Leica DM 2500 microscope with a HC PLAN APO 20x/0.7 NA and a HCX PL APO 100x/1.40-0.70 objective or a Leica DMi8 microscope with a HC PL FLUOTAR L 20x/0.40 and a HC PL APO 40x/0.75 objective and equipped with the image processing and analysis software LasX (Leica). The villus height/crypt depth ratios were obtained from morphometric measurements of five well-orientated villi. The villous to crypt ratio was calculated by dividing the villous height by the corresponding crypt depth. Villus height was measured from the tip to the shoulder of the villus or up to the top of the crypt of Lieberkuhn. The crypt depth was measured as the distance from the top of the crypt of Lieberkuhn to the deepest level of the crypt. The intra-epithelial lymphocyte count was assessed by counting the amount of intra-epithelial lymphocytes among at least 100 enterocytes. Additional 5μm sections were processed for immunohistochemical detection of Granzyme

B. Slides were deparaffinized, rehydrated, and washed in 1X PBS. Sections were incubated in Citrate buffer (1 M pH 6.0) for 20 min at 68 °C. Then the sections were permeabilized with 0.3% Triton X-100 at room temperature for 30 minutes. Endogenous peroxidase activity was quenched for 15 minutes with 2% hydrogen peroxide in PBS. Sections were blocked with normal donkey serum (Vector Laboratories) for 1 hour and incubated with polyclonal Goat IgG anti-mouse Granzyme B (R&D Systems) for 2 hours at room temperature. Sections were then washed in PBS, incubated with biotinylated anti-goat IgG (Vector Laboratories) for 1 hour at room temperature, and stained using the avidin-biotin complex method (Vectastain ABC kit; Vector Laboratories). Color was developed using 3,3'-diaminobenzidine (Dako Diagnostics) containing hydrogen peroxide. Slides were counterstained with Harris modified hematoxylin, dehydrated, cleared, mounted, and examined under light microscopy as described above.

2.5.8 Immunohistochemistry

Mice were euthanized and intestines were resected. Distal ileum pieces were snap-frozen in optimum cutting temperature (OCT) compound (Tissue-Tek) submerged in isopentane cooled with liquid nitrogen. Frozen tissues were cryosectioned (5 μm thickness) and sections were fixed for ten minutes in acetone. Slides were sequentially rehydrated for 10 minutes in 1X PBS, treated for 30 minutes at room temperature with 1X PBS containing 3% bovine serum albumin (BSA), and incubated for 1 hour at room temperature with Alexa Fluor 594 anti-mouse CD3 (17A2, rat IgG2b, Biolegend), purified anti-mouse CD138 (281-2, rat IgG2a, BD Biosciences), anti-mouse IgA-biotin (goat IgG,

Southern Biotech), or anti-transglutaminase 2 (rabbit polyclonal, produced by Pacific Immunology as described before (Plugis and Khosla, 2015) diluted in 1X PBS containing 1% BSA. After three washes in PBS, slides were then incubated for 1 hour at room temperature with secondary antibody goat anti-rat IgG Alexa Fluor 488, goat anti-rat IgG Alexa Fluor 633, Alexa Fluor 594 streptavidin, or goat anti-rabbit Alexa Fluor 488 (Molecular Probes). For IgA staining, slides were blocked for 1 hour at room temperature in Tris-buffered saline (TBS) containing 0.05% Tween 20 (TBS-T) and 3% BSA, and the antibodies were diluted in TBS-T containing 1% BSA. After three washes in PBS, slides were mounted with Fluoromount-G containing DAPI (Southern Biotech).

2.5.9 RNA extraction, cDNA synthesis, and quantitative real-time PCR

Total RNA isolation was performed on epithelial and LP cells using the RNeasy Mini Kit (Qiagen). RNA concentration and quality were determined by UV spectrophotometry (Epoch Microplate Spectrophotometer, BioTek). cDNA synthesis was performed using qScript cDNA SuperMix (QuantaBio) according to the manufacturer's instructions. Expression analysis was performed in technical duplicate via quantitative real-time PCR on an Applied Biosystems® StepOne™ Real-Time PCR Systems (Applied Biosystems) with a Power SYBR Green Master Mix (Thermo Fisher Scientific). Expression levels were quantified and normalized to Gapdh expression using the following murine primer pairs:

Gapdh: 5'-AGGTCGGTGTGAACGGATTTG-3', 5'-TGTAGACCATGTAGTTGAGGTCA-3'

Ifng:5'-ATGAACGCTACACACTGCATC-3', 3'-TCTAGGCTTTCAATGACTGTGC-5'

Qa1: 5'- AACACACGGAGAGTCAAGGG-3', 3'-ATCAAGGCCATCATAGGCGAA-5'. Expression analysis for murine GzmB, Prf1 and Rae1 was performed with TaqMan gene expression assays and normalized to Gapdh (Thermo Fisher Scientific). Relative gene expression levels were determined using the delta–delta Ct method.

2.5.10 Gene expression microarray

RNA from mouse samples was obtained as described above, quantified spectrophotometrically, and the quality was assessed with the Agilent 2100 Bioanalyzer (Agilent Technologies). Only samples with no evidence for RNA degradation (RNA integrity number >8) were kept for further experiments. Genome-wide gene expression profiling of the epithelium and Lp of five individual DQ8, DQ8-IL-15^{LPxIEC}, and IL-15^{LPxIEC} mice were determined by using the MouseWG-6 v2.0 Expression BeadChips from Illumina. Low-level microarray analyses were performed in R, using the Bioconductor software package lumi (De et al., 2008). We first applied a variance stabilizing transformation to all arrays (Lin et al., 2008) and then quantile normalized the data. After normalization, we removed probes with intensities indistinguishable from background noise (as measured by the negative controls present on each array).

2.5.11 Identifying genes differentially expressed between mouse strains.

To identify genes differently expressed between the different strains of mice, we used a linear modeling-based approach. Specifically, we used the Bioconductor limma package (Smyth, 2004) to fit, for each gene, a linear model with individual treatment (i.e.,

gluten feeding), and mice strains as fixed effects. For each gene, we subsequently used the empirical Bayes approach of Smyth (Smyth, 2004) to calculate a moderated t statistic and P value. We corrected for multiple testing using the false discovery rate (FDR) approach of Benjamini and Hochberg (Benjamini and Hochberg, 1995).

2.5.12 Patients

One duodenal biopsy was obtained from ninety-six individuals undergoing upper gastrointestinal endoscopy during diagnostic work-up at the University of Chicago Medicine and at Mayo Clinic, including forty-five non-celiac controls and fifthy-one untreated CeD patients (active CeD) for subsequent RNA-sequencing. Control subjects included 29 females and 16 males and underwent upper gastrointestinal endoscopy during a diagnostic work-up for anemia, failure to thrive or other intestinal disorders not associated with CeD. All controls had normal small intestinal histology, no family history of CeD, no significant levels of anti-TG2 IgA antibodies in the serum. Active CeD patients included 31 females and 20 males, all had positive anti-TG2 antibodies and small intestinal enteropathy with increased infiltration of IELs, crypts hyperplasia and villous atrophy, according to currently accepted diagnostic guidelines (Husby et al., 2012). Each subject signed an informed consent as provided by the Institutional Review Board of each institution (IRB-12623B for the University of Chicago and IRB-1491-03 for Mayo Clinic).

2.5.13 RNA-sequencing on gut biopsies from control and coeliac disease patients

A single duodenal bioptic fragment was directly submerged in RNA-later (QIAGEN), kept at 4°C for 24 hours and then frozen at -80°C upon RNA later removal until processing. Defrost tissues were homogenized using magnetic beads and a Cell Tissue Homogenizer (Bullet blender by *Next Advance*) and RNA was extracted using RNeasy columns (QIAGEN). RNA integrity was assessed by Bioanalyzer (Agilent). All included samples showed RNA integrity number (RIN) above 8. RNA-sequencing libraries were prepared using the SMARTer® Stranded Total RNA Sample Prep Kit-HI Mammalian by Clontech Laboratories (Takara), according to manufacturer's instructions. Libraries quality was checked by Bioanalyzer (Agilent) prior to pooling and sequencing. Indexed cDNA libraries were pooled in equimolar amounts and sequenced with single-end 50bp reads with a high output Flow Cell (8 lane flow cell) on an Illumina HiSeq4000 at the University of Chicago Genomic Facility.

Adaptor sequences and low quality score bases (Phred score < 20) were first trimmed using Trim Galore (version 0.2.7). The resulting reads were then mapped to the human genome reference sequence (Ensembl GRCh37 release 75) using Kallisto v0.43.0 (Bray et al., 2016) with a GRch38 transcript annotation GTF file downloaded from Ensembl rel 87. Gene expression was normalized across samples using the weighted trimmed mean of M-values algorithm (TMM), as implemented in the R package edgeR (Robinson et al., 2010). After normalization, we log-transformed the data using the voom function in the limma package (Ritchie et al., 2015). For all downstream analyses, we excluded non-coding and lowly expressed genes with a median read count lower than 20

in all samples. Following this pre-processing of the data, we fitted the log-transformed expression estimates to linear models using the lmFit function from the limma package (Ritchie et al., 2015) to look at differences in gene expression between control and celiac disease patients, while taking into account variation in sex and age of the donors. Gene ontology enrichment analysis were performed in Gorilla (Eden et al., 2009). We corrected for multiple testing using the FDR approach of Benjamini and Hochberg (Benjamini and Hochberg, 1995).

2.5.14 Statistical Analysis.

Tests were performed as indicated in figure legends using GraphPad Prism. Data are presented as mean ± SEM. The statistical test used and p values are indicated in each figure legend. P values of < 0.05 were considered to be statistically significant. *P $<$ 0.05, **P < 0.01, ***P < 0.001 and ****P < 0.0001. ns = non-significant.

2.6 Acknowledgments

We thank patients with coeliac disease and their family members, as well as the University of Chicago Celiac Disease Center, for supporting our research. We thank Charlotte Zaouter from BZ-Histo Services Inc. (Montreal, Quebec, Canada) for her technical assistance with the histological processing of intestinal samples. We also thank the Human Tissue Resource Center and the Integrated Light Microscopy Core Facility at the University of Chicago. This work was supported by grants from NIH: R01 DK67180 and

R01 DK63158, and Digestive Diseases Research Core Center P30 DK42086 at the University of Chicago as well as by funding from F. Oliver Nicklin associated with the First Analysis Institute of Integrative Studies and the Regenstein Foundation to B.J., from the CIHR (catalyst grant in environments, genes, and chronic disease) to V.A. and L.B.B., the SickKids Foundation (NI15-040) and the Canadian Celiac Association to V.A., from NIH: R01 DK063158 and R01 DK100619 to C.K., award from the Wallonie-Bruxelles International-World Excellence and from FRQNT to T.L. The “Carlino fellowship for celiac disease research” from the University of Chicago Celiac Disease Center supported V.D.

2.7 Author contributions

V.A. and B.J. designed the research and supervised all investigations. S.M.K, T.L. J.D.E., B.A.P., C.C., R.B., M.A.Z., A.D., V.Y. and V.A. performed experiments and analyzed the data. V.D. and I.L. performed the human RNA-seq. experiment. E.V.M. and I.H. undertook serology experiments. O.T., J.C.G., and L.B.B. performed the computational analysis. C.K., J.A.M. and L.B.B. provided intellectual input and technical support. S.M.K, V.A. and B.J. wrote the manuscript. All authors provided critical review of the manuscript.

2.8 Competing interests

The authors declare no competing financial interests. B.J. and J.A.M. have been consultants to Celimmune and Bionix. Correspondence and requests for materials should be addressed to V.A. (valerie.abadie@umontreal.ca) and B.J. (bjabri@bsd.uchicago.edu).

2.9 Extended Data Figures

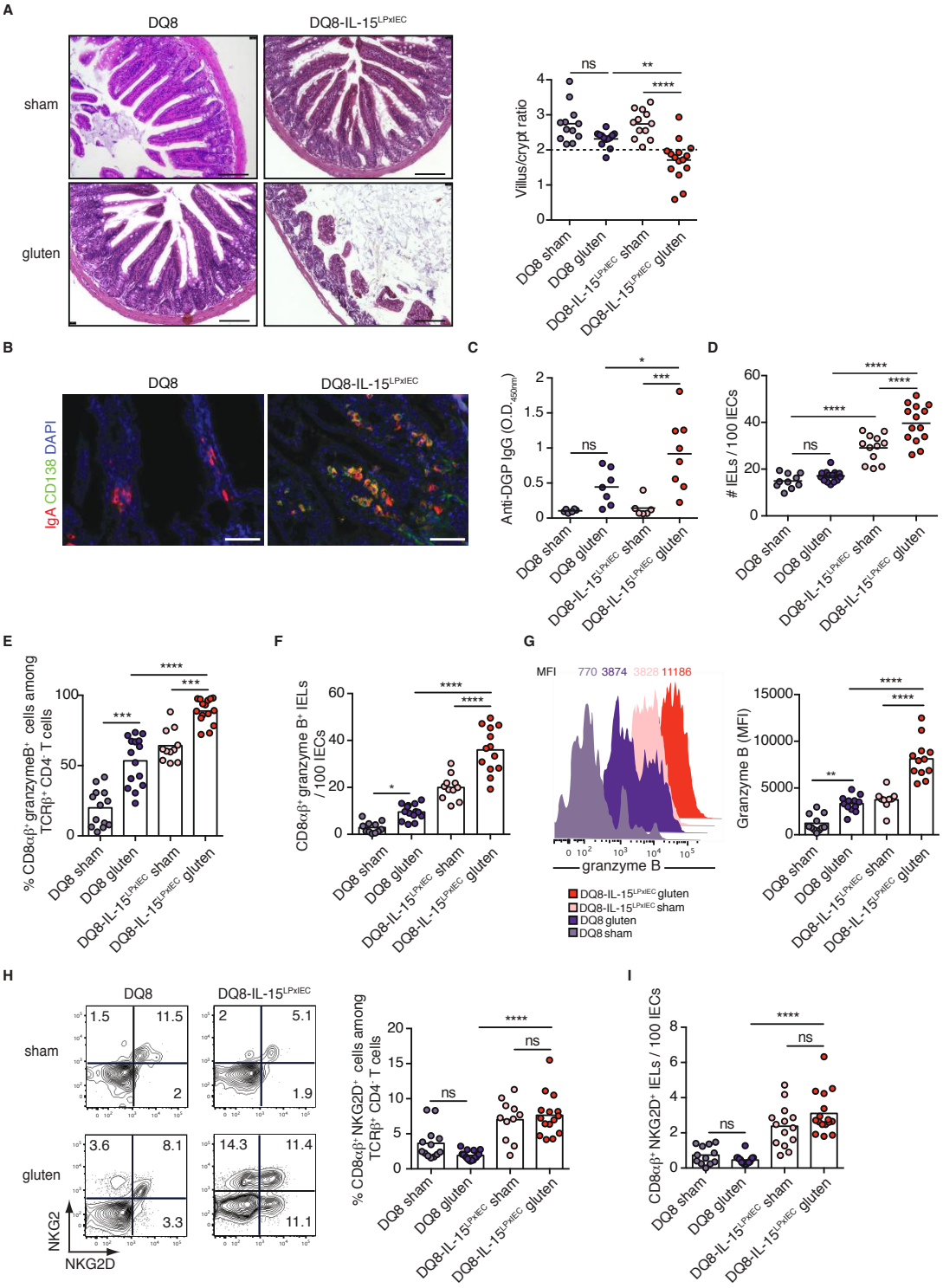

Extended Data Figure 2.1. Overexpression of IL-15 in HLA-humanized DQ8 mice confers susceptibility to development of coeliac disease-like features in a gluten-dependent manner.

Extended Data Figure 2.1., continued.
(A-I) Ten-week old DQ8 and DQ8-IL-15^{LPxIEC} mice that were raised on a GFD were maintained on a GFD (sham) or fed with gluten for 30 days (gluten).
(A) H&E staining of paraffin-embedded ileum sections. The graph depicts the ratio of the morphometric assessment of villous height to crypt depth. Scale bar, 100 μm.
(B) IgA (red) and CD138^{+} plasma cells (green) were distinguished by immunohistochemistry (IHC) staining of frozen ileum sections.
(C) Serum anti-deamidated gliadin peptides (DGP) IgG levels as measured by ELISA. Sera were collected thirty days after gluten feeding.
(D) Quantification of intraepithelial lymphocytes (IELs) among intraepithelial cells (IECs) was performed on H&E stained ileum sections.
(E-I) The intestinal epithelium was isolated and analyzed by flow cytometry. IELs were identified as TCRβ^{+} CD4^{-} CD8$\alpha\beta^{+}$ cells. Granzyme B^{+} IELs are indicated by (E) percentage, (F) absolute number / 100 IECs, and (G) MFI. NKG2D^{+} NKG2^{-} IELs are indicated by (H) percentage and (I) absolute number / 100 IECs.
Data are representative of two [(C)] and four independent experiments [(A), (D), (E), (F), (G), (H), (I)]. *P < 0.05, **P < 0.01, ***P < 0.001, ****P < 0.0001; One-way ANOVA / Tukey's multiple comparison.

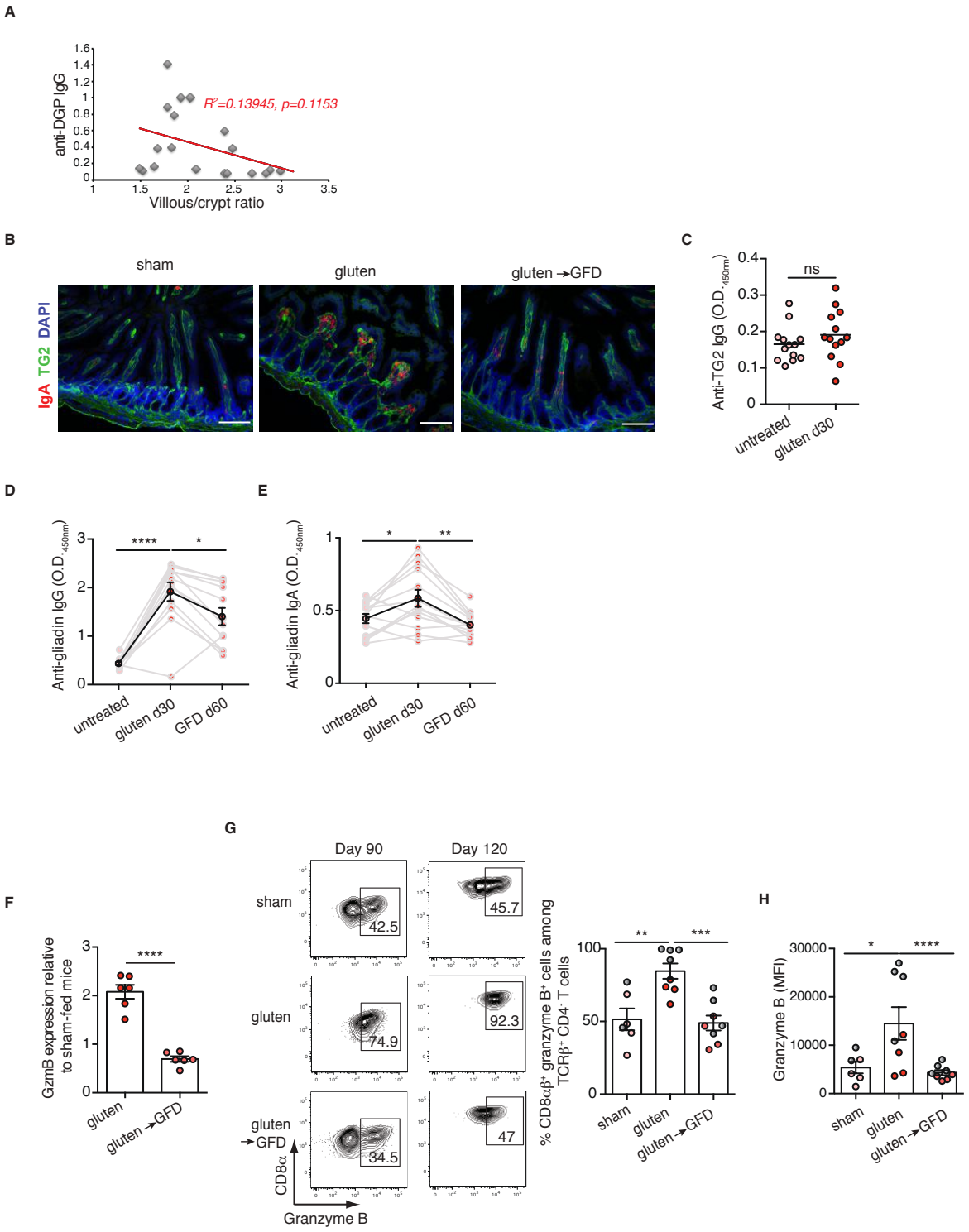

Extended Data Figure 2.2. A gluten-free diet decreases the anti-gluten antibody response and the levels of cytotoxic intraepithelial lymphocytes.

Extended Data Figure 2.2., continued.
(A-E) Ten-week old DQ8-IL-15^{LPxIEC} mice that were raised on a gluten-free diet (GFD) were maintained on a GFD (denoted "sham"), fed with gluten for 30 days ("gluten"), or fed with gluten for 30 days and then reverted to a GFD ("gluten→GFD") for 30 days.
(A) Correlation between the degree of villous atrophy and the levels of anti-DGP antibodies in sham and gluten-fed DQ8-IL-15^{LPxIEC} mice.
(B) Mucosal IgA deposits (red) and transglutaminase 2 (TG2, green) were identified by immunohistochemistry (IHC) staining of frozen ileum sections.
(C) Serum anti-TG2 IgG antibodies levels measured by ELISA thirty days after gluten feeding.
(D, E) Serum anti-gliadin (C) IgG and (D) IgA levels were measured by ELISA. Sera were collected sequentially in the same mice before gluten feeding (untreated), thirty days after gluten feeding (gluten d30), and thirty days after reversion to a GFD (GFD d60). The black line represents the average for each of the groups.
(F) Expression of *GzmB* in the intestinal epithelium was measured by qPCR. Relative expression levels in gluten and gluten→GFD groups were normalized against the expression levels observed in sham-fed DQ8-IL-15^{LPxIEC} mice.
(G, H) Ten-week old DQ8-IL-15^{LPxIEC} mice that were raised on a gluten-free diet (GFD) were maintained on a GFD (denoted "sham"), fed with gluten for 30 days ("gluten"), or fed with gluten for 30 days and then reverted to a GFD ("gluten→GFD") for 60 (day 90) or 90 days (day 120). The intestinal epithelium was isolated and analyzed by flow cytometry. IELs were identified as TCRβ^+ CD4$^-$ CD8$\alpha\beta^+$ cells. Granzyme B$^+$ IELs are indicated by (F) percentage and (G) MFI.
Data represent four [(B) to (D)] or two [(E), (F) and (G)] independent experiments. Error bars, SEM. *$P < 0.05$, **$P < 0.01$, ***$P < 0.001$, ****$P < 0.0001$; RM One-way ANOVA / Tukey's multiple comparison [(C), (D), (F) and (G)], unpaired Student's *t*-test [(E)].

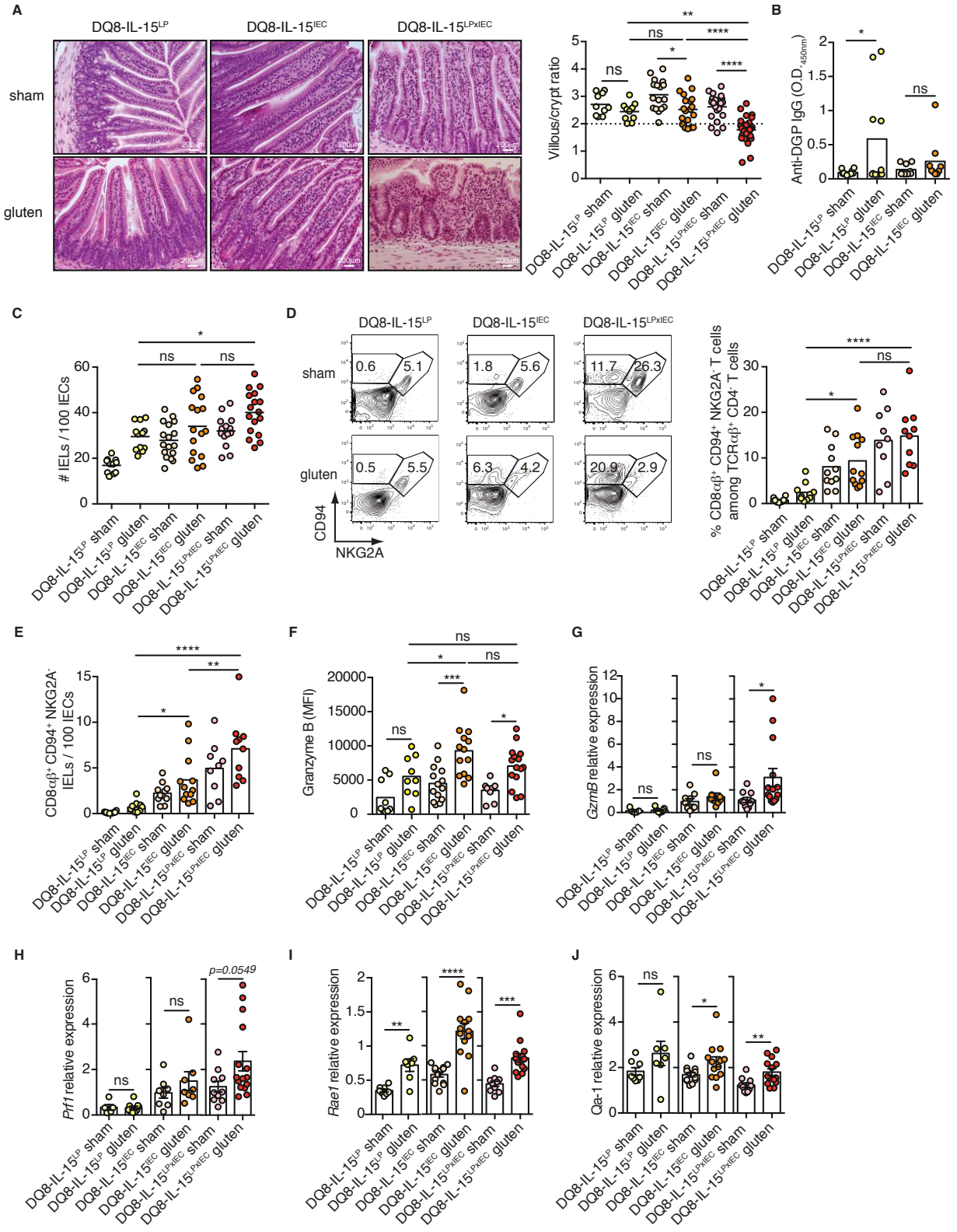

Extended Data Figure 2.3. IL-15 expression in both the lamina propria and epithelium confers IELs with a cytotoxic phenotype and the ability to kill epithelial cells.

Extended Data Figure 2.3., continued.
(A-J) Ten-week old DQ8-IL-15^{LP}, DQ8-IL-15^{IEC}, and DQ8-IL-15^{LPxIEC} mice that were raised on a GFD were maintained on a GFD (sham) or fed with gluten for 30 days (gluten).
(A) H&E staining of paraffin-embedded ileum sections. The graph depicts the ratio of the morphometric assessment of villous height to crypt depth.
(B) Serum anti-deamidated gliadin peptides (DGP) IgG levels were measured by ELISA in (A) DQ8-IL-15^{LP} and (B) DQ8-IL-15^{IEC} mice. Sera were collected thirty days after gluten feeding.
(C) Quantification of intraepithelial lymphocytes (IELs) among intraepithelial cells (IECs) was performed on H&E stained ileum sections.
(D-F) The intestinal epithelium was isolated and analyzed by flow cytometry. IELs were identified as TCRβ^+ CD4$^-$ CD8$\alpha\beta^+$ cells. CD94$^+$NKG2A$^-$ IELs are indicated by (D) percentage and (E) absolute number / 100 IECs. Intracellular granzyme B mean fluorescence intensity (MFI) was measured (F).
(G-J) Expression of (G) *GzmB*, (H) *Prf1*, (I) *Rae1,* and (J) *Qa-1* in the intestinal epithelium was measured by qPCR. Relative expression levels in sham and gluten-fed mice for each strain are shown.
Data are representative of at least three independent experiments. *P < 0.05, **P < 0.01, ***P < 0.001, ****P < 0.0001; One-way ANOVA / Tukey's multiple comparison [(A), (C), (D), (E), (F) unpaired Student's *t*-test [(B), (G), (H), (I) and (J)].

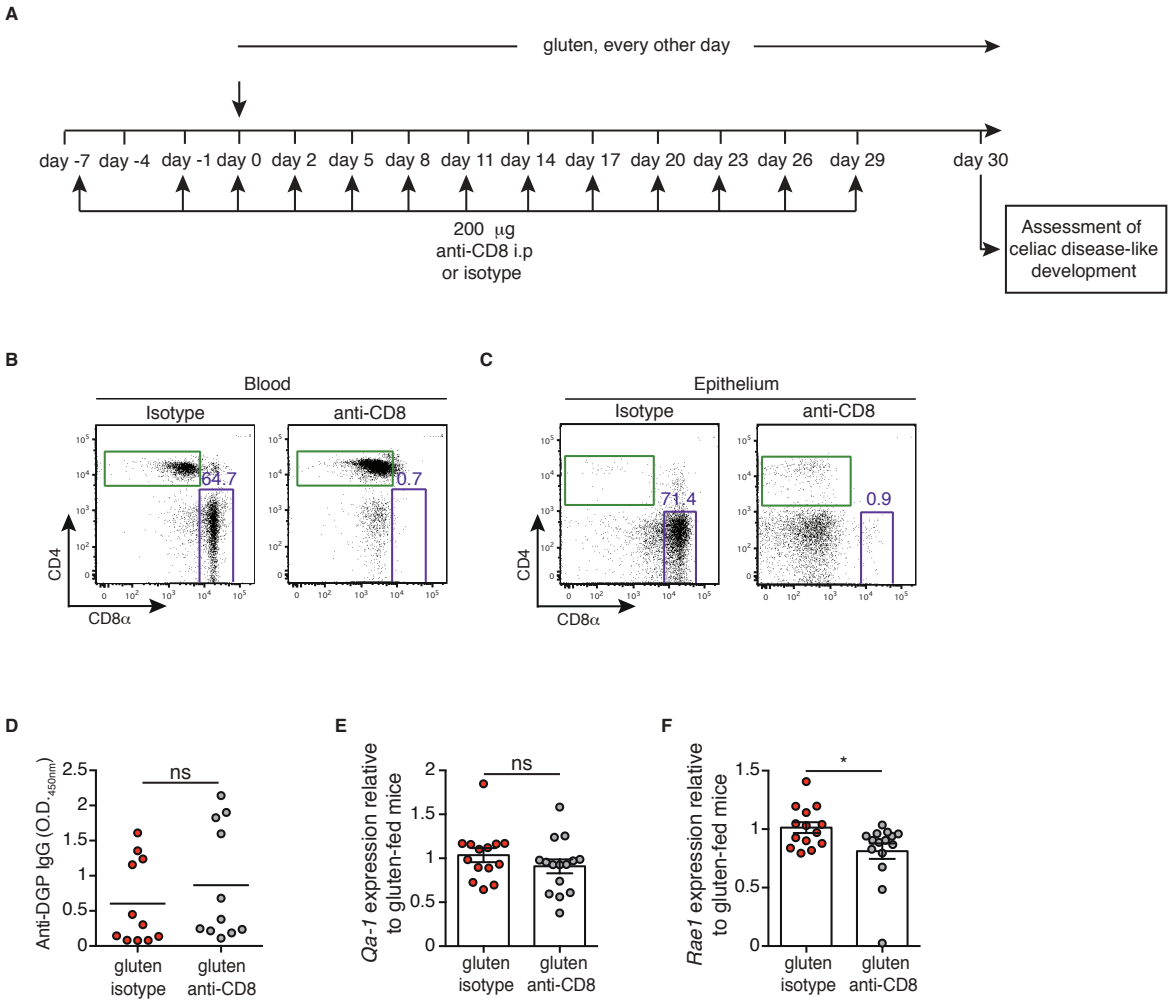

Extended Data Figure 2.4. Effect of IELs depletion on antibodies production and epithelial stress markers.

(**A-F**) Ten-week old DQ8-IL-15^{LPxIEC} mice were treated with 200 or 400 µg of depleting anti-CD8α antibody (clone 2.43) or its isotype control (rat IgG2b) twice prior to and during the course of gluten.

(**A**) Experimental scheme.

(**B, C**) Representative dot-plots showing depletion efficiency in the (B) blood and (C) epithelium of DQ8-IL-15^{LPxIEC} mice after 30 days of anti-CD8α treatment.

(D) Anti-deamidated gluten peptides (DGP) IgG levels from serum collected thirty days after gluten feeding.

(E, F) *Qa-1* (E) and *Rae1* (F) gene expression in the intestinal epithelium was determined by qPCR. Relative expression levels were normalized against the expression levels observed in gluten-fed DQ8-IL-15^{LPxIEC} mice.

Data represent four independent experiments. *P < 0.05; unpaired Student's *t*-test

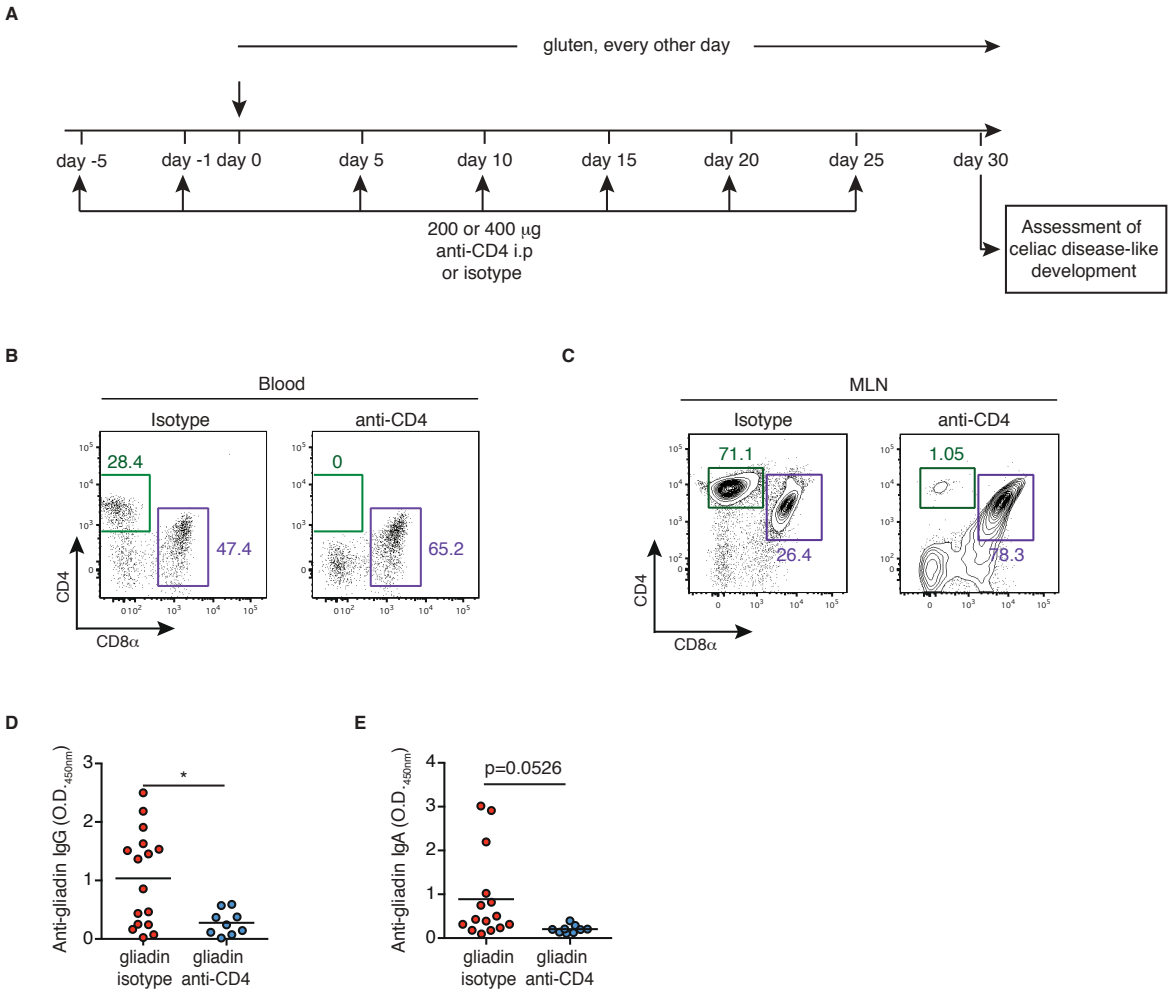

Extended Data Figure 2.5. Anti-gliadin antibody titers are decreased in CD4-depleted DQ8-IL-15^{LPxIEC} mice.

(**A-E**) Ten-week old DQ8-IL-15^{LPxIEC} mice were treated with 200 or 400 μg of depleting anti-CD4 antibody (clone GK1.5) or its isotype control (rat IgG2b) twice prior to and during the course of gluten feeding.

(**A**) Experimental scheme.

(**B, C**) Representative dot-plots showing depletion efficiency in the (B) blood and (C) mesenteric lymph nodes (MLN) of DQ8-IL-15^{LPxIEC} mice.

(**D, E**) Anti-gliadin (D) IgG and (E) IgA levels were measured by ELISA from serum collected thirty days after gluten feeding.

Data represent four independent experiments. *P < 0.05; unpaired Student's *t*-test.

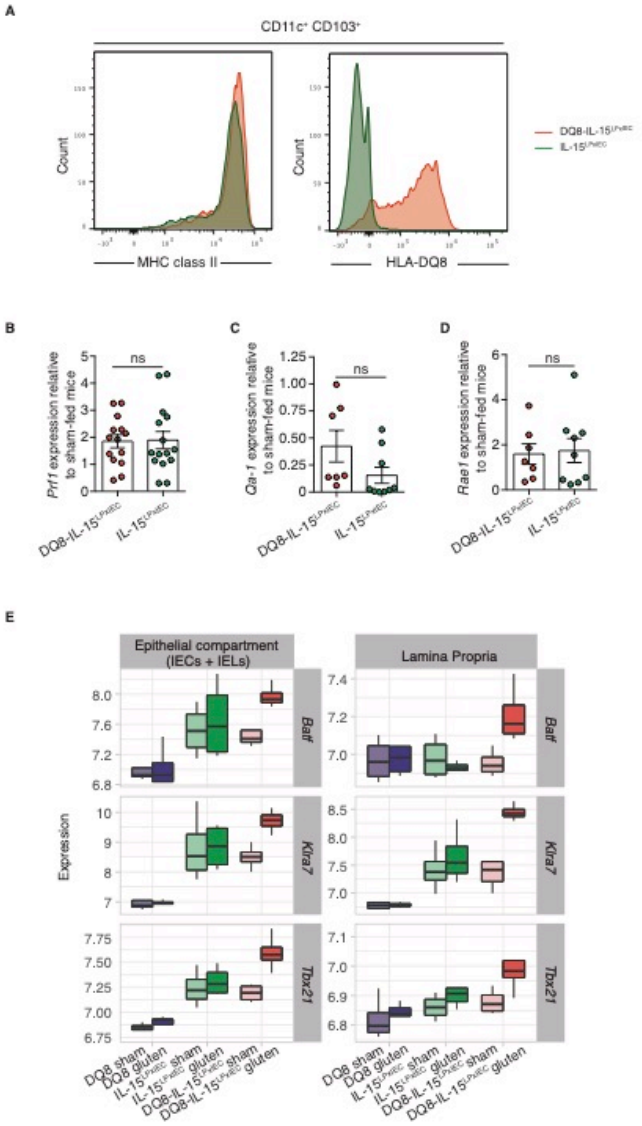

Extended Data Figure 2.6. HLA-DQ8 is required to amplify gluten-specific adaptive immunity to the threshold required for tissue destruction.

(A) Cells isolated from MLN of DQ8-IL-15^{LPxIEC} and IL-15^{LPxIEC} mice. CD11c^{+} CD103^{+} dendritic cells were analyzed by flow cytometry for their expression of MHC class II and HLA-DQ8 molecules.

(**B-E**) Ten-week old DQ8-IL-15^{LPxIEC}, IL-15^{LPxIEC}, and DQ8 mice that were raised on a GFD were maintained on a GFD (sham) or fed with gluten for 30 days (gluten).

(**B**) Expression of perforin (*Prf1*) in the intestinal epithelium was measured by qPCR. Relative expression levels were normalized against the expression levels observed in sham-fed DQ8-IL-15^{LPxIEC} mice and sham-fed IL-15^{LPxIEC}.

(**C, D)** Expression of *Qa-1* (D) and *Rae1* (E) in the intestinal epithelium was measured by qPCR. Relative expression levels were normalized against the expression levels observed in sham-fed DQ8-IL-15^{LPxIEC} mice and sham-fed IL-15^{LPxIEC}.

(**E**) Examples of genes that are significantly up-regulated in response to gluten uniquely in DQ8-IL-15^{LPxIEC} mice.

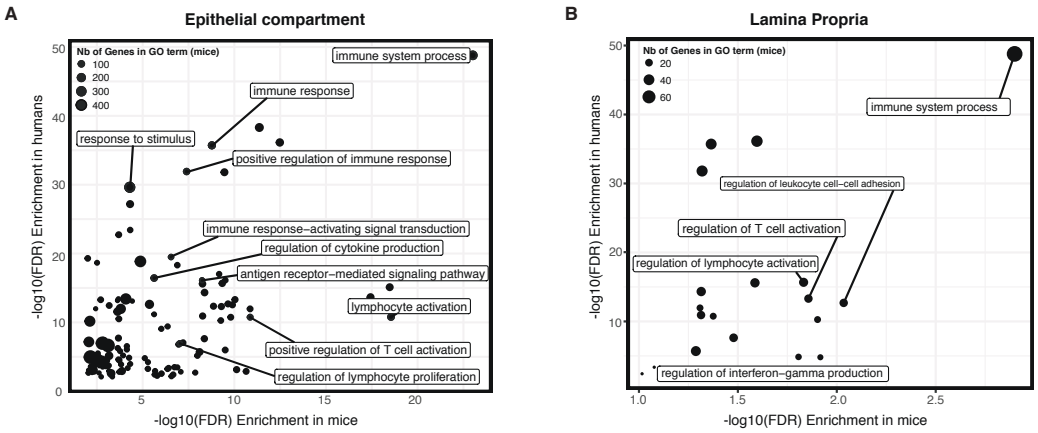

Extended Data Figure 2.7. Similar gene regulatory mechanisms underlie the development of CeD in humans and DQ8-IL-15^{LPxIEC} mice.
Contrast between the gene ontology terms enriched among genes induced by gluten challenge in DQ8-IL-15^{LPxIEC} mice (depicted in the form of –log10 p-values on the x-axis) and the gene ontology terms enriched among genes differently expressed between CeD patients and healthy controls (depicted in the form of –log10 p-values on the x-axis) in the epithelial compartment (A) and the Lp (B).

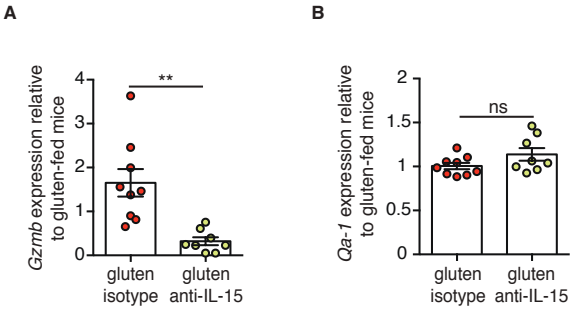

Extended Data Figure 2.8. Anti-IL-15 treatment effect on epithelial gene expression.
Ten-week old DQ8-IL-15^{LPxIEC} mice that were raised on a GFD were fed with gluten for 3 weeks, returned to a GFD for 30 days, and then rechallenged with gluten and concurrently treated with an anti-IL-15 antibody or isotype control for an additional 3 weeks. All readouts were taken at the endpoint of the experiment unless otherwise indicated.
Expression of (A) *GzmB,* and (B) *Qa-1* in the intestinal epithelium were measured by qPCR. Relative expression levels were normalized to gluten-fed mice.

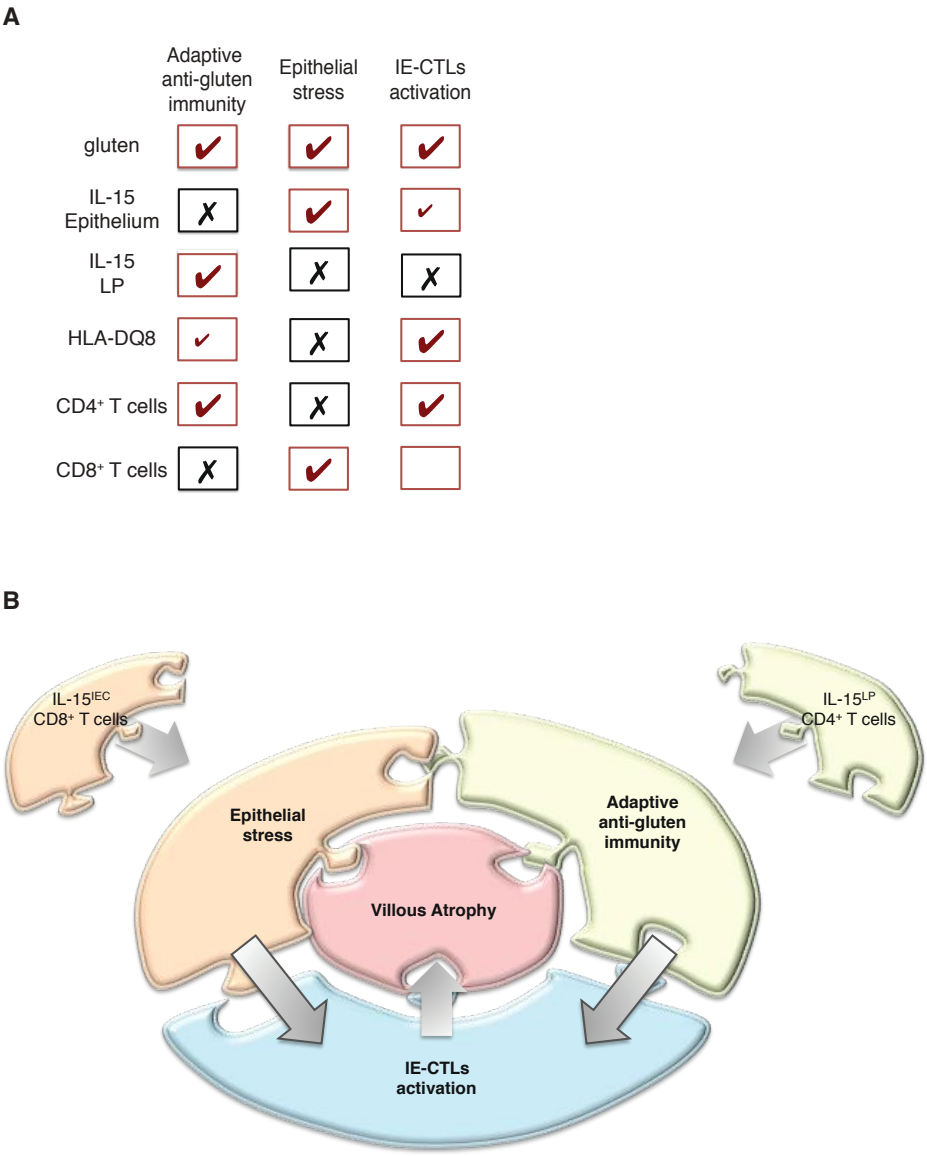

Extended Data Figure 2.9. Interplay between IL-15, gluten, and HLA-DQ8 promote the development of villous atrophy

(A) Representation of the requirements of gluten, the over-expression of IL-15 in IECs or the Lp, presence of HLA-DQ8, $CD4^+$ and $CD8^+$ T cells for promoting adaptive anti-gluten immunity, epithelial stress and IE-CTLs activation. Checked boxes illustrate requirements, crossed boxes illustrate no requirements, empty box = not applicable.

(B) CeD can be represented as a jigsaw puzzle where each piece representing one component of the anti-gluten immune response must interlock to lead to the development of VA.

IL-15 overexpression in the Lp promotes adaptive anti-gluten T cell immunity while IL-15 overexpression in the epithelium favors the expression of non-classical MHC class I molecules on IECs. Individually, these two immune pathways are insufficient to license IE-CTLs with a fully activated killer phenotype and development of VA. When concomitantly upregulated, they promote the licensing of IE-CTLs to kill stressed IECs and VA.

CHAPTER 3. PHARMACOLOGICAL INHIBITION OF TRANSGLUTAMINASE 2 ATTENUATES DEVELOPMENT OF CELIAC DISEASE IN A HUMANIZED MOUSE MODEL

Authors: Sangman M. Kim†[1,2], Brad A. Palanski†[6], Jordan D. Ernest[1,2], Raul Aguirre-Gamboa[9], Thomas Lejeune[10,11], Cisca Wijmenga[9], Luis B. Barreiro[12,13], Valérie Abadie[5,10,11], Chaitan Khosla[6,7,8], and Bana Jabri[1,2,3,4,5]

Affiliations:

[1]Committee on Immunology, [2]Department of Medicine, [3]Department of Pathology, [4]University of Chicago Celiac Disease Center, [5]Section of Gastroenterology, Hepatology and Nutrition, Department of Pediatrics, University of Chicago, Chicago, Illinois, USA.

[6]Department of Chemistry, [7]Department of Chemical Engineering, [8]Stanford ChEM-H; Stanford University, Stanford, CA, USA.

[9]Department of Genetics, University Medical Center Groningen, University of Groningen, 9713 AV Groningen, the Netherlands

[10]Department of Microbiology, Infectiology, and Immunology, University of Montreal, [11]Sainte-Justine Hospital Research Centre, Montreal, Quebec, Canada

[12]Department of Genetics, Sainte-Justine Hospital Research Centre, [13]Department of Pediatrics Faculty of Medicine; University of Montreal, Montreal, Quebec, Canada.

†These authors contributed equally to this work.

3.1. Abstract

Celiac disease (CeD) is an autoimmune disorder that currently affects 1 in 100 individuals worldwide. In genetically susceptible individuals, consumption of gluten (a common dietary protein found in wheat and related species) drives an inflammatory Th1 response in the small intestine, resulting in local enteropathy as well as systemic malaise. The enzymatic activity of the disease autoantigen, transglutaminase 2 (TG2) is thought to initiate and/or amplify this Th1 response by deamidating gluten-derived peptides, which renders them more potent T cell antigens. The only treatment for CeD is a strict, lifelong adherence to a gluten-free diet. However, complete avoidance of gluten is often impossible, and symptoms persist in a significant fraction of patients. Thus, non-dietary therapies are urgently needed. Recently, we reported a humanized mouse model of CeD that develops all of the key characteristics of the human form of the disease. Here, we test the effects of pharmacological inhibition of TG2 in this model using specific, active site directed inhibitors. We show that TG2 inhibition results in significantly reduced intestinal enteropathy in gluten-fed mice. This reduction in enteropathy was associated with reduced TG2 enzymatic activity *in vivo*, as well as a reduction in the Th1-associated antibody response. Transcriptional analysis identified immune associated pathways that are regulated by TG2 inhibition. Our results provide the first experimental evidence for the emerging hypothesis that TG2 is one of the most attractive targets for CeD treatment.

3.2. Introduction

Celiac disease (CeD) is an autoimmune disorder that affects approximately 1 in 100 individuals worldwide (Rubio-Tapia et al., 2012; Lionetti et al., 2015). The onset of CeD may occur at any age, and for unclear reasons, its prevalence is rising (Rubio-Tapia et al., 2009; Rubio-Tapia et al., 2012; Ludvigsson et al., 2013). In genetically susceptible (HLA-DQ2 or DQ8) individuals, dietary consumption of gluten (a common dietary protein in wheat, rye, and barley) drives a Th1 inflammatory response that classically presents as enteropathy of the small intestine, and results in diarrhea, malabsorption, abdominal pain, bloating, and failure to thrive (Sollid, 2002). Extraintestinal manifestations of CeD, such as anemia, osteoporosis, dermatitis herpetiformis (blistering skin rash) and gluten ataxia (a neurological condition), are also increasingly recognized (Leffler et al., 2015). The only accepted treatment for CeD is lifelong avoidance of dietary gluten. However, symptoms and enteropathy commonly persist in patients who attempt to adhere to a gluten-free diet (GFD), which impairs their quality of life (Rubio-Tapia et al., 2010; Ghazzawi et al., 2014). Pharmacological interventions for CeD are urgently needed.

Transglutaminase 2 (TG2), a ubiquitously expressed enzyme, plays a central role in celiac disease pathogenesis. It is the disease autoantigen, and its enzymatic activity is thought to be required for initiating and/or amplifying the Th1 inflammatory response to gluten (Di Sabatino et al., 2012; Klöck et al., 2012). TG2 in the small intestine deamidates glutamine residues of proteolytically resistant peptides derived from dietary gluten. This deamidation reaction markedly increases the binding affinity of these peptides for HLA-DQ2 or 8 and renders them much more potent T cell antigens (Shan et al., 2002; Kim et

al., 2004; Henderson et al., 2007; Qiao et al., 2009). Therefore, inhibition of TG2 activity is thought to be one of the promising avenues for a non-dietary CeD therapy, but experimental support for this hypothesis is lacking (Plugis and Khosla, 2015).

We recently developed a triple transgenic mouse model (DQ8-IL-15^{LPxIEC}) of CeD that recapitulates the key phenotypic, serological, and transcriptional signatures of human CeD (**Chapter 2**). Additionally, we have previously reported the development of a potent and specific class of TG2 inhibitors that irreversibly target its active site (Klöck et al., 2014). We have demonstrated that these inhibitors are effective in blocking small-intestinal TG2 activity in living mice and have also validated a chemical biological approach for monitoring TG2 activity *in vivo* (Plugis et al., 2017). Here, we use two TG2 inhibitors to answer the long-standing question of whether TG2 activation is a critical step in development of CeD pathology. Our results suggest that TG2 inhibition is a promising option for pharmacological CeD therapy.

3.3. Results

Previously, we have shown that DQ8-IL-15^{LPxIEC} mice develop villous atrophy and the other key features of human CeD upon gluten feeding (**Chapter 2**). To test the hypothesis that TG2 catalyzed deamidation of gluten derived peptides is an essential step in the development of a Th1 immune response to gluten and villous atrophy, we utilized two pharmacological inhibitors of TG2, ERW1041E and CK805 (**Figure 3.1A**). The first of these inhibitors was previously validated to block small intestinal TG2 activity in an acute mouse model of TG2 activation (Plugis et al., 2017), and the second is a closely related analog with increased potency (Klöck et al., 2014).

As a first step, we confirmed that both ERW1041E and CK805 could reach reasonable plasma concentrations following intraperitoneal (IP) injection. Both of these inhibitors reached similar concentrations five minutes after dosing and had comparable half-lives (**Figure 3.2**). Although the circulating half-lives of these compounds are short, they irreversibly bind to the TG2 active site and thus their effective half-lives for TG2 inhibition are likely much longer. Based on the prior observation that ERW1041E had an effective inhibitory half-life of ~12 hours in a mouse model of pulmonary hypertension, we chose to dose both ERW1041E and CK805 twice daily by IP injection. To determine the effects of TG2 inhibition on development of celiac disease features, DQ8-IL-15^{LPxIEC}, were fed gluten for 30 days with and without co-administration of a TG2 inhibitor. A third group was maintained on a sham (gluten-free) diet as a negative control (**Figure 3.1B**).

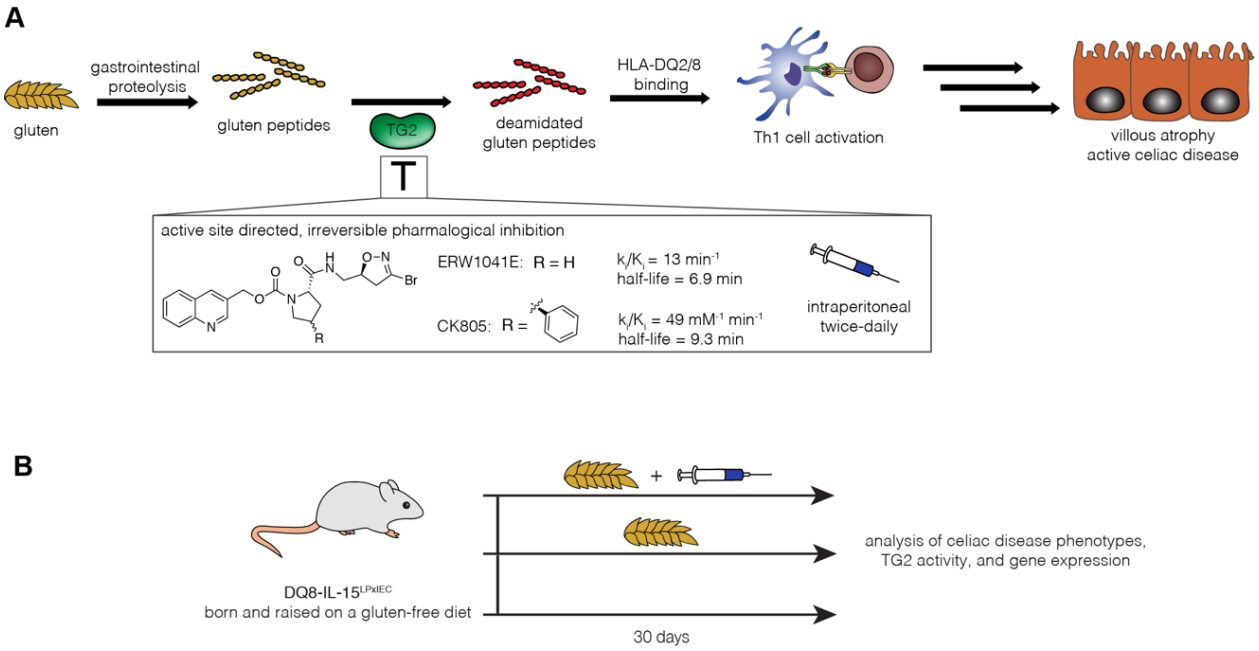

Figure 3.1. Pharmacological TG2 inhibition in a mouse model of CeD pathogenesis. (**A**) Role of TG2 in initiating and/or amplifying the immune response to gluten. TG2 deamidates selected Gln residues of peptides derived from dietary wheat, which increases their binding affinity to HLA-DQ2 or 8 on antigen presenting cells which renders them potent T cell antigens, eventually leading to CeD. Blocking TG2 activity with pharmacological inhibitors is hypothesized to prevent development of CeD features (inset). (**B**) Schematic and timeline for prophylactic administration of TG2 inhibitors in an established mouse model of CeD pathogenesis.

A

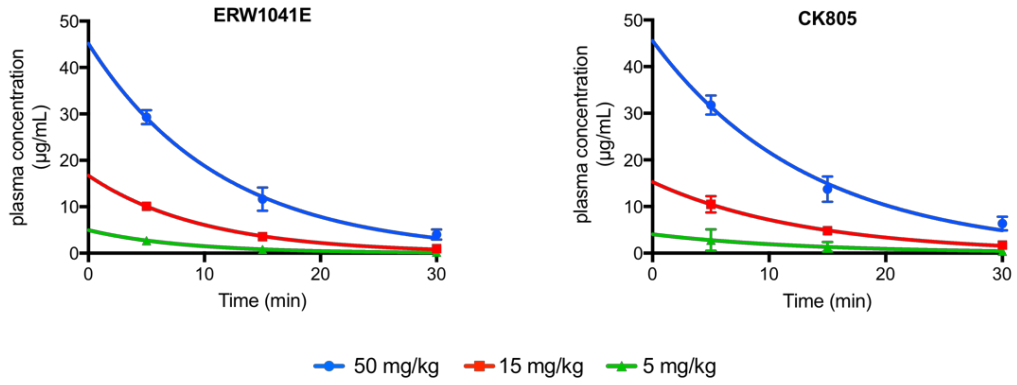

B

Dose (mg/kg)	50	15	5
C_0 (µg/mL)	45.21	16.73	4.99
k (min^{-1})	0.088	0.101	0.12
$t_{1/2}$ (min)	7.91	6.86	5.82

Dose (mg/kg)	50	15	5
C_0 (µg/mL)	45.56	15.28	4.05
k (min^{-1})	0.074	0.076	0.074
$t_{1/2}$ (min)	9.32	9.16	9.36

Figure 3.2. Pharmacokinetic profiling of TG2 inhibitors ERW1041E and CK805 following IP injection.
(**A**) Inhibitors were administered at three doses, and survival bleeds were taken at three subsequent time points. Plasma levels of TG2 were quantified by triple quadrupole mass spectrometry, as previously described (Klöck et al., 2012). Lines are least squares fits to C=C0exp(-kt), where C is the concentration, C0 is the initial concentration, k is a rate constant, and t is the time. (**B**) Parameters obtained from least squares fitting. t1/2 denotes the calculated half-life.

In clinical practice, the villous height to crypt depth ratio is regarded as a gold standard in assessment of CeD pathogenesis (Adelman et al., 2018). We therefore first asked if TG2 inhibition could prevent a reduction in the villous/crypt ratio in gluten-fed mice. As expected, gluten but not sham feed mice developed villous atrophy and a significantly reduced villous/crypt ratio upon 30 days of gluten feeding (**Fig. 3.3A, B**). Administration of ERW1041E appeared to result in some protection against development of gluten-induced intestinal enteropathy, but the increase in the villous/crypt ratio was not statistically significant (**Fig. 3.3A**). In contrast, administration of the more potent inhibitor CK805 resulted in greater protection of the villous architecture and a significantly

increased villous/crypt ratio (**Fig. 3.3B**).

Next, we wanted to assess the effects of TG2 inhibition on the development of adaptive immunity to gluten. To do so, we measured the levels of anti-gluten IgA antibodies in circulation (**Fig. 3.3C**) and from duodenal explants (**Fig. 3.3D**), as the IgA subclass is most used in diagnosis of CeD in humans. As previously reported (**Chapter 2**), the IgA antibody response was relatively weak in gluten fed mice. However, the trend toward reduction in IgA antibodies was stronger for CK805 than for ERW1041E (**Fig. 3.3C, D**). Importantly, CK805 also showed a stronger trend toward reducing circulating antibodies of the circulating IgG2c subclass, which are indicative of an ongoing Th1 immune response (**Fig. 3.3E**). Taken together with the fact that CK805 but not ERW1041E significantly attenuated development of villous atrophy, we decided to focus on further characterization of the former, more potent TG2 inhibitor.

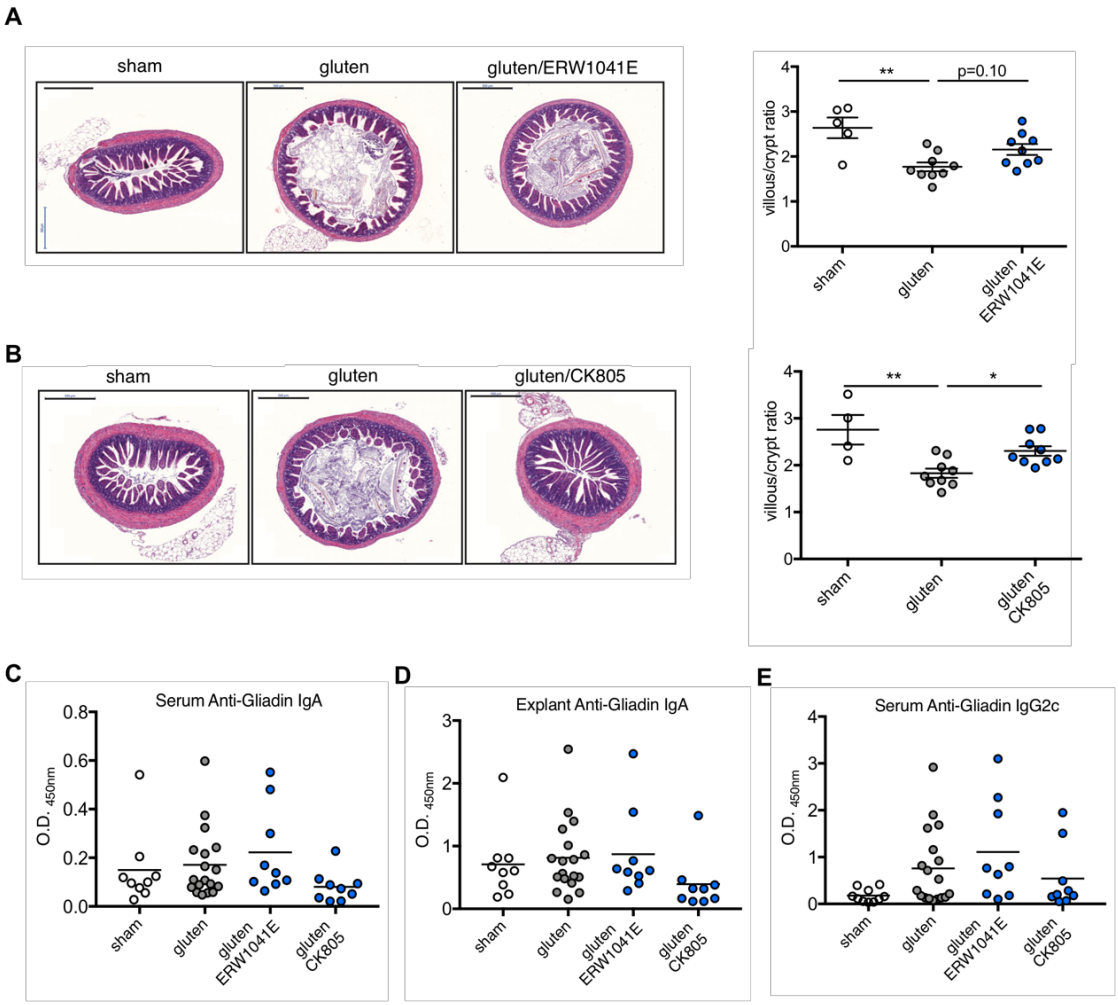

Figure 3.3. TG2 inhibition attenuates development of villous atrophy and Th1 immunity in a mouse model of celiac disease.

Ten-week old DQ8-IL-15^{LPxIEC} mice that were raised on a gluten-free diet (GFD) were maintained on a GFD ("sham"), fed with gluten for 30 days ("gluten"), or fed with gluten for 30 days along with twice-daily administration of TG2 inhibitors (ERW1041E or CK805). (**A-B**) Hematoxylin and eosin (H&E) staining of paraffin-embedded ileum sections. The graph depicts the ratio of the morphometric assessment of villous height to crypt depth. Scale bar, 200 μm. (**C-E**) Measurement of anti-gliadin antibody levels by ELISA. Data for each of the two inhibitors come from two independent experiments. Error bars, SEM. *P < 0.05, **P < 0.01; One-way analysis of variance (ANOVA) / Tukey's multiple comparison.

TG2 activation is thought to be a key step in the development of CeD pathogenesis. There is some evidence gathered from ex vivo studies that human CeD patients have elevated levels of small intestinal TG2 activity compared to healthy controls (Esposito et al., 2003),

but this finding has never been confirmed in vivo. We therefore administered 5-biotinamidopentylamine (5-BP), a chemical biological probe of TG2 activity to living DQ8-IL-15LPxIEC mice and then assessed their intestinal TG2 activity post-mortem, using a previously validated protocol (Palanski and Khosla, 2018).

Compared to sham-fed mice, gluten-fed mice had elevated levels of TG2 activity, as judged by 5-BP incorporation. CK805 restored TG2 activity to approximately the same level as in the sham-fed mice, confirming the efficacy of CK805 in inhibiting its target (**Fig. 3.4A**). As a second, more disease-relevant manner of assessing the ability of CK805 to prevent TG2-mediated deamidation of gluten peptides, we measured levels of antibodies to native and deamidated gliadin peptides in vehicle and CK805 treated gluten-fed mice. We hypothesized that in CK805 but not vehicle-treated mice, there would be a reduction in the level of anti-deamidated gluten peptide antibodies. Indeed, CK805 significantly reduced circulating IgG levels of anti-deamidated gluten antibodies compared to antibodies against native gluten (**Fig. 3.4C**). There was no difference in vehicle treated mice (**Fig. 3.4B**). This difference was modest, and in future studies we will therefore directly assess the magnitude of the anti-gliadin T-cell response by ELISpot.

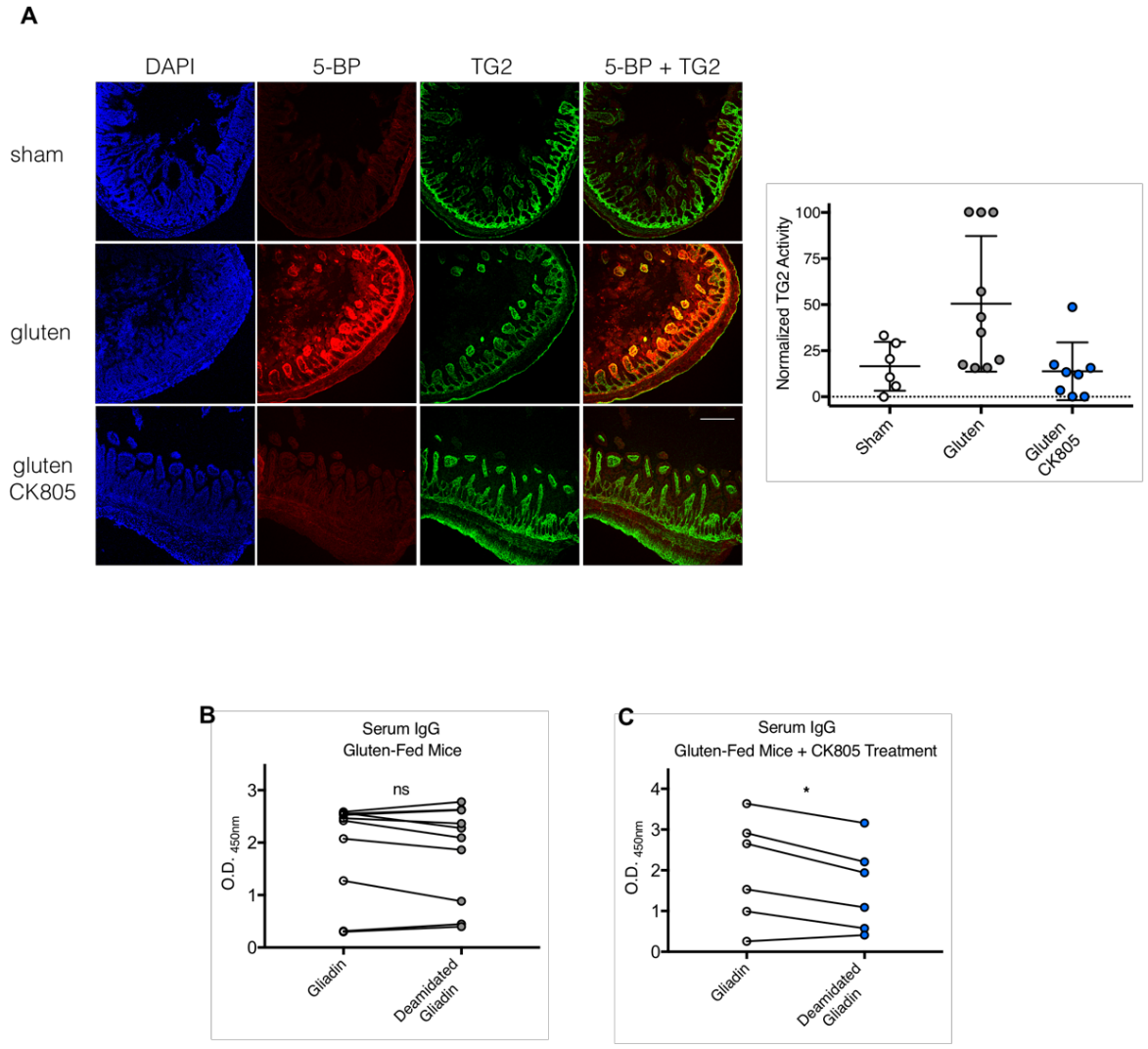

Figure 3.4. TG2 activity is increased in DQ8-IL-15LPxIEC upon gluten feeding and blocked by administration of CK805.
(**A**) Immunohistochemical analysis of ileum sections from mice injected with the TG2 activity probe 5-BP prior to sacrifice. The amount of 5-BP incorporation (red staining) reflects the amount of in vivo TG2 activity. The graph depicts a quantitative analysis of TG2 activity (5-BP staining divided by TG2 staining intensity) from three independent experiments. To allow comparison between experiments, data were min-max normalized within each experiment. (**B-C**) Serum IgG levels of antibodies against native and deamidated gliadin peptides as determined by ELISA. *P < 0.05, paired t-test.

As an unbiased first step toward gaining mechanistic insight into how TG2 inhibition prevents development of CeD phenotypes, we performed transcriptional

analysis of the intestinal epithelium and lamina propria. For our initial analysis, samples from small cohorts of sham-fed, gluten-fed, and gluten-fed, CK805-treated mice were analyzed by RNAseq. Encouragingly, principal component analysis of differentially expressed genes from each of the intestinal compartments showed clustering of the mice according to their treatment group (**Figure 3.5A**).

Reactome pathway enrichment (Sidiropoulos et al., 2017) demonstrated that several pathways that were deregulated upon gluten feeding were unaffected when CK805 was administered along with gluten (**Figure 3.5B, C**). The most enriched pathway involved genes involved in biological oxidations, many of which were also shown to be differentially regulated in human CeD patients (Bragde et al., 2018). Additionally, there was also significant enrichment in the immune related ontology of neutrophil degranulation. Although the roles of neutrophils in CeD have not been widely studied, CeD patients have elevated levels of neutrophils in their small intestine compared to healthy controls (Sarikaya et al., 2014). Furthermore, genetic studies have suggested that TG2 plays a role in neutrophil differentiation and function (Balajthy, 2006), but this function has not been well studied. Overall, this preliminary study highlights the promise of transcriptomics in elucidating the mechanisms by which TG2 inhibition may prevent induction of Th1 immunity in response to gluten. Analysis of selected genes by qPCR, as well as additional RNAseq studies involving larger cohorts of mice, are ongoing.

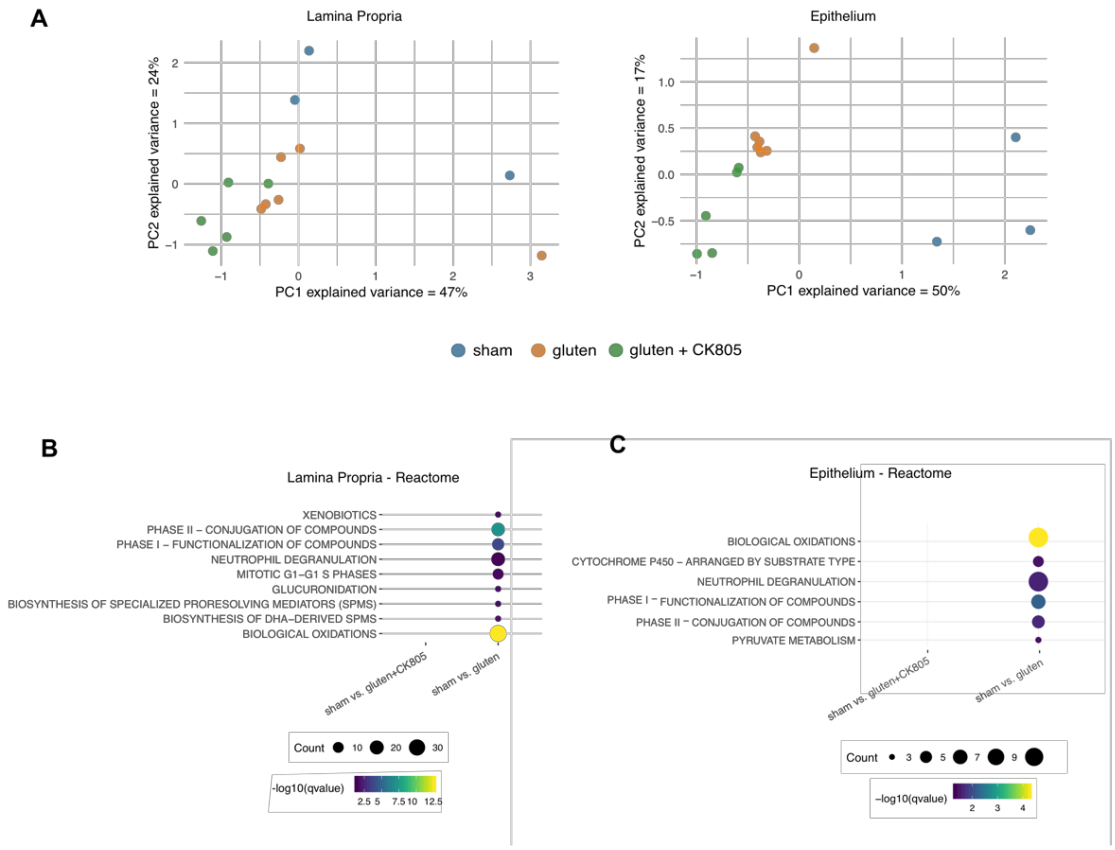

Figure 3.5. Transcriptional analysis of sham, gluten-fed, and gluten-fed mice prophylactically treated with TG2 inhibitor CK805.

(**A**) Principal component analysis of differentially expressed genes. (**B-C**) Reactome pathway enrichment of differentially expressed genes. Pathways that are deregulated upon gliadin feeding but not upon gliadin feeding in conjunction with CK805 administration are shown.

3.4 Ongoing work

3.4.1 Quantification of the Th1 response

Given the suspected role of TG2 in the amplification of the gluten-specific $CD4^+$ T cell response (**Chapter 1.2.3**), we are currently attempting to quantify the IFNγ levels in mLN and LP $CD4^+$ T cells from mice that are fed with gluten with and without CK805 treatment. We will accomplish this by flow cytometry on bulk mLN and LP fractions stimulated with PMA ionomycin, Golgi-plug, and deamidated gliadin. Additionally, we will culture mLN and LP single cell suspensions with or without deamidated gliadin and measure IFNγ levels by ELISA (as described in DePaolo et al., 2011). Finally, we are currently in the process of creating TCR transgenic mice that have specificity for native, deamidated, or both forms of gliadin, and this will clarify the role of TG2 in the amplification of the gluten-specific T cell response in a quantitative and temporal manner (as described in detail in **Section 4.2**).

3.4.2 Expansion of RNAseq study

Although there are some interesting insights that we can draw from our initial RNAseq analysis, our study is underpowered as stands, leading to an underestimation of the genes and pathways that might be different between our groups. We are currently expanding this analysis to include more mice and also including a group of mice that is sham fed, and treated with CK805. The reason for this is that we were surprised to find that the number of differentially expressed genes compared to sham fed mice in the gluten feeding + CK805 treated group was greater than the effect of gluten feeding alone,

meaning that the way in which TG2 inhibition was leading to a significant reduction in villous atrophy was not simply by preventing certain gene expression changes from occurring, and TG2 inhibition has gluten independent effects that impact gene expression. We would like to dissociate these effects with those that affect the abrogation of tissue destruction in the context of gluten feeding.

3.4.3 CK805 Treatment

We have demonstrated that CK805 can lead to the prevention of villous atrophy when mice are treated over the course of initial gluten feeding. We are currently performing “treatment” experiments in mice that are fed with gluten for 30 days, reverted to a gluten free diet for 30 days (to allow for the restoration of small intestinal architecture and the reversal of all phenotypes; **Fig. 2.1**), and then re-exposed to gluten with or without concurrent CK805 treatment. This experimental scheme would mimic a celiac patient that has been on a gluten free diet, who eats gluten while using CK805 as a treatment.

3.5 Methods

3.5.1 Mice

Mice used in these studies are on the C57BL/6 background. Mice were maintained under specific pathogen-free conditions at the University of Chicago and at the Sainte-Justine University Hospital Research Center. Importantly, no differences in the outcome of the experiments were observed between the two institutions, enabling to pool the data. HLA-DQ8 transgenic mice (DQ8) and DQ8-D^d-IL-15tg mice expressing IL-15 under the minimal MHC class I D^d promoter (named DQ8-IL-15^{LP} in the present study) were previously described (DePaolo et al., 2011). Villin-IL-15^{IEL} mice expressing IL-15 under the intestine-specific villin promoter of IECs (Meisel et al., 2017) were crossed to HLA-DQ8 mice. IL-15^{LP} mice were then crossed onto DQ8-IL-15^{IEC} mice to obtain the first generation DQ8-IL-15^{LPxIEC} mice. Next generations were obtained by backcrossing DQ8-IL-15^{LPxIEC} mice with DQ8-villin-IL-15^{IEL} mice. All mice expressing HLA-DQ8 also express I-A^b MHC class II molecules. All strains were maintained on a gluten-free chow (AIN76A, Envigo). For all experiments, mice were used at 10 weeks of age. All experiments were performed in accordance with the Institutional Biosafety Committee and the Institutional Care and Use Committee of the University of Chicago, and with the Canadian Council on Animal Care guidelines and the Institutional Committee for Animal Care in Research of the Sainte-Justine University Hospital Research Center.

3.5.2 ERW1041E synthesis

Commercial proline methyl ester hydrochloride (15.69 g, 95 mmol) was dissolved

in 150 mL DMF and catalytic N,N-dimethylpyridin-4-amine (1.930 g, 15.79 mmol) was added, followed by triethylamine (11.01 mL, 79 mmol). The mixture was stirred and a white solid precipitated. Separately, quinolin-3-ylmethyl 1H-imidazole-1-carboxylate (5b) (20 g, 79 mmol) was dissolved in 100 mL methylene chloride and then added to the reaction mixture. The mixture was stirred overnight at RT, before the volatiles were evaporated to about 70 mL. A white solid was filtered off. The filtrate was diluted with 300 mL water and some hydrochloric acid (1 M) was added to reach pH 5–6. The cloudy mixture was diluted with 500 mL ethyl acetate, partitioned, and the organic layer washed with brine (4 × 150 mL). The organic layer was dried over sodium sulfate and evaporated under reduced pressure, yielding (S)-2-methyl 1-(quinolin-3-ylmethyl) pyrrolidine-1,2-dicarboxylate (21.5 g, 68.4 mmol, 87% yield) that was used in the next step without prior purification.

The saponification of the intermediate ester and the subsequent amide coupling were performed similar to the previously reported protocol (Watts et al., 2006). The ester (21.5 g, 68.4 mmol) was thus dissolved in 200 mL THF/MeOH 1:1 and LiOH (1 M in water) was added in small aliquots until the starting material had disappeared by TLC (9:1 ethyl acetate/hexanes). An equivalent amount of hydrochloric acid (1 M) was added and the volatiles were removed under reduced pressure. The crude oil was diluted with lightly acidic water and extracted with ethyl acetate (4 × 150 mL). The combined organic extracts were dried over sodium sulfate and evaporated under reduced pressure, furnishing (S)-1-((quinolin-3-ylmethoxy)carbonyl) pyrrolidine-2-carboxylic acid (18.8 g, 62.6 mmol, 92% yield) as a yellow oil.

An aliquot of the free acid (17.8 g, 59.3 mmol) that was used without purification from the previous step, EDCI·HCl (13.07 g, 68.2 mmol), and 1H-benzo[d][1,2,3]triazol-1-ol (8.01 g, 59.3 mmol) were dissolved in DMF (120 mL) and 4-methylmorpholine (NMM) (6.52 mL, 59.3 mmol) was added. The mixture was stirred for 10 min, and enantiomerically enriched (S)-(3-bromo-4,5-dihydroisoxazol-5-yl)methanamine (S-DHI)(10.61 g, 59.3 mmol) was added dropwise. The mixture was stirred at RT for 2 h before it was diluted with 250 mL water. This mixture was diluted with 600 mL ethyl acetate and extracted. The organic layer was washed with brine (4 × 200 mL), dried over sodium sulfate and evaporated under reduced pressure, furnishing the desired product in good yield and purity. The crude material was purified on a short silica gel column (10 cm diameter, 15 cm length) with a stepwise gradient of 600 mL 80% EtOAc/pentane, 600 mL 90% EtOAc/pentane, 1000 mL EtOAc, 600 mL 5% MeOH in EtOAc, 1000 mL 10% MeOH in EtOAc. After pooling all fractions containing product and evaporation of the volatiles, (S)-quinolin-3-ylmethyl 2-((((S)-3-bromo-4,5-dihydroisoxazol-5-yl)methyl)carbamoyl)pyrrolidine-1-carboxylate (22.55 g, 48.9 mmol, 82% yield) was obtained as a viscous oil that foamed under high vacuum. A fine amorphous solid was obtained by crushing the solidified foam. 1H NMR (400 MHz, DMSO-d6, mixture of rotational isomers) δ 8.93 and 8.84 (2 d, J = 1.9 Hz, 1H), 8.20–8.37 (m, 2H), 7.90–8.06 (m, 2H), 7.69–7.83 (m, 1H), 7.62 (t, J = 7.6 Hz, 1H), 5.16–5.37 (m, 2H), 4.73 and 4.59 (2 m, 1H), 4.27 and 4.19 (dd, J = 2.8, 8.2 Hz dd, J = 3.5, 8.4 Hz, 1H), 3.12–3.56 (m, 5H), 2.92–3.10 (m, 1H), 1.99–2.24 (m, 1H), 1.71–1.91 (m, 3H).

3.5.3 CK805 synthesis

The title compound was prepared from commercial (2*S*,4*S*)-1-(*tert*-butoxycarbonyl)-4-phenylpyrrolidine-2-carboxylic by the general procedure, furnishing (2*S*,4*S*)-quinolin-3-ylmethyl 2-((((*S*)-3-bromo-4,5-dihydroisoxazol-5-yl)methyl)carbamoyl)-4-phenylpyrrolidine-1-carboxylate (81 mg, 0.151 mmol, 43.9% yield over three steps) as a white solid. ^{1}H NMR (500 MHz, DMSO-d_6, mixture of rotational isomers) δ 8.93 and 8.86 (2 d, *J* = 2.2 Hz, 1H), 8.41 and 8.35 (2 t, *J* = 6.1 Hz, 1H), 8.36 and 8.27 (2 d, J = 1.6 Hz, 1H), 8.03 (d, *J* = 8.3 Hz, 1H), 7.99 (dd, *J* = 17.0, 8.0 Hz, 1H), 7.77 (ddt, *J* = 8.1, 6.9, 1.1 Hz, 1H), 7.67–7.60 (m, 1H), 7.35–7.27 (m, 4H), 7.26–7.19 (m, 1H), 5.37–5.20 (m, 2H), 4.80–4.71 and 4.66–4.59 (2 m, 1H), 4.46 and 4.37 (2 dd, *J* = 8.8, 2.2 Hz, 1H), 3.98 and 3.91 (2 dd, *J* = 9.8, 7.6 Hz, 1H), 3.54–3.18 (m, 5H, partly obscured by residual water), 3.04 (ddd, *J* = 26.4, 17.6, 7.2 Hz, 1H), 2.43–2.28 (m, 1H), 2.18–2.08 (m, 1H). ^{13}C NMR (126 MHz, DMSO-d_6, mixture of rotational isomers) δ 172.52 (d, *J* = 33.1 Hz), 153.68 (d, *J* = 41.6 Hz), 150.50 (d, *J* = 25.3 Hz), 147.12 (d, *J* = 7.8 Hz), 140.62 (d, *J* = 22.0 Hz), 138.02 (d, *J* = 26.7 Hz), 134.42 (d, *J* = 52.0 Hz), 129.98 (d, *J* = 4.6 Hz), 129.65 (d, *J* = 8.8 Hz), 128.76 (d, *J* = 3.2 Hz), 128.54 (d, *J*= 4.4 Hz), 128.09 (d, *J* = 15.0 Hz), 127.27 (d, *J* = 3.9 Hz), 127.15 (d, *J* = 3.3 Hz), 126.86 (d, *J* = 21.8 Hz), 80.11 (d, *J* = 14.2 Hz), 64.03 (d, *J* = 15.0 Hz), 59.93 (d, *J* = 75.6 Hz), 52.98 (d, *J* = 61.1 Hz), 43.41, 41.56 (d, *J* = 59.3 Hz), 40.99 (d, *J* = 36.4 Hz), 37.82 (d, *J* = 132.7 Hz). HRMS (ESI-QTOF) *m*/*z*: calculated for $C_{26}H_{26}BrN_4O_4^+$ $[M + H]^+$, 537.11319; found, 537.11300.

3.5.4 Pharmacokinetic analysis

Using the inhibitors formulated as above, cohorts of five male C57BL/6J mice (6–8 weeks of age) were fasted for approximately 6 h and then each dosed by intraperitoneal injection at the doses indicated for each inhibitor. Blood was collected by cheek bleeding in tubes containing Heparin sodium salt (Sigma) at 10, 20, and 30 min postdosing.

Plasma was obtained from whole blood by sedimenting the cells for 20 min in a benchtop microcentrifuge and removing the supernatant liquid. The plasma was stored at –20 °C until analysis. For analysis, the plasma samples were thawed on ice, and 25 µL (group A) or 10 µL (group B and standard curve) were withdrawn. To each sample, an equal volume of internal standard (IS) spiking solution (1 µM **5b** in 95% water, 4.9% acetonitrile, and 0.1% DMSO) was added, followed by an equal volume of blank spiking solution (95% water, 4.9% acetonitrile, and 0.1% DMSO). To generate standard curves, blank plasma was taken and an equal volume of IS spiking solution added, followed by an equal volume of compound spiking solution (24.4 ng/mL to 12.5 µg/mL per compound, separated in the same groups, in 95% water, 4.9% acetonitrile, and 0.1% DMSO). The volumes of all samples were increased to 250 µL by the addition of water and well mixed. Then, 600 µL of ethyl acetate were added and the samples thoroughly shaken and vortexed. The phases were separated by brief centrifugation, and then 500 µL of ethyl acetate were withdrawn to a microcentrifuge tube, 300 µL of new ethyl acetate added, and the extraction repeated. Another 300 µL were then withdrawn, and the combined extracts were evaporated. To reconstitute the residues, 20 µL of methanol were added to each tube and thoroughly vortexed. After brief centrifugation, 80 µL of water with 0.1%

formic acid were added and the tubes thoroughly vortexed again. The liquids were withdrawn, passed through 0.45 µm centrifugal filter units, and analyzed by LC-MS (ESI-QTOF).

Total ion chromatograms were extracted for the most prevalent masses of each compound ([M + H]+ and its ^{81}Br isotopologues, and the peaks integrated. The peak areas of analytes were normalized by the peak area of the internal standard. Standard curves were used to calculate the concentration of analytes in the plasma samples

3.5.5 Gluten feeding and TG2 inhibition

To study the response to dietary gluten, mice were transferred from a GFD to a standard rodent chow at the beginning of each experiment and allowed to consume the gluten-containing chow *ad libitum*. Additionally, supplemental gluten (20mg crude gliadin (Sigma-Aldrich)) was administered via intragastric gavage, every other day for thirty days, using a 22-gauge round-tipped needle (Cadence Science). ERW1041E and CK805 were dosed intraperitoneally twice daily at 25 mg/kg, in a vehicle of 20% DMSO, 40% PBS, and 40% PEG-400. Control mice received an equivalent dose of vehicle alone.

3.5.6 5-Biotinamidopentylamine Hydrochloride (5-BP·HCl) synthesis

d-(+)-Biotin (3.26 g, 13.35 mmol) and *tert*-butyl (5-aminopentyl)carbamate (2.7 g, 13.35 mmol), prepared by the method of Lee et al., 2007 and EDCI·HCl (2.94 g, 15.35 mmol) were suspended in acetonitrile (70 mL). Water (30 mL) was added, followed by NMM (2.70 g, 26.7 mmol). The mixture was stirred for 3 h, whereafter the volatiles were

removed under reduced pressure, furnishing the crude product as a yellow oil. The oil was diluted with water and a first crop of the product could be filtered off. On standing for several days, a number of additional crops of product could be filtered off, accounting for a moderate additional yield. The crude product was loaded onto a silica gel column in ethyl acetate with methanol and eluted slowly with a gradient up to 15% methanol in ethyl acetate. Upon evaporation of the pooled fractions, *tert*-butyl 5-(biotinamidopentyl) carbamate (3.0 g, 7.00 mmol, 52.4% yield) was obtained as a gel that slowly solidified under vacuum. An aliquot of the white solid (2.5 g, 5.83 mmol) was suspended in 15 mL of 4 M HCl in dioxane and stirred for 10 min. Then, 15 mL of methanol were added and residual suspended solids dissolved. Stirring was continued for another 10 min. The crude mixture was slowly added to 220 mL diethyl ether under vigorous stirring and stirring continued for 1 h. During this time, a sticky oil had formed on the walls of the flask. The solvent was decanted off and the flask washed with additional ether. Then, the oily solid was taken up in methanol and the clear solution evaporated under reduced pressure, yielding the title compound as an off-white foam (1.3 g, 3.56 mmol, 61.1% yield). ^{1}H NMR (500 MHz, D_2O) δ 4.53 (d, J = 5.13 Hz, 1H), 4.35 (d, J = 7.32 Hz, 1H), 3.27 (br. s., 1H obscured by residual methanol solvent signal), 3.12 (d, J = 5.62 Hz, 2H), 2.81–2.98 (m, 3H), 2.71 (d, J = 13.43 Hz, 1H), 2.08–2.26 (m, 2H), 1.15–1.79 (m, 12H). ^{13}C NMR (126 MHz, D_2O) δ 177.3, 165.8, 62.7, 60.9, 56.0, 40.3, 40.0, 39.6, 36.0, 28.53, 28.45, 28.3, 27.0, 25.8, 23.6.

3.5.7 Preparation of chymotrypsin-digested gliadin (CT-gliadin), peptic-tryptic digests of gliadin (PT-gliadin) and deamidated gliadin peptides (DGP)

CT-gliadin was prepared as previously described (Bouziat et al., 2017). To obtain DGP, CT-gliadin was dissolved in a 10mM $CaCl_2$ solution containing Guinea pig liver transglutaminase (Zedira) and incubated overnight at 37°C with continuous shaking. Concentration of DGP was calculated based on the concentration of the CT-glia and the volume added during deamidation. To obtain PT-gliadin, gliadin was digested in 0.2 N HCl (pH 1.8) with pepsin (Sigma) for 2h at 37°C. Once the pH adjusted to 8.0, the digest was incubated with purified trypsin for 4h at 37°C, and thereafter with cotazym (lipase from porcine pancreas Type II, Sigma) for 2h under constant stirring. Concentration of PT-gliadin was determined using a BCA assay (Pierce).

3.5.8 Anti-gluten and anti DGP ELISA

Serum was harvested thirty or sixty days after mice received the first gliadin feeding. For anti-gluten IgG2c, IgG and IgA ELISA, high-binding ELISA 96-well plates (Nunc, Thermo-Scientific) were coated with 50 µl of 100 µg/ml CT-gliadin in 100 mM Na_2HPO_4 overnight at 4 °C. Plates were washed three times with PBS containing 0.05% Tween-20 (PBS-T) and blocked with 200 µl of 2% BSA in PBS-T for 2 hours at room temperature. Serum was assessed in duplicate and at two dilutions, typically 1/50 and 1/200. Sera were incubated overnight at 4 °C and plates were washed three times with PBS-T. Specific anti-mouse Ig-horseradish peroxidase (HRP) (Southern Biotech) in blocking buffer was added to plates and incubated for 1 hour at room temperature. Plates

were washed five times with PBS-T. 50 µl HRP substrate TMB (Thermo-Scientific) was added and the reaction stopped by the addition of 50 µl 2N H_2SO_4 (Fluka Analytical). Absorbance was read at 450 nm on Molecular Devices Versamax tunable microplate reader. For anti-DGP IgG ELISA, deamidated PTD gliadin was coated onto Immulon-2 HB ELISA plates (Thermo Scientific) at a concentration of 100μg/ml in 0.1M Na2HPO4 (Sigma Aldrich) and incubated overnight at 4C. Blocking buffer of 4% BSA/0.05% tween/1X PBS was used, and sera diluted at 1/200 with diluent of 0.1%BSA/0.05%tween/1XPBS. Biotinylated anti-mouse IgG and streptavidin-HRP (Both Jackson Immunoresearch) were used as the detection reagents. TMB (Sigma Aldrich) was used as the substrate. Plates were then read at 450nm. Levels of anti-DGP IgG and anti-gliadin IgG, IgG2c, IgA were expressed in OD values.

3.5.9 Histology

Hematoxylin & Eosin staining was performed on 5µM thick sections of 10% formalin-fixed paraffin-embedded ileum. Slides were analyzed using a Leica DM 2500 microscope with a HC PLAN APO 20x/0.7 NA and a HCX PL APO 100x/1.40-0.70 objective or a Leica DMi8 microscope with a HC PL FLUOTAR L 20x/0.40 and a HC PL APO 40x/0.75 objective and equipped with the image processing and analysis software LasX (Leica). The villus height/crypt depth ratios were obtained from morphometric measurements of five well-orientated villi. The villous to crypt ratio was calculated by dividing the villous height by the corresponding crypt depth. Villus height was measured from the tip to the shoulder of the villus or up to the top of the crypt of Lieberkuhn. The

crypt depth was measured as the distance from the top of the crypt of Lieberkuhn to the deepest level of the crypt. The intra-epithelial lymphocyte count was assessed by counting the amount of intra-epithelial lymphocytes among at least 100 enterocytes. Additional 5μm sections were processed for immunohistochemical detection of Granzyme B. Slides were deparaffinized, rehydrated, and washed in 1X PBS. Sections were incubated in Citrate buffer (1 M pH 6.0) for 20 min at 68 °C. Then the sections were permeabilized with 0.3% Triton X-100 at room temperature for 30 minutes. Endogenous peroxidase activity was quenched for 15 minutes with 2% hydrogen peroxide in PBS. Sections were blocked with normal donkey serum (Vector Laboratories) for 1 hour and incubated with polyclonal Goat IgG anti-mouse Granzyme B (R&D Systems) for 2 hours at room temperature. Sections were then washed in PBS, incubated with biotinylated anti-goat IgG (Vector Laboratories) for 1 hour at room temperature, and stained using the avidin-biotin complex method (Vectastain ABC kit; Vector Laboratories). Color was developed using 3,3'-diaminobenzidine (Dako Diagnostics) containing hydrogen peroxide. Slides were counterstained with Harris modified hematoxylin, dehydrated, cleared, mounted, and examined under light microscopy as described above.

3.5.10 Visualization and quantification of TG2 activity

Six and three hours prior to euthanasia, mice were injected i.p. (100 mg/kg) with 5-(biotinamido)-pentylamine (5BP), a substrate for TG2 transamidation activity, which was synthesized following a published protocol (13). Small intestinal pieces were collected and frozen in OCT (Tissue-Tek). Frozen sections of 5 μm thickness were cut,

fixed in 1% paraformaldehyde, and TG2 protein was visualized by staining with a rabbit polyclonal anti-TG2 antibody (custom produced by Pacific Immunology), followed by AF647-conjugated goat anti-rabbit IgG (LifeTechnologies). TG2 enzymatic activity was measured using 5BP crosslinking, and was visualized by costaining with AF555-conjugated streptavidin (LifeTechnologies). Images were acquired at 10x magnification using a Leica SP8 Laser Scanning Confocal microscope. TG2 activity was quantified by systematically taking two sections of small intestine from each mouse, quantifying the 5BP signal / TG2 protein signal on a per villi basis. The mean 5BP signal / TG2 signal is shown for each mouse that was assessed.

3.5.11 RNA extraction, cDNA synthesis, RNAseq

Total RNA isolation was performed on epithelial and LP cells using the RNeasy Mini Kit (Qiagen). RNA concentration and quality were determined by UV spectrophotometry (Epoch Microplate Spectrophotometer, BioTek). RNA was extracted using RNeasy columns (QIAGEN). RNA integrity was assessed by Bioanalyzer (Agilent). All included samples showed RNA integrity number (RIN) above 8. RNA-sequencing libraries were prepared using the SMARTer® Stranded Total RNA Sample Prep Kit-HI Mammalian by Clontech Laboratories (Takara), according to manufacturer's instructions. Libraries quality was checked by Bioanalyzer (Agilent) prior to pooling and sequencing. Indexed cDNA libraries were pooled in equimolar amounts and sequenced with single-end 50bp reads with a high output Flow Cell (8 lane flow cell) on an Illumina HiSeq4000 at the University of Chicago Genomic Facility.

CHAPTER 4. DISCUSSION

4.1 Crosstalk between tissue stress and adaptive immunity

4.1.1 The crosstalk between tissues and effector lymphocytes

The causative agent of CeD is foreign, meaning that despite the presence of autoantibodies against TG2, it is not strictly an autoimmune disorder. However, the loss of tolerance to what should be an innocuous antigen, the specific killing of enterocytes, and the large number of susceptibility loci that are shared between CeD and other autoimmune disorders (Trynka et al., 2010; Cho and Feldman, 2015) suggests that the insight that we glean from our study of CeD will have great relevance to organ-specific autoimmune disorders.

The LOT seen in potential CeD patients without apparent small intestinal enteropathy (**Section 1.1.3)**, and the lack of villous atrophy seen in mouse models that solely have the induction of Th1 immunity against oral antigen (**Section 1.3.1**) convincingly demonstrate that the LOT to gluten is not sufficient for the development of tissue destruction. Intriguingly, what can be seen in these models of LOT (**Table 1.2**), and in gluten fed DQ8-IL-15^{LP} mice (**Extended data Fig. 2.3**) is the fact that Th1 immunity leads to an increase in the number of IELs in the epithelium, however, in the absence of additional input, it appears that these cells do not have the ability to kill.

This is in line with observations from a mouse model of T1D that has β islet cells that are engineered to express lymphocytic choriomeningitis virus (LCMV) glycoprotein (GP) under the control of the rat insulin promoter (Lang et al., 2005). When these mice

were infected with LCMV, GP-specific $CD8^+$ T cells infiltrated the pancreas and killed the GP expressing β islet cells, causing diabetes (Lang et al., 2005). In contrast, when mice were immunized with LCMV-GP peptide, although there is a large infiltration of activated GP-specific $CD8^+$ T cells into the pancreas, there was no β islet cell killing and no disease, and the authors demonstrate that the missing component of disease is the TLR- and type I IFN-dependent upregulation of MHC class I on the surface of the β islet cells (Lang et al., 2005).

Epithelial IL-15 in DQ8-IL-15^{LPxIEC} mice is required for the gluten-dependent upregulation of stress ligands Rae-1 and Qa1 on the surface of IECs (**Extended data Fig. 2.3I, J**), and surface expression of these ligands is what permits licensed IE-CTL to target these IECs for killing, explaining why villous atrophy only develops with epithelial IL-15 overexpression (**Extended data Fig. 2.3A**). The role for the tissue inflammation in the development of organ-specific autoimmunity is further corroborated by genomic studies in T1D patients. GWAS studies identified more than 50 loci associated with T1D risk, and RNAseq analysis on human pancreatic islets indicate that >60% of the candidate genes are expressed in islet cells, including pathways related to innate immunity and antiviral activity (Eizirik et al., 2012; Eizirik et al, 2013). In MS, CNS-resident microglia and astrocytes produce a range of inflammatory mediators that recruit and activate lymphocytes (Dendrou et al., 2015), while rheumatoid arthritis is characterized by aberrant fibroblast-like synoviocytes that contribute directly to local cartilage destruction, but also secrete cytokines and chemokines that maintain and exacerbate tissue-specific adaptive immunity (McInnes and Schett, 2011). In psoriasis, damaged keratinocytes

produce uncontrolled levels of canthelicidin antimicrobial peptide (CAMP) as well as other proinflammatory cytokines and chemokines, and this drives the activation and proliferation of tissue-antigen-specific T cells (Greb et al., 2016). We have demonstrated that the inflammatory status of the intestinal epithelium, and the crosstalk between this tissue and the invading lymphocytes appears to be a necessary factor in the pathogenesis of CeD, and the dialogue between target tissues and adaptive immunity appears to be a key component of other organ-specific autoimmune disorders as well.

4.1.2 The triggers and impact of antigen-specific adaptive immunity

The development of self-antigen-specific Th1 or Th17 immunity is thought to play a role in the pathogenesis and/or perpetuation of many autoimmune disorders, including T1D, MS, rheumatoid arthritis, psoriasis, autoimmune uveitis, and Crohn's disease (which like CeD is not a classic autoimmune disorder, but involves LOT and tissue destruction in response to what should be a tolerance-inducing antigen, in this case the microbiota) (Sospreda and Martin, 2005; Luger et al., 2008; Palmer and Weaver, 2010; Baumgart and Sandborn, 2012; Patel and Kuchroo, 2015). Understanding how LOT occurs in the context of CeD and the role it plays in tissue destruction can give us insight into the genesis and impact of the $CD4^+$ T cell response in these other organ-specific autoimmune diseases.

As discussed in **Section 1.1.2**, two factors that can lead to the induction of Th1 immunity against gluten in mice are infection with viruses that induce an IRF1-dependent pro-inflammatory transcriptional signature in the inductive sites of the gut immune system

(Bouziat et al., 2017; Bouziat et al., 2018), and the overexpression of IL-15 in the LP of mice at the time of gluten exposure (DePaolo et al., 2011). Exactly when and how IL-15 is dysregulated during the course of disease is a remaining question of huge importance. Additional factors that have been implicated in the LOT to gluten are type I IFN, and dysbiosis (Kim et al., 2015), and a role for both pathogenic infection (Ercolini and Miller, 2009) and the microbiota (Yurkovetskiy et al., 2015) has been proposed in the pathogenesis of many autoimmune disorders.

To understand the role that $CD4^+$ T cells play in tissue destruction, we used GK1.5 to deplete $CD4^+$ T cells over the course 30 days of gluten feeding (although one caveat with this experimental approach is that we are depleting all $CD4^+$ T cells, because targeted depletion of gluten-specific $CD4^+$ T cells was not possible). We demonstrate that this leads to an abrogation of the gluten-specific antibody response (**Fig. 2.3A, B** and **Extended data Fig. 2.5D,E**), demonstrating that the activation of gluten-specific B cells appears to be T dependent as was previously hypothesized (Spencer and Sollid, 2016). Importantly, $CD4^+$ T cells were required for the expansion of IE-CTLs with a fully activated phenotype (**Fig. 2.3D-G**) suggesting that the Th1 response seen in CeD patients directly contributes to IE-CTL licensing, expansion, and/or survival. Finally, without LP IL-15 driving the LOT to gluten (**Extended data Fig. 2.3A**), or without $CD4^+$ T cells (**Fig. 2C**), tissue destruction does not occur, and the magnitude of tissue destruction is directly correlated to the number of $NKG2D^+$ and granzyme B^+ IE-CTL that are present in the epithelium (**Fig. 2.2E-G**). IFNγ causes the upregulation of HLA-E on human enterocytes (Meresse et al., 2006), providing a potential link between Th1 immunity and stress ligands.

In our models, it appears that $CD4^+$ T cells are dispensable for the upregulation of stress ligands on IECs (**Fig. 2.3H, I**), however the full impact of the gluten-driven $CD4^+$ T cell response on the epithelium remains to be assessed by RNA sequencing.

In summary, it appears that the reason that LOT is required for the pathogenesis of CeD is that without it, it is not possible to get to the number of hyperactivated IE-CTL necessary to cause tissue destruction. The quantitative nature of disease development is further emphasized by the requirement for both HLA-DQ8 and TG2 enzymatic activity in the development of villous atrophy.

4.2 The amplification of adaptive immunity

4.2.1 The role of disease predisposing MHC class II molecules

Our observation that although IL-15^{LPxIEC} mice also exhibit the LOT to gluten, HLA-DQ8 is required for the licensing of IE-CTL and the development of villous atrophy (**Fig. 2.4A-G**) demonstrates that there is something unique about HLA-DQ8 that is required for optimal disease development (particularly given the fact that our HLA-DQ8^{+} mice are otherwise equivalent for endogenous MHC class II molecule I-A^{b} as shown in **Extended data Fig. 2.6A**). As discussed at length in **Section 1.2.3**, the property that distinguishes HLA-DQ2 and HLA-DQ8 from other MHC class II molecules is their affinity for the negatively-charged glutamate residues that are found in gliadin peptides that have been modified by TG2 (as well as their ability to accommodate proline residues).

Comparative transcriptional analysis between strains (**Fig. 2H, I and Extended data Fig. 2.6E**) demonstrates that some pathways are enriched by gluten feeding (particularly those related to metabolic processes), some pathways are enriched by IL-15 overexpression (including pathways involved in antigen processing and presentation in the LP), but that the presence of both IL-15-mediated LOT, and DQ8-mediated amplification is required for complete immune activation (**Fig. 2H, I and Extended data Fig. 2.6E)** and for IE-CTLs to reach the levels required for tissue destruction (**Fig. 2.4A, D-G**).

Of note, the observation that CeD predisposing HLA molecules are not required for the LOT to gluten (**Fig. 2.4A-C**) suggests that LOT to gluten can occur in individuals that do not have CeD predisposing MHC haplotypes. The presence of anti-deamidated

gliadin peptide IgG in the serum of IL-15^{LPxIEC} mice (**Fig. 2.4B**), is consistent with the presence of gluten-specific antibodies in HLA-DQ2^{-}/DQ8^{-} individuals (Kaukinen et al., 2002), and suggests that there may be gluten-dependent TG2 activation in these mice and a T cell response against deamidated gliadin peptides, and this remains to be clarified.

4.2.2 Posttranslational modifications of antigens

Observations from patients have shown that the enzymatic activity of TG2 plays a central role in CeD pathogenesis (**Section 1.2.3**; **Section 3.2**). One of the roadblocks in the generation of pathophysiologically relevant mouse models of CeD until this point has been the lack of models with *in vivo* TG2 activation (Costes et al., 2015). The DQ8-IL-15^{LPxIEC} mouse model has TG2 activation after 30 days of gluten feeding (**Fig. 3.4A**). Interestingly, IL-15 overexpression in the epithelium and LP is not sufficient to drive TG2 activation, as the majority of mice on a GFD have a 5-BP signal that is similar to levels seen with mice that are treated with TG2 inhibitor (**Fig. 3.4A**). We are currently investigating how gluten-feeding drives the activation of TG2 in this model (**Section 5.2**), as well as during the course of infection with the LOT-inducing pathogen, reovirus T1L (**Fig.1.3; Section 5.3**).

Importantly, the activity of TG2 is required for the development of villous atrophy in gluten-fed DQ8-IL-15^{LPxIEC} mice (**Fig. 3.3A, B**), further illustrating the requirement for the amplification of the anti-gluten CD4^{+} T cell response. Deamidation of gluten causes it to have a higher binding affinity for HLA-DQ8 (**Section 1.2.3**). The increased binding

affinity of deamidated gluten to HLA-DQ2 and HLA-DQ8 is relevant to the magnitude of the $CD4^+$ T cell response of CeD because it has been shown that the half-life of MHC-peptide interaction is proportional to number of T cells that can be activated by a specific MHC-peptide combination (Henrickson et al., 2008). Additionally, deamidation allows for the recruitment of $CD4^+$ T cells with different TCR specificities than those that can be stimulated by native gluten peptide when it is presented by HLA-DQ8 (Hovhannisyan et al., 2008), and the magnitude of a $CD4^+$ T cell response is directly related to the initial population size of naïve T cells (Moon et al., 2007). Of particular relevance will be future studies that investigate the kinetics of TG2 activation juxtaposed against the induction of Th1 immunity in T cells that have specificity for native or deamidated gliadin peptides (**Section 5.1**).

It has been widely suggested that the posttranslational modification of antigens may play a role in breaking tolerance to self-antigens through the creation of neoepitopes that can activate T cells that have not been negatively selected in the thymus. This has been proposed in autoimmune disorders including T1D, systemic lupus erythematosus, rheumatoid arthritis, collagen-induced arthritis, atherosclerosis, and MS (Doyle and Mamula, 2001; Sollid and Jabri, 2011). Here we have demonstrated in the context of CeD that posttranslational modifications and the creation of additional epitopes can also play a critical role in the amplification of adaptive immunity to reach the threshold necessary for pathology.

4.3 The pathogenesis of complex immune disorders

The specific causes of most autoimmune diseases are not known. MHC class II genes are associated with many autoimmune disorders (**Section 4.2.1**), as are polymorphisms of non-MHC genes, particularly variants in genes that code for innate and adaptive immunity (Abadie et al., 2011; Cho and Feldman, 2015), however these MHC haplotypes and disease predisposing factors are also found in many individuals that do not develop disease, highlighting the complex and multifactorial nature of these disorders. CeD provides a unique opportunity to understand how autoimmune disorders develop because of the amount that is known about disease pathogenesis (**Chapter 1**). The DQ8-IL-15^{LPxIEC} mouse model has allowed us to directly investigate the respective contributions of disease-predisposing HLA molecules, dietary gluten, auto-antigen TG2, and the innate and adaptive immune responses in the development of tissue destruction (**Chapter 2 and 3**).

Based on these studies, our current belief is that the development of organ-specific autoimmunity is one that requires a dialogue between the inflamed target tissues and antigen-specific adaptive immune cells (**Section 4.1**). The production of cytokines, chemokines, and proinflammatory molecules (such as IL-15) from tissue cells leads to the recruitment, activation, and proliferation of adaptive immune cells, and in the case of CeD, the upregulation of stress ligands appears to be necessary for the specific targeting of IECs.

Additionally, there is a requirement for the amplification of adaptive immunity to reach the inflammatory threshold necessary for the development of pathology and full-

blown disease (**Section 4.2**). In DQ8-IL-15^{LPxIEC} mice, the activation of TG2 and resultant posttranslational modification of gluten, and the recruitment of additional CD4^{+} T cells with specificity for deamidated gluten peptides presented by HLA-DQ8 appears to be required for the development of tissue destruction. How TG2 and other enzymes associated with the pathogenesis of autoimmunity become activated during the course of disease will be a key question with important therapeutic implications (**Section 5.2 and 5.3**). The incomplete penetrance of villous atrophy development (**Fig. 2.1**) and TG2 activation (**Fig. 3.4**) in gluten fed DQ8-IL-15^{LPxIEC} mice suggests that there are additional, potentially stochastic, events that contribute to the development of CeD.

This illustrates the fact that the autoimmune disorders are likely the result of multiple factors, that could include predisposing genes and environmental inputs that can influence the target tissues, the aberrant activation of adaptive immunity, and the activity of enzymes and processes that can amplify this adaptive immune response. In turn, these components of disease interact with one another, and this series of unfortunate events can lead to the development of disease (**Fig. 4.1**). The events that are required to reach the disease threshold explains why these disorders are not more common, why many of these disorders have variable ages of onset, and also why they are so difficult to treat. Future studies with the DQ8-IL-15^{LPxIEC} mouse model and its variants (**Section 5**) will provide further insight into the pathogenesis and treatment of CeD and autoimmunity.

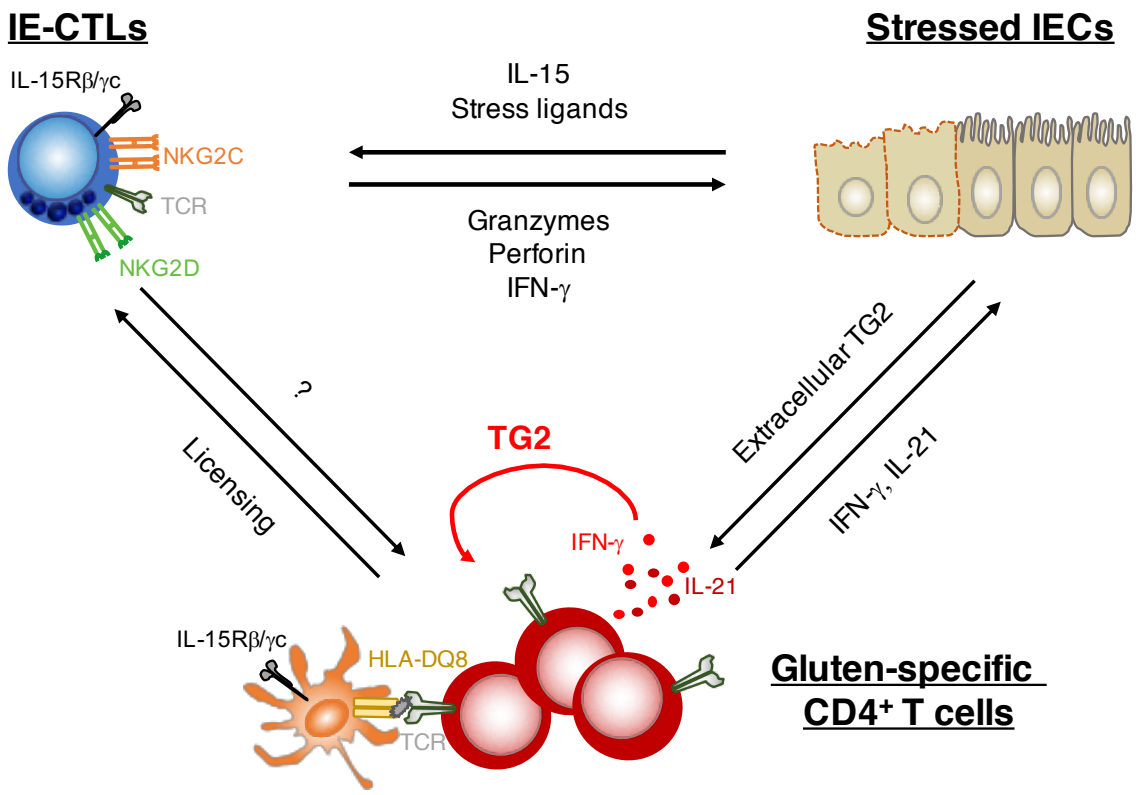

Figure 4.1. Celiac disease pathogenesis
The interplay between the three main components of disease is illustrated.
1. IL-15 overexpression in the LP causes the activation of inflammatory DCs, which cause the induction of gluten-specific Th1 immunity and the secretion of IFNγ and IL-21. IFNγ and other environmental factors cause the activation of TG2, which amplifies the gluten-specific $CD4^+$ T cell response.
2. IL-15 overexpression in the epithelium leads to the upregulation of stress ligands on the surface of IECs, and drives the activation of IE-CTL. The amplified $CD4^+$ T cell response is required for full licensing of IE-CTL, and these hyperactivated IE-CTL mediate tissue destruction through the production cytotoxic molecules and IFNγ. We did not observe an impact of IEL depletion on the gluten-specific adaptive immune response, but there may be uncharacterized effects.
3. Tissue destruction can lead to the liberation of intracellular TG2, further amplifying the gluten-specific $CD4^+$ T cell response to the point of total villous atrophy.
Non-MHC genetic factors and environmental inputs (such as infections, perturbations of the microbiota, toxins and drugs) can contribute to all three components of disease.

CHAPTER 5. FUTURE DIRECTIONS

5.1 Remaining questions

We have demonstrated the requirement for $CD4^+$ T cells in the production of disease-specific antibodies, as well as the licensing of IE-CTL and the development of villous atrophy through depletion of $CD4^+$ cells over the course of gluten feeding (**Section 2** and **Section 4.1.2**). Furthermore, the combined requirement for HLA-DQ8 and TG2 activity in the development of disease suggests that there needs to be an amplification of gluten-specific Th1 immunity to reach the threshold necessary for IE-CTL licensing and subsequent tissue destruction (**Section 2, Section 3,** and **Section 4.2**).

Here, I discuss ongoing and future studies that will allow us to investigate the dynamics of the gluten-specific $CD4^+$ T cell response while determining the role of TG2-mediated deamidation of gluten in the amplification of the Th1 response (**Section 5.2**). We will use additional mouse models to investigate the differences in Th1 magnitude between mice bearing HLA-DQ2 and HLA-DQ8, as well as the temporal requirements for IL-15 overexpression in the development of CeD phenotypes (**Section 5.2**). Finally, we will investigate the mechanism of TG2 activation in DQ8-IL-15^{LPxIEC} mice (**Section 5.3**) as well as in the context of reovirus infection (**Section 5.4**).

5.2 Investigation into the dynamics of CeD pathogenesis

5.2.1 The gluten-specific CD4⁺ T cell response

We demonstrated the requirement for HLA-DQ8, and TG2 activity for the development of disease, leading us to hypothesize that an amplification of the gluten-specific CD4 T cell response is occurring and required for the development of villous atrophy in our DQ8-IL-15^{LPxIEC} mice. However, our lack of tools for isolating the DQ8-restricted gluten-specific CD4⁺ T cells has prevented a direct measurement of this gluten-specific Th1 response.

Preliminary studies using DQ8 tetramers loaded with either the immunodominant gliadin-α1 peptide or the gliadin-γ1 peptide (Tollefsen et al. 2006) did not stain the CD4⁺ T cells from the mLN and LP of gluten-fed DQ8-IL-15^{LPxIEC} mice (**Fig. 5.1**).

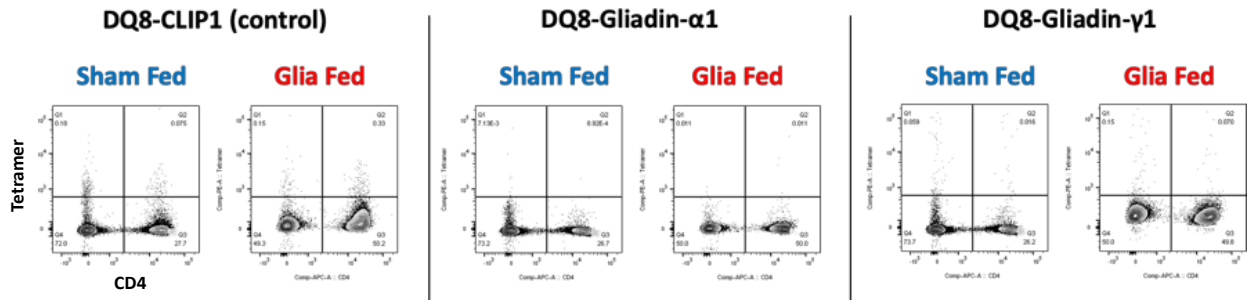

Figure 5.1. DQ8 gliadin tetramer staining
DQ8-IL-15^{LPxIEC} mice were fed with gluten for 30 days. mLN and LP cells were stained for CD4⁺ and with gliadin peptide loaded DQ8 tetramers (or CLIP1 loaded control tetramer) prepared and stained according to previous reports (Tollefsen et al, 2006). Representative mLN flow plots are shown, n=3 / group. Cells were pre-gated on CD45⁺ TCRb⁺ CD19⁻ CD11c⁻ CD14⁻ MHCII⁻ NK1.1⁻ population. No positive staining was seen in the mLN or LP in sham or gluten fed mice. In the same experiment, we had 100% positive staining for human T cell clones generated from CeD patients with specificity for these peptides.

This lack of positive staining with DQ8-gliadin tetramers likely reflects the rarity of DQ-restricted gluten-specific CD4⁺ T cells; these cells only make up 0.1-1.2% of all CD4⁺ T

cells in active CeD small intestines (Bodd et al., 2013). Therefore, we will attempt to stain for these cells after enrichment by using cell sorting to first isolate only $CD4^+$ T cells, or we can enrich with the DQ8-gliadin tetramers themselves (Benlagha et al., 2005; Moon et al., 2007). Once we are able to directly stain and isolate DQ8-restricted gluten-specific $CD4^+$ T cells, this will allow us to perform transcriptional analysis on these cells and confirm that in our mouse model, they are Th1 in nature. Importantly, this will allow us to confirm that in mice that lack DQ8 (IL-15^{LPxIEC} mice) or in gluten-fed DQ8-IL-15^{LPxIEC} mice treated with TG2 inhibitors, the magnitude of anti-gluten Th1 immunity is lower than in gluten-fed DQ8-IL-15^{LPxIEC} mice that develop villous atrophy. Additionally, it will allow for a direct correlation between the magnitude of the gluten-specific Th1 response and IE-CTL activation as well as measurements of tissue destruction.

Additionally, we are going to create TCR transgenic mice that have TCRs with specificity for gluten to measure the temporal dynamics and magnitude of the gluten-specific $CD4^+$ T cell response. Previous studies from our lab have identified the sequences of TCRs that have specificity for native gluten peptide (N-TCR), TCRs that have specificity for deamidated gluten peptide (D-TCR), and TCRs that can recognize both (N=D-TCR) presented by HLA-DQ8 (Hovhannisyan et al., 2008). We will generate TCR transgenic mice that have $CD4^+$ cells bearing these TCRs to dissect the role $CD4^+$ dynamics as well as the requirement for deamidation on the peptide response of $CD4^+$ T cells in DQ8-IL-15^{LPxIEC} mice over the course of gluten feeding. We will perform a time-course study that examines the activation, expansion, and functionality of T cells with N-, D-, and N=D- TCRs during the development of CeD, juxtaposed against the dynamics of

TG2 activation in these mice. We predict that at earlier timepoints, we will see the activation and expansion of N-TCR T cells and that upon the activation of TG2, we will see a stronger and more diverse T cell response that also includes T cells with D- and N=D-TCRs.

5.2.2 Comparison of disease pre-disposing HLA molecules

We have recently received HLA-DQ2tg mice (de Kauwe et al., 2009), that we are crossing to our IL-15^{LPxIEC} mice. HLA-DQ2 poses a significantly higher risk for developing CeD than HLA-DQ8, with 90% of CeD patients having at least one copy of HLA-DQ2 (Karrell et al., 2003), and by having both HLA-DQ2^{+} and HLA-DQ8^{+} mice we will be able to directly investigate why this is the case. The gluten epitopes that are presented by HLA-DQ2 and HLA-DQ8 are distinct, and it is currently believed that the ability of the HLA-DQ2 binding pocket to facilitate a wider range of gluten peptides explains why HLA-DQ2 confers a greater disease risk (Jabri and Sollid, 2009; Tjon et al., 2010). If this is indeed the case then we can expect to see a gluten-dependent Th1 response that is greater in magnitude in HLA-DQ2^{+} mice, and greater disease penetrance. Additionally, it has been proposed that although HLA-DQ8 is able to present native gluten peptides, HLA-DQ2 cannot (Hovhannisyan et al., 2008; Sollid, 2017), and having both of these strains will eventually allow us to indirectly and directly address this question, through a combination of TG2 activation, serology, and T cell dynamics.

5.2.3 Spatial and temporal modulation of IL-15 overexpression

Finally, due to previous issues with mice utilizing the D^d promoter, I generated an alternative IL-15tg construct that utilizes the CMV+β-actin promoter which has strong expression in all tissue sites across all strains of mice (**Fig. 5.2**).

Figure 5.2. IL-15 tg SK2 construct.
Flox sites are indicated with arrows. Cre expression drives the excision of GFP and this results in the transcription of transgenic IL15.

Transgenic mice with this SK2 construct only express IL-15 in the presence of a Cre recombinase, thus giving us a mouse in which we have the ability to turn on IL-15 expression in specific cell types or tissues by crossing these mice to mice expressing Cre recombinase under the control of tissue specific promoters. This also gives us the option to use inducible Cre systems in which the expression of IL15 can be driven by administration of compounds such as tamoxifen, allowing for the temporal control of IL15 expression. The progeny of SK2tg mice crossed with Rosa26-Cre/ERT2 mice have IL-15 production in the epithelium and LP upon tamoxifen treatment (**Fig. 5.3**), and this will allow us to investigate the impact of IL-15 overexpression in intestines of adult mice, without the impact of constitutive IL-15 expression during development. Furthermore, this will allow for an assessment of the dynamics of our CeD phenotypes immediately upon IL-15 overexpression to more clearly elucidate the role of IL-15 on these phenotypes.

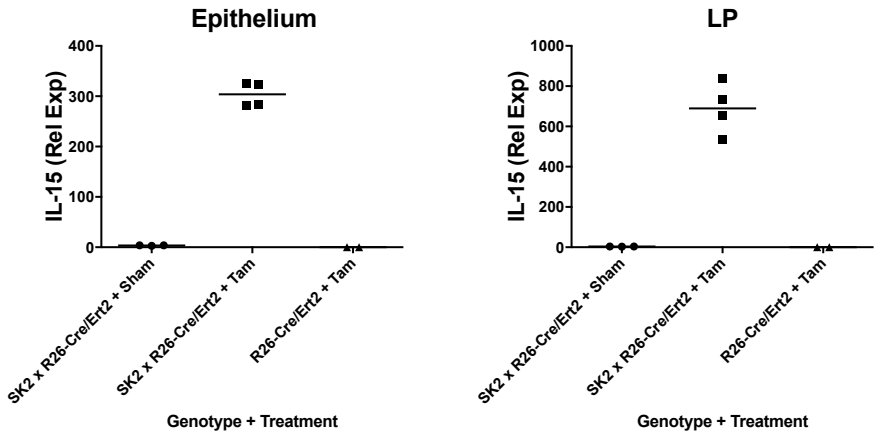

Figure 5.3. IL-15 induction upon tamoxifen treatment of IL-15tg mice
IL-15tg SK2 mice were crossed with Rosa26-Cre/ERT2 mice (purchased from Jackson Laboratories). 14 days after gavage with tamoxifen, IL-15 levels were measured in the small intestinal epithelium and LP by qPCR. IL-15 expression, relative to housekeeping gene GAPDH are shown. Vehicle gavaged mice (SK2 x R26-Cre/Ert2 + Sham) or tamoxifen gavaged mice lacking the IL-15tg SK2 construct (R26-Cre/Ert2 + Tam) were used as controls.

5.3 Investigation of the mechanism of gluten-dependent TG2 activation in the DQ8-IL-15^{LPxIEC} mouse model

5.3.1 Investigate TG2 activation during the pathogenesis of CeD.

We have seen the gluten-dependent activation of TG2 in DQ8-IL-15^{LPxIEC} mice (**Chapter 3**) and will further investigate how and when TG2 is activated during the progression of disease. Given the demonstration that IFNγ positively regulates TG2 activity (DiRaimondo et al., 2012), one plausible hypothesis is that TG2 is activated by IFNγ produced by CD4$^+$ T cells that are specific against native gluten peptides. To determine if the Th1 immune response is required for the TG2 activity, we will utilize neutralizing antibodies against IL-12 and IFNγ to block Th1 differentiation, and Th1 effector function, respectively, and see the effects on TG2 activity. It will also be informative to test whether TG2 activation requires HLA-DQ8 by feeding gluten to IL-15^{LPxIEC} mice, especially given the fact that we see anti-DGP IgG in the serum of these mice (**Fig. 2.4B**). If our hypothesis that Th1 immunity can drive the activation of TG2 is correct, one would expect to see lower levels of TG2 activity in IL-15^{LPxIEC} mice given the lower levels of immune activation seen in these mice (**Fig. 2H,I and Extended data Fig. 2.6E**).

5.3.2 Investigate the molecular mechanisms of TG2 activation.

The activation of the deamidation activity of TG2 is a two-step process involving the release or export of intracellular TG2 into the extracellular space, and the reduction of a disulfide bond that locks TG2 in an inactive conformation (**Section 1.2.2**). Trx is a

redox protein that has the ability to reduce this disulfide bond in vitro (Jin et al., 2011), and injection of Trx into mice causes the activation of intestinal TG2 (Plugis et al., 2017). We have generated preliminary data that demonstrates that Trx is upregulated upon gluten feeding in DQ8-IL-15^{LPxIEC} mice, and it also appears to be upregulated in the serum of CeD patients (**Fig 5.4**). Additionally, we have access to a small molecule inhibitor of Trx, NP161, through our coloration with the Khosla lab at Stanford University (Plugis et al., 2017). Therefore, to demonstrate that Trx plays a role in the activation of TG2 in DQ8-IL-15^{LPxIEC} mice, we will treat mice with NP161 over the course of gluten feeding, and determine whether they have TG2 activation. If Trx is required for the activation of TG2 in our model, inhibition of Trx would presumably abrogate the CeD-associated phenotypes that we see downregulated upon TG2 inhibition (**Chapter 3**), further validating Trx and TG2 as promising therapeutic targets.

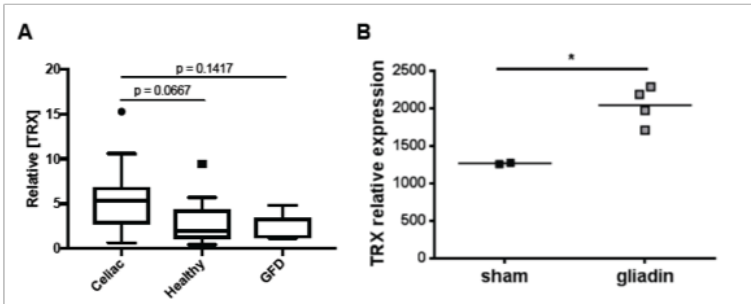

Figure 5.4. Upregulation of Trx in CeD
(A) Serum TRX levels in CeD patients (n=15), healthy controls (n=12), and CeD patients on a gluten-free diet (GFD, n=8). Statistics were performed using a two-tailed Mann-Whitney U Test. (B) TRX expression in gliadin-fed DQ8-Dd-villin IL-15 tg mice. Mice were sham- or gliadin-fed 10 days, and lamina propria cells were isolated. TRX gene expression in the lamina propria was determined by qPCR (p=0.0157; student t test)

5.4 Investigation of the mechanism of reovirus-induced activation of TG2.

Infection with reovirus T1L leads to the activation of TG2 (**Fig. 1.3**). We have demonstrated that T1L infection drives the production of Type I IFNs as well as the polarization of Tbet^{+} IFNγ producing CD4 T cells (Th1) specific to oral antigen (Bouziat et al., 2017). We will investigate the host factors that are required for the T1L mediated activation of TG2 by utilizing knockout mice. After these studies are performed, we can further fine tune our hypothesis – we also recognize the possibility that there could be multiple pathways that can lead to the activation of TG2 and that this redundancy may obscure the contribution of a single candidate pathway.

5.4.1 Determine whether detection of viral dsRNA by pattern recognition receptors (PRRs) is required for the T1L mediated activation of TG2.

Given that viral dsRNA analog polyI:C is sufficient to activate TG2 in vivo (Siegel et al., 2008), it will be necessary to determine whether the T1L mediated activation of TG2 is caused by detection of the recognition of viral dsRNA by PRRs. TLR3 and RIG-I/MDA5 are the known sensors of dsRNA, and signaling through these receptors converges upon the phosphorylation and nuclear localization of transcription factor IRF3. Therefore, we will utilize IRF3$^{-/-}$ mice and based on the results of this infection, we can further determine which PRRs could be associated with TG2 activation.

5.4.2 Determine whether Type I IFN signaling is required for the T1L mediated activation of TG2.

One consequence of viral recognition by PRRs is the production of Type I IFNs. T1L drives the production of Type I IFN and IFN stimulated genes in PP, mLN, and small intestinal LP of infected mice and we have preliminary experiments that show that oral IFNβ administration is sufficient to drive the activation of TG2 in vivo. Therefore, it will be important to determine whether the T1L mediated activation of TG2 is dependent on Type I IFN signaling by infecting $IFNAR^{-/-}$ mice and determining whether we see TG2 activation.

5.4.3 Determine whether IRF1 signaling is required for T1L mediated activation of TG2.

Another signaling pathway that we have seen upregulated upon T1L infection is the IRF1 pathway, and signaling through this pathway can occur in the absence of Type I IFN signaling (i.e. in $IFNAR^{-/-}$ mice) in response to infection. It is known that IRF1 signaling can lead to the production of inflammatory molecules IL-12, IFNγ, and IL-1β and we have data that demonstrates that when $IRF1^{-/-}$ mice are infected with T1L, there is no longer Th1 polarization of oral antigen specific naïve T cells. Given the demonstrated impact of IRF1 in this model, it will be informative to investigate whether TG2 can become activated in T1L infected $IRF1^{-/-}$ mice as a potential alternative mechanism to IRF3 and/or type I IFN-mediated activation.

5.5 Treatments for celiac disease

The overarching goal of this work is the generate and implement new therapeutic strategies for CeD to increase the quality of life for individuals with disease, particularly those that are non-responsive to a GFD. We have used the DQ8-IL-15^{LPxIEC} mouse model to demonstrate the promise of anti-IL15 (**Fig. 2.5C-L**) and TG2 inhibitors (**Fig. 3.3 and 3.4**) in the treatment and prevention of disease, and will continue to test potential therapeutic strategies and fine-tune our understanding of disease pathogenesis with the ultimate goal of finding a cure for CeD.

BIBLIOGRAPHY

Abadie, V., and Jabri, B. (2014). IL-15: a central regulator of celiac disease immunopathology. Immunological Reviews *260*, 221–234.

Abadie, V., Sollid, L.M., Barreiro, L.B., and Jabri, B. (2011). Integration of genetic and immunological insights into a model of celiac disease pathogenesis. Annu. Rev. Immunol. *29*, 493–525.

Adelman, D.C., Murray, J., Wu, T.-T., Mäki, M., Green, P.H., and Kelly, C.P. (2018). Measuring Change In Small Intestinal Histology In Patients With Celiac Disease. Am. J. Gastroenterol. *113*, 339–347.

Balajthy, Z., Csomós, K., Vámosi, G., Szántó, A., Lanotte, M., and Fésüs, L. (2006). Tissue-transglutaminase contributes to neutrophil granulocyte differentiation and functions. Blood *108*, 2045–2054.

Bamford, R.N., DeFilippis, A.P., Azimi, N., Kurys, G., and Waldmann, T.A. (1998a). The 5' untranslated region, signal peptide, and the coding sequence of the carboxyl terminus of IL-15 participate in its multifaceted translational control. J. Immunol. *160*, 4418–4426.

Bamford, R.N., DeFilippis, A.P., Azimi, N., Kurys, G., and Waldmann, T.A. (1998b). The 5′ Untranslated Region, Signal Peptide, and the Coding Sequence of the Carboxyl Terminus of IL-15 Participate in Its Multifaceted Translational Control. The Journal of Immunology *160*, 4418–4426.

Bauer, S., Groh, V., Wu, J., Steinle, A., Phillips, J.H., Lanier, L.L., and Spies, T. (1999). Activation of NK cells and T cells by NKG2D, a receptor for stress-inducible MICA. Science *285*, 727–729.

Baumgart, D.C., and Sandborn, W.J. (2012). Crohn's disease. The Lancet *380*, 1590–1605.

Belkin, A.M. (2011). Extracellular TG2: emerging functions and regulation. FEBS J. *278*, 4704–4716.

Benjamini, Y., and Hochberg, Y. (1995). Controlling the False Discovery Rate: A Practical and Powerful Approach to Multiple Testing. Journal of the Royal Statistical Society. Series B (Methodological) *57*, 289–300.

van Berge-Henegouwen, G.P., and Mulder, C.J. (1993). Pioneer in the gluten free diet: Willem-Karel Dicke 1905-1962, over 50 years of gluten free diet. Gut *34*, 1473–1475.

Black, K.E., Murray, J.A., and David, C.S. (2002). HLA-DQ determines the response to exogenous wheat proteins: a model of gluten sensitivity in transgenic knockout mice. J. Immunol. *169*, 5595–5600.

Bouziat, R., Hinterleitner, R., Brown, J.J., Stencel-Baerenwald, J.E., Ikizler, M., Mayassi, T., Meisel, M., Kim, S.M., Discepolo, V., Pruijssers, A.J., et al. (2017). Reovirus infection triggers inflammatory responses to dietary antigens and development of celiac disease. Science *356*, 44–50.

Bouziat, R., Biering, S.B., Kouame, E., Sangani, K.A., Kang, S., Ernest, J.D., Varma, M., Brown, J.J., Urbanek, K., Dermody, T.S., et al. Murine Norovirus Infection Induces TH1 Inflammatory Responses to Dietary Antigens. Cell Host & Microbe *0*.

Bragde, H., Jansson, U., Fredrikson, M., Grodzinsky, E., and Söderman, J. (2018). Celiac disease biomarkers identified by transcriptome analysis of small intestinal biopsies. Cell. Mol. Life Sci. *75*, 4385–4401.

Braud, V.M., Allan, D.S., O'Callaghan, C.A., Söderström, K., D'Andrea, A., Ogg, G.S., Lazetic, S., Young, N.T., Bell, J.I., Phillips, J.H., et al. (1998). HLA-E binds to natural killer cell receptors CD94/NKG2A, B and C. Nature *391*, 795–799.

Bray, N.L., Pimentel, H., Melsted, P., and Pachter, L. (2016). Near-optimal probabilistic RNA-seq quantification. Nat. Biotechnol. *34*, 525–527.

Cammarota, G., Cuoco, L., Cianci, R., Pandolfi, F., and Gasbarrini, G. (2000). Onset of coeliac disease during treatment with interferon for chronic hepatitis C. Lancet *356*, 1494–1495.

Canova, C., Zabeo, V., Pitter, G., Romor, P., Baldovin, T., Zanotti, R., and Simonato, L. (2014). Association of maternal education, early infections, and antibiotic use with celiac disease: a population-based birth cohort study in northeastern Italy. Am. J. Epidemiol. *180*, 76–85.

Carson, W.E., Fehniger, T.A., Haldar, S., Eckhert, K., Lindemann, M.J., Lai, C.F., Croce, C.M., Baumann, H., and Caligiuri, M.A. (1997). A potential role for interleukin-15 in the regulation of human natural killer cell survival. J. Clin. Invest. *99*, 937–943.

Chen, Y., Inobe, J., Marks, R., Gonnella, P., Kuchroo, V.K., and Weiner, H.L. (1995). Peripheral deletion of antigen-reactive T cells in oral tolerance. Nature *376*, 177–180.

Cho, J.H., and Feldman, M. (2015). Heterogeneity of autoimmune diseases: pathophysiologic insights from genetics and implications for new therapies. Nat. Med. *21*, 730–738.

Colpitts, S.L., Stoklasek, T.A., Plumlee, C.R., Obar, J.J., Guo, C., and Lefrançois, L. (2012). Cutting edge: the role of IFN-α receptor and MyD88 signaling in induction of IL-15 expression in vivo. J. Immunol. *188*, 2483–2487.

Coombes, J.L., Siddiqui, K.R.R., Arancibia-Cárcamo, C.V., Hall, J., Sun, C.-M., Belkaid, Y., and Powrie, F. (2007). A functionally specialized population of mucosal CD103+ DCs induces Foxp3+ regulatory T cells via a TGF-beta and retinoic acid-dependent mechanism. J. Exp. Med. *204*, 1757–1764.

Costes, L.M.M., Meresse, B., Cerf-Bensussan, N., and Samsom, J.N. (2015a). The role of animal models in unravelling therapeutic targets in coeliac disease. Best Pract Res Clin Gastroenterol *29*, 437–450.

Costes, L.M.M., Meresse, B., Cerf-Bensussan, N., and Samsom, J.N. (2015b). The role of animal models in unravelling therapeutic targets in coeliac disease. Best Practice & Research Clinical Gastroenterology *29*, 437–450.

Curotto de Lafaille, M.A., Kutchukhidze, N., Shen, S., Ding, Y., Yee, H., and Lafaille, J.J. (2008). Adaptive Foxp3+ regulatory T cell-dependent and -independent control of allergic inflammation. Immunity *29*, 114–126.

Decker, E., Hornef, M., and Stockinger, S. (2011). Cesarean delivery is associated with celiac disease but not inflammatory bowel disease in children. Gut Microbes *2*, 91–98.

Dendrou, C.A., Fugger, L., and Friese, M.A. (2015). Immunopathology of multiple sclerosis. Nature Reviews Immunology *15*, 545–558.

DePaolo, R.W., Abadie, V., Tang, F., Fehlner-Peach, H., Hall, J.A., Wang, W., Marietta, E.V., Kasarda, D.D., Waldmann, T.A., Murray, J.A., et al. (2011). Co-adjuvant effects of retinoic acid and IL-15 induce inflammatory immunity to dietary antigens. Nature *471*, 220–224.

Di Niro, R., Mesin, L., Zheng, N.-Y., Stamnaes, J., Morrissey, M., Lee, J.-H., Huang, M., Iversen, R., du Pré, M.F., Qiao, S.-W., et al. (2012). High abundance of plasma cells secreting transglutaminase 2-specific IgA autoantibodies with limited somatic hypermutation in celiac disease intestinal lesions. Nat. Med. *18*, 441–445.

Di Sabatino, A., Pickard, K.M., Gordon, J.N., Salvati, V., Mazzarella, G., Beattie, R.M., Vossenkaemper, A., Rovedatti, L., Leakey, N.A.B., Croft, N.M., et al. (2007). Evidence for the role of interferon-alfa production by dendritic cells in the Th1 response in celiac disease. Gastroenterology *133*, 1175–1187.

Di Sabatino, A., Vanoli, A., Giuffrida, P., Luinetti, O., Solcia, E., and Corazza, G.R. (2012). The function of tissue transglutaminase in celiac disease. Autoimmun Rev *11*, 746–753.

Dieterich, W., Ehnis, T., Bauer, M., Donner, P., Volta, U., Riecken, E.O., and Schuppan, D. (1997). Identification of tissue transglutaminase as the autoantigen of celiac disease. Nat. Med. *3*, 797–801.

DiRaimondo, T.R., Klöck, C., and Khosla, C. (2012). Interferon-γ Activates Transglutaminase 2 via a Phosphatidylinositol-3-Kinase-Dependent Pathway: Implications for Celiac Sprue Therapy. J Pharmacol Exp Ther *341*, 104–114.

Doyle, H.A., and Mamula, M.J. (2001). Post-translational protein modifications in antigen recognition and autoimmunity. Trends in Immunology *22*, 443–449.

Du, P., Kibbe, W.A., and Lin, S.M. (2008). lumi: a pipeline for processing Illumina microarray. Bioinformatics *24*, 1547–1548.

Du Pré, M.F., Kozijn, A.E., van Berkel, L.A., ter Borg, M.N.D., Lindenbergh–Kortleve, D., Jensen, L.T., Kooy–Winkelaar, Y., Koning, F., Boon, L., Nieuwenhuis, E.E.S., et al. (2011). Tolerance to Ingested Deamidated Gliadin in Mice is Maintained by Splenic, Type 1 Regulatory T Cells. Gastroenterology *141*, 610-620.e2.

Dubois, P.C.A., Trynka, G., Franke, L., Hunt, K.A., Romanos, J., Curtotti, A., Zhernakova, A., Heap, G.A.R., Adány, R., Aromaa, A., et al. (2010). Multiple common variants for celiac disease influencing immune gene expression. Nat. Genet. *42*, 295–302.

Eden, E., Navon, R., Steinfeld, I., Lipson, D., and Yakhini, Z. (2009). GOrilla: a tool for discovery and visualization of enriched GO terms in ranked gene lists. BMC Bioinformatics *10*, 48.

Eizirik, D.L., Colli, M.L., and Ortis, F. (2009). The role of inflammation in insulitis and beta-cell loss in type 1 diabetes. Nat Rev Endocrinol *5*, 219–226.

Eizirik, D.L., Sammeth, M., Bouckenooghe, T., Bottu, G., Sisino, G., Igoillo-Esteve, M., Ortis, F., Santin, I., Colli, M.L., Barthson, J., et al. (2012). The Human Pancreatic Islet Transcriptome: Expression of Candidate Genes for Type 1 Diabetes and the Impact of Pro-Inflammatory Cytokines. PLOS Genetics *8*, e1002552.

Ercolini, A.M., and Miller, S.D. (2009). The role of infections in autoimmune disease. Clin Exp Immunol *155*, 1–15.

Esposito, C., Paparo, F., Caputo, I., Porta, R., Salvati, V.M., Mazzarella, G., Auricchio, S., and Troncone, R. (2003). Expression and enzymatic activity of small intestinal tissue transglutaminase in celiac disease. Am. J. Gastroenterol. *98*, 1813–1820.

Fehniger, T.A., and Caligiuri, M.A. (2001). Interleukin 15: biology and relevance to human disease. Blood *97*, 14–32.

Ferguson, A., Arranz, E., and O'Mahony, S. (1993). Clinical and pathological spectrum of coeliac disease--active, silent, latent, potential. Gut *34*, 150–151.

Freitag, T.L., Rietdijk, S., Junker, Y., Popov, Y., Bhan, A.K., Kelly, C.P., Terhorst, C., and Schuppan, D. (2009). Gliadin-primed CD4+CD45RBlowCD25– T cells drive gluten-dependent small intestinal damage after adoptive transfer into lymphopenic mice. Gut *58*, 1597–1605.

Friedman, A., and Weiner, H.L. (1994). Induction of anergy or active suppression following oral tolerance is determined by antigen dosage. Proc. Natl. Acad. Sci. U.S.A. *91*, 6688–6692.

Galipeau, H.J., Rulli, N.E., Jury, J., Huang, X., Araya, R., Murray, J.A., David, C.S., Chirdo, F.G., McCoy, K.D., and Verdu, E.F. (2011). Sensitization to gliadin induces moderate enteropathy and insulitis in nonobese diabetic-DQ8 mice. J. Immunol. *187*, 4338–4346.

Gallucci, S., Lolkema, M., and Matzinger, P. (1999). Natural adjuvants: endogenous activators of dendritic cells. Nat. Med. *5*, 1249–1255.

Ghazzawi, Y., Rubio-Tapia, A., Murray, J.A., and Absah, I. (2014). Mucosal healing in children with treated celiac disease. J. Pediatr. Gastroenterol. Nutr. *59*, 229–231.

Giri, J.G., Kumaki, S., Ahdieh, M., Friend, D.J., Loomis, A., Shanebeck, K., DuBose, R., Cosman, D., Park, L.S., and Anderson, D.M. (1995). Identification and cloning of a novel IL-15 binding protein that is structurally related to the alpha chain of the IL-2 receptor. EMBO J. *14*, 3654–3663.

Grabstein, K.H., Eisenman, J., Shanebeck, K., Rauch, C., Srinivasan, S., Fung, V., Beers, C., Richardson, J., Schoenborn, M.A., Ahdieh, M., et al. (1994). Cloning of a T cell growth factor that interacts with the beta chain of the interleukin-2 receptor. Science *264*, 965–968.

Greb, J.E., Goldminz, A.M., Elder, J.T., Lebwohl, M.G., Gladman, D.D., Wu, J.J., Mehta, N.N., Finlay, A.Y., and Gottlieb, A.B. (2016). Psoriasis. Nat Rev Dis Primers *2*, 16082.

Greco, L., Romino, R., Coto, I., Di Cosmo, N., Percopo, S., Maglio, M., Paparo, F., Gasperi, V., Limongelli, M.G., Cotichini, R., et al. (2002). The first large population based twin study of coeliac disease. Gut *50*, 624–628.

Green, P.H.R., and Cellier, C. (2007). Celiac disease. N. Engl. J. Med. *357*, 1731–1743.

Groh, V., Bahram, S., Bauer, S., Herman, A., Beauchamp, M., and Spies, T. (1996). Cell stress-regulated human major histocompatibility complex class I gene expressed in gastrointestinal epithelium. Proc. Natl. Acad. Sci. U.S.A. *93*, 12445–12450.

Groh, V., Steinle, A., Bauer, S., and Spies, T. (1998). Recognition of stress-induced MHC molecules by intestinal epithelial gammadelta T cells. Science *279*, 1737–1740.

Günther, C., Buchen, B., He, G.-W., Hornef, M., Torow, N., Neumann, H., Wittkopf, N., Martini, E., Basic, M., Bleich, A., et al. (2015). Caspase-8 controls the gut response to microbial challenges by Tnf-α-dependent and independent pathways. Gut *64*, 601–610.

Hayday, A., Theodoridis, E., Ramsburg, E., and Shires, J. (2001). Intraepithelial lymphocytes: exploring the Third Way in immunology. Nat. Immunol. *2*, 997–1003.

Henderson, K.N., Tye-Din, J.A., Reid, H.H., Chen, Z., Borg, N.A., Beissbarth, T., Tatham, A., Mannering, S.I., Purcell, A.W., Dudek, N.L., et al. (2007). A structural and immunological basis for the role of human leukocyte antigen DQ8 in celiac disease. Immunity *27*, 23–34.

Hovhannisyan, Z., Weiss, A., Martin, A., Wiesner, M., Tollefsen, S., Yoshida, K., Ciszewski, C., Curran, S.A., Murray, J.A., David, C.S., et al. (2008). The role of HLA-DQ8 beta57 polymorphism in the anti-gluten T-cell response in coeliac disease. Nature *456*, 534–538.

Hüe, S., Mention, J.-J., Monteiro, R.C., Zhang, S., Cellier, C., Schmitz, J., Verkarre, V., Fodil, N., Bahram, S., Cerf-Bensussan, N., et al. (2004). A direct role for NKG2D/MICA interaction in villous atrophy during celiac disease. Immunity *21*, 367–377.

Husby, S., Koletzko, S., Korponay-Szabó, I.R., Mearin, M.L., Phillips, A., Shamir, R., Troncone, R., Giersiepen, K., Branski, D., Catassi, C., et al. (2012). European Society for Pediatric Gastroenterology, Hepatology, and Nutrition guidelines for the diagnosis of coeliac disease. J. Pediatr. Gastroenterol. Nutr. *54*, 136–160.

International Multiple Sclerosis Genetics Consortium (2013). Network-based multiple sclerosis pathway analysis with GWAS data from 15,000 cases and 30,000 controls. Am. J. Hum. Genet. *92*, 854–865.

Iwata, M., Hirakiyama, A., Eshima, Y., Kagechika, H., Kato, C., and Song, S.-Y. (2004). Retinoic acid imprints gut-homing specificity on T cells. Immunity *21*, 527–538.

Jabri, B., and Abadie, V. (2015). IL-15 functions as a danger signal to regulate tissue-resident T cells and tissue destruction. Nat. Rev. Immunol. *15*, 771–783.
Jabri, B., and Sollid, L.M. (2006). Mechanisms of disease: immunopathogenesis of celiac disease. Nat Clin Pract Gastroenterol Hepatol *3*, 516–525.

Jabri, B., de Serre, N.P., Cellier, C., Evans, K., Gache, C., Carvalho, C., Mougenot, J.F., Allez, M., Jian, R., Desreumaux, P., et al. (2000). Selective expansion of intraepithelial lymphocytes expressing the HLA-E-specific natural killer receptor CD94 in celiac disease. Gastroenterology *118*, 867–879.

Järvinen, T.T., Kaukinen, K., Laurila, K., Kyrönpalo, S., Rasmussen, M., Mäki, M., Korhonen, H., Reunala, T., and Collin, P. (2003). Intraepithelial lymphocytes in celiac disease. Am. J. Gastroenterol. *98*, 1332–1337.

Jin, X., Stamnaes, J., Klöck, C., DiRaimondo, T.R., Sollid, L.M., and Khosla, C. (2011). Activation of Extracellular Transglutaminase 2 by Thioredoxin. J. Biol. Chem. *286*, 37866–37873.

Karell, K., Louka, A.S., Moodie, S.J., Ascher, H., Clot, F., Greco, L., Ciclitira, P.J., Sollid, L.M., and Partanen, J. (2003a). Hla types in celiac disease patients not carrying the DQA1*05-DQB1*02 (DQ2) heterodimer: results from the european genetics cluster on celiac disease. Human Immunology *64*, 469–477.

Karell, K., Louka, A.S., Moodie, S.J., Ascher, H., Clot, F., Greco, L., Ciclitira, P.J., Sollid, L.M., Partanen, J., and European Genetics Cluster on Celiac Disease (2003b). HLA types in celiac disease patients not carrying the DQA1*05-DQB1*02 (DQ2) heterodimer: results from the European Genetics Cluster on Celiac Disease. Hum. Immunol. *64*, 469–477.

Kaukinen, K., Partanen, J., Mäki, M., and Collin, P. (2002). HLA-DQ typing in the diagnosis of celiac disease. Am. J. Gastroenterol. *97*, 695–699.

de Kauwe, A.L., Chen, Z., Anderson, R.P., Keech, C.L., Price, J.D., Wijburg, O., Jackson, D.C., Ladhams, J., Allison, J., and McCluskey, J. (2009). Resistance to celiac disease in humanized HLA-DR3-DQ2-transgenic mice expressing specific anti-gliadin CD4+ T cells. J. Immunol. *182*, 7440–7450.

Kennedy, M.K., Glaccum, M., Brown, S.N., Butz, E.A., Viney, J.L., Embers, M., Matsuki, N., Charrier, K., Sedger, L., Willis, C.R., et al. (2000). Reversible Defects in Natural Killer and Memory Cd8 T Cell Lineages in Interleukin 15–Deficient Mice. Journal of Experimental Medicine *191*, 771–780.

Kim, C.-Y., Quarsten, H., Bergseng, E., Khosla, C., and Sollid, L.M. (2004). Structural basis for HLA-DQ2-mediated presentation of gluten epitopes in celiac disease. Proc. Natl. Acad. Sci. U.S.A. *101*, 4175–4179.

Kim, S.M., Mayassi, T., and Jabri, B. (2015). Innate immunity: actuating the gears of celiac disease pathogenesis. Best Pract Res Clin Gastroenterol *29*, 425–435.

Klöck, C., Diraimondo, T.R., and Khosla, C. (2012). Role of transglutaminase 2 in celiac disease pathogenesis. Semin Immunopathol *34*, 513–522.

Klöck, C., Herrera, Z., Albertelli, M., and Khosla, C. (2014). Discovery of potent and specific dihydroisoxazole inhibitors of human transglutaminase 2. J. Med. Chem. *57*, 9042–9064.

Kondrashova, A., Mustalahti, K., Kaukinen, K., Viskari, H., Volodicheva, V., Haapala, A.-M., Ilonen, J., Knip, M., Mäki, M., Hyöty, H., et al. (2008). Lower economic status and inferior hygienic environment may protect against celiac disease. Ann. Med. *40*, 223–231.

Korneychuk, N., Ramiro-Puig, E., Ettersperger, J., Schulthess, J., Montcuquet, N., Kiyono, H., Meresse, B., and Cerf-Bensussan, N. (2014). Interleukin 15 and $CD4^+$ T cells cooperate to promote small intestinal enteropathy in response to dietary antigen. Gastroenterology *146*, 1017–1027.

Korneychuk, N., Meresse, B., and Cerf-Bensussan, N. (2015). Lessons from rodent models in celiac disease. Mucosal Immunol *8*, 18–28.

Kutlu, T., Brousse, N., Rambaud, C., Le Deist, F., Schmitz, J., and Cerf-Bensussan, N. (1993). Numbers of T cell receptor (TCR) alpha beta+ but not of TcR gamma delta+ intraepithelial lymphocytes correlate with the grade of villous atrophy in coeliac patients on a long term normal diet. Gut *34*, 208–214.

Lang, K.S., Recher, M., Junt, T., Navarini, A.A., Harris, N.L., Freigang, S., Odermatt, B., Conrad, C., Ittner, L.M., Bauer, S., et al. (2005). Toll-like receptor engagement converts T-cell autoreactivity into overt autoimmune disease. Nat. Med. *11*, 138–145.

Laparra, J.M., Olivares, M., Gallina, O., and Sanz, Y. (2012). Bifidobacterium longum CECT 7347 Modulates Immune Responses in a Gliadin-Induced Enteropathy Animal Model. PLOS ONE *7*, e30744.

Lebrec, H., Horner, M.J., Gorski, K.S., Tsuji, W., Xia, D., Pan, W.-J., Means, G., Pietz, G., Li, N., Retter, M., et al. (2013). Homeostasis of human NK cells is not IL-15 dependent. J. Immunol. *191*, 5551–5558.

Lee, D.W., Ha, H., and Lee, W.K. (2007). Selective Mono-BOC Protection of Diamines. Synthetic Communications *37*, 737–742.

Lee, K.H., Wucherpfennig, K.W., and Wiley, D.C. (2001). Structure of a human insulin peptide-HLA-DQ8 complex and susceptibility to type 1 diabetes. Nat. Immunol. *2*, 501–507.

Leffler, D.A., Edwards-George, J., Dennis, M., Schuppan, D., Cook, F., Franko, D.L., Blom-Hoffman, J., and Kelly, C.P. (2008). Factors that influence adherence to a gluten-free diet in adults with celiac disease. Dig. Dis. Sci. *53*, 1573–1581.

Leffler, D.A., Green, P.H.R., and Fasano, A. (2015). Extraintestinal manifestations of coeliac disease. Nat Rev Gastroenterol Hepatol *12*, 561–571.

Lefrançois, L., and Lycke, N. (2001). Isolation of mouse small intestinal intraepithelial lymphocytes, Peyer's patch, and lamina propria cells. Curr Protoc Immunol *Chapter 3*, Unit 3.19.

Lin, S.M., Du, P., Huber, W., and Kibbe, W.A. (2008). Model-based variance-stabilizing transformation for Illumina microarray data. Nucleic Acids Res. *36*, e11.

Lionetti, E., Gatti, S., Pulvirenti, A., and Catassi, C. (2015). Celiac disease from a global perspective. Best Pract Res Clin Gastroenterol *29*, 365–379.

Liu, S., Cerione, R.A., and Clardy, J. (2002). Structural basis for the guanine nucleotide-binding activity of tissue transglutaminase and its regulation of transamidation activity. Proc. Natl. Acad. Sci. U.S.A. *99*, 2743–2747.

Lodolce, J.P., Boone, D.L., Chai, S., Swain, R.E., Dassopoulos, T., Trettin, S., and Ma, A. (1998). IL-15 Receptor Maintains Lymphoid Homeostasis by Supporting Lymphocyte Homing and Proliferation. Immunity *9*, 669–676.

Lodolce, J.P., Burkett, P.R., Boone, D.L., Chien, M., and Ma, A. (2001). T Cell–Independent Interleukin 15rα Signals Are Required for Bystander Proliferation. Journal of Experimental Medicine *194*, 1187–1194.

Lorand, L., and Graham, R.M. (2003). Transglutaminases: crosslinking enzymes with pleiotropic functions. Nat. Rev. Mol. Cell Biol. *4*, 140–156.

Ludvigsson, J.F., Rubio-Tapia, A., van Dyke, C.T., Melton, L.J., Zinsmeister, A.R., Lahr, B.D., and Murray, J.A. (2013). Increasing incidence of celiac disease in a North American population. Am. J. Gastroenterol. *108*, 818–824.

Luger, D., Silver, P.B., Tang, J., Cua, D., Chen, Z., Iwakura, Y., Bowman, E.P., Sgambellone, N.M., Chan, C.-C., and Caspi, R.R. (2008). Either a Th17 or a Th1 effector response can drive autoimmunity: conditions of disease induction affect dominant effector category. J. Exp. Med. *205*, 799–810.

Lundin, K.E., Scott, H., Hansen, T., Paulsen, G., Halstensen, T.S., Fausa, O., Thorsby, E., and Sollid, L.M. (1993). Gliadin-specific, HLA-DQ(alpha 1*0501,beta 1*0201) restricted T cells isolated from the small intestinal mucosa of celiac disease patients. J. Exp. Med. *178*, 187–196.

Lundin, K.E.A., Scott, H., Fausa, O., Thorsby, E., and Sollid, L.M. (1994). T cells from the small intestinal Mucosa of a DR4, DQ7/DR4. DQ8 celiac disease patient preferentially recognize gliadin when presented by DQ8. Human Immunology *41*, 285–291.

Ma, L.J., Acero, L.F., Zal, T., and Schluns, K.S. (2009). Trans-presentation of IL-15 by intestinal epithelial cells drives development of CD8alphaalpha IELs. J. Immunol. *183*, 1044–1054.

Marsh, M.N. (1992). Gluten, major histocompatibility complex, and the small intestine. A molecular and immunobiologic approach to the spectrum of gluten sensitivity ('celiac sprue'). Gastroenterology *102*, 330–354.

Mayassi, T., and Jabri, B. (2018). Human intraepithelial lymphocytes. Mucosal Immunology *11*, 1281.

McDonald, B.D., Bunker, J.J., Ishizuka, I.E., Jabri, B., and Bendelac, A. (2014). Elevated T cell receptor signaling identifies a thymic precursor to the TCRαβ(+)CD4(-)CD8β(-) intraepithelial lymphocyte lineage. Immunity *41*, 219–229.

McDonald, B.D., Bunker, J.J., Erickson, S.A., Oh-Hora, M., and Bendelac, A. (2015). Crossreactive αβ T Cell Receptors Are the Predominant Targets of Thymocyte Negative Selection. Immunity *43*, 859–869.

McInnes, I.B., and Schett, G. (2011). The Pathogenesis of Rheumatoid Arthritis. New England Journal of Medicine *365*, 2205–2219.

Mearin, M.L., Biemond, I., Peña, A.S., Polanco, I., Vazquez, C., Schreuder, G.T., Vries, R.R. de, and Rood, J.J. van (1983). HLA-DR phenotypes in Spanish coeliac children: their contribution to the understanding of the genetics of the disease. Gut *24*, 532–537.

Meresse, B., Malamut, G., and Cerf-Bensussan, N. (2012). Celiac disease: an immunological jigsaw. Immunity *36*, 907–919.

Mesin, L., Sollid, L.M., and Di Niro, R. (2012). The intestinal B-cell response in celiac disease. Front Immunol *3*, 313.

Molberg, O., Kett, K., Scott, H., Thorsby, E., Sollid, L.M., and Lundin, K.E. (1997). Gliadin specific, HLA DQ2-restricted T cells are commonly found in small intestinal biopsies from coeliac disease patients, but not from controls. Scand. J. Immunol. *46*, 103–109.

Molberg, O., Mcadam, S.N., Körner, R., Quarsten, H., Kristiansen, C., Madsen, L., Fugger, L., Scott, H., Norén, O., Roepstorff, P., et al. (1998). Tissue transglutaminase selectively modifies gliadin peptides that are recognized by gut-derived T cells in celiac disease. Nat. Med. *4*, 713–717.

Monteleone, G., Pender, S.L., Alstead, E., Hauer, A.C., Lionetti, P., McKenzie, C., and MacDonald, T.T. (2001). Role of interferon alpha in promoting T helper cell type 1 responses in the small intestine in coeliac disease. Gut *48*, 425–429.

Mozo, L., Gómez, J., Escanlar, E., Bousoño, C., and Gutiérrez, C. (2012). Diagnostic value of anti-deamidated gliadin peptide IgG antibodies for celiac disease in children and IgA-deficient patients. J. Pediatr. Gastroenterol. Nutr. *55*, 50–55.

Mucida, D., Park, Y., Kim, G., Turovskaya, O., Scott, I., Kronenberg, M., and Cheroutre, H. (2007). Reciprocal TH17 and regulatory T cell differentiation mediated by retinoic acid. Science *317*, 256–260.

Murphy, K.M., and Weaver, C. (2016). Janeway's Immunobiology (New York, NY: W. W. Norton & Company).

Nilsen, E.M., Lundin, K.E., Krajci, P., Scott, H., Sollid, L.M., and Brandtzaeg, P. (1995). Gluten specific, HLA-DQ restricted T cells from coeliac mucosa produce cytokines with Th1 or Th0 profile dominated by interferon gamma. Gut *37*, 766–776.

Nilsen, E.M., Jahnsen, F.L., Lundin, K.E., Johansen, F.E., Fausa, O., Sollid, L.M., Jahnsen, J., Scott, H., and Brandtzaeg, P. (1998). Gluten induces an intestinal cytokine response strongly dominated by interferon gamma in patients with celiac disease. Gastroenterology *115*, 551–563.

Oberhuber, G., Vogelsang, H., Stolte, M., Muthenthaler, S., Kummer, J.A., Kummer, A.J., and Radaszkiewicz, T. (1996). Evidence that intestinal intraepithelial lymphocytes are activated cytotoxic T cells in celiac disease but not in giardiasis. Am. J. Pathol. *148*, 1351–1357.

Ohta, N., Hiroi, T., Kweon, M.-N., Kinoshita, N., Jang, M.H., Mashimo, T., Miyazaki, J.-I., and Kiyono, H. (2002). IL-15-dependent activation-induced cell death-resistant Th1 type CD8 alpha beta+NK1.1+ T cells for the development of small intestinal inflammation. J. Immunol. *169*, 460–468.

Palanski, B.A., and Khosla, C. (2018). Cystamine and Disulfiram Inhibit Human Transglutaminase 2 via an Oxidative Mechanism. Biochemistry *57*, 3359–3363.

Park, D., Choi, S.S., and Ha, K.-S. (2010). Transglutaminase 2: a multi-functional protein in multiple subcellular compartments. Amino Acids *39*, 619–631.

Patel, D.D., and Kuchroo, V.K. (2015). Th17 Cell Pathway in Human Immunity: Lessons from Genetics and Therapeutic Interventions. Immunity *43*, 1040–1051.

Pinkas, D.M., Strop, P., Brunger, A.T., and Khosla, C. (2007). Transglutaminase 2 undergoes a large conformational change upon activation. PLoS Biol. *5*, e327.

Ploski, R., Ek, J., Thorsby, E., and Sollid, L.M. (1993). On the HLA-DQ(alpha 1*0501, beta 1*0201)-associated susceptibility in celiac disease: a possible gene dosage effect of DQB1*0201. Tissue Antigens *41*, 173–177.

Plugis, N.M., and Khosla, C. (2015). Therapeutic approaches for celiac disease. Best Pract Res Clin Gastroenterol *29*, 503–521.

Plugis, N.M., Palanski, B.A., Weng, C.-H., Albertelli, M., and Khosla, C. (2016). Thioredoxin-1 Selectively Activates Transglutaminase 2 in the Extracellular Matrix of the Small Intestine: Implications for Celiac Disease. J. Biol. Chem. jbc.M116.767988.

Plugis, N.M., Palanski, B.A., Weng, C.-H., Albertelli, M., and Khosla, C. (2017). Thioredoxin-1 Selectively Activates Transglutaminase 2 in the Extracellular Matrix of the Small Intestine: IMPLICATIONS FOR CELIAC DISEASE. J. Biol. Chem. *292*, 2000–2008.

Qiao, S.-W., Bergseng, E., Molberg, O., Jung, G., Fleckenstein, B., and Sollid, L.M. (2005). Refining the rules of gliadin T cell epitope binding to the disease-associated DQ2 molecule in celiac disease: importance of proline spacing and glutamine deamidation. J. Immunol. *175*, 254–261.

Qiao, S.-W., Sollid, L.M., and Blumberg, R.S. (2009). Antigen presentation in celiac disease. Curr. Opin. Immunol. *21*, 111–117.

Ráki, M., Beitnes, A.-C.R., Lundin, K.E.A., Jahnsen, J., Jahnsen, F.L., and Sollid, L.M. (2013). Plasmacytoid dendritic cells are scarcely represented in the human gut mucosa and are not recruited to the celiac lesion. Mucosal Immunol *6*, 985–992.

Rezende, R.M., and Weiner, H.L. (2017). History and mechanisms of oral tolerance. Seminars in Immunology *30*, 3–11.

Ritchie, M.E., Phipson, B., Wu, D., Hu, Y., Law, C.W., Shi, W., and Smyth, G.K. (2015). limma powers differential expression analyses for RNA-sequencing and microarray studies. Nucleic Acids Res. *43*, e47.

Roberts, A.I., Lee, L., Schwarz, E., Groh, V., Spies, T., Ebert, E.C., and Jabri, B. (2001). Cutting Edge: NKG2D Receptors Induced by IL-15 Costimulate CD28-Negative Effector CTL in the Tissue Microenvironment. The Journal of Immunology *167*, 5527–5530.

Robinson, M.D., McCarthy, D.J., and Smyth, G.K. (2010). edgeR: a Bioconductor package for differential expression analysis of digital gene expression data. Bioinformatics *26*, 139–140.

Rubio-Tapia, A., and Murray, J.A. (2010). Classification and management of refractory coeliac disease. Gut *59*, 547–557.

Rubio-Tapia, A., Kyle, R.A., Kaplan, E.L., Johnson, D.R., Page, W., Erdtmann, F., Brantner, T.L., Kim, W.R., Phelps, T.K., Lahr, B.D., et al. (2009). Increased prevalence and mortality in undiagnosed celiac disease. Gastroenterology *137*, 88–93.

Rubio-Tapia, A., Rahim, M.W., See, J.A., Lahr, B.D., Wu, T.-T., and Murray, J.A. (2010). Mucosal recovery and mortality in adults with celiac disease after treatment with a gluten-free diet. Am. J. Gastroenterol. *105*, 1412–1420.

Rubio-Tapia, A., Ludvigsson, J.F., Brantner, T.L., Murray, J.A., and Everhart, J.E. (2012). The prevalence of celiac disease in the United States. Am. J. Gastroenterol. *107*, 1538–1544; quiz 1537, 1545.

Santin, I., and Eizirik, D.L. (2013). Candidate genes for type 1 diabetes modulate pancreatic islet inflammation and β-cell apoptosis. Diabetes Obes Metab *15 Suppl 3*, 71–81.

Sarikaya, M., Dogan, Z., Ergul, B., and Filik, L. (2014). Neutrophil-to-lymphocyte ratio as a sensitive marker in diagnosis of celiac disease. Ann Gastroenterol *27*, 431–432.

Sarkar, N.K., Clarke, D.D., and Waelsch, H. (1957). An enzymically catalyzed incorporation of amines into proteins. Biochim. Biophys. Acta *25*, 451–452.

Schluns, K.S., Nowak, E.C., Cabrera-Hernandez, A., Puddington, L., Lefrançois, L., and Aguila, H.L. (2004). Distinct cell types control lymphoid subset development by means of IL-15 and IL-15 receptor alpha expression. Proc. Natl. Acad. Sci. U.S.A. *101*, 5616–5621.

Schuppan, D., Pickert, G., Ashfaq-Khan, M., and Zevallos, V. (2015). Non-celiac wheat sensitivity: Differential diagnosis, triggers and implications. Best Practice & Research Clinical Gastroenterology *29*, 469–476.

Setty, M., Discepolo, V., Abadie, V., Kamhawi, S., Mayassi, T., Kent, A., Ciszewski, C., Maglio, M., Kistner, E., Bhagat, G., et al. (2015). Distinct and Synergistic Contributions of Epithelial Stress and Adaptive Immunity to Functions of Intraepithelial Killer Cells and Active Celiac Disease. Gastroenterology *149*, 681-691.e10.

Shan, L., Molberg, Ø., Parrot, I., Hausch, F., Filiz, F., Gray, G.M., Sollid, L.M., and Khosla, C. (2002). Structural Basis for Gluten Intolerance in Celiac Sprue. Science *297*, 2275–2279.

Shires, J., Theodoridis, E., and Hayday, A.C. (2001). Biological Insights into TCRγδ+ and TCRαβ+ Intraepithelial Lymphocytes Provided by Serial Analysis of Gene Expression (SAGE). Immunity *15*, 419–434.

Sidiropoulos, K., Viteri, G., Sevilla, C., Jupe, S., Webber, M., Orlic-Milacic, M., Jassal, B., May, B., Shamovsky, V., Duenas, C., et al. (2017). Reactome enhanced pathway visualization. Bioinformatics *33*, 3461–3467.

Siegel, M., Strnad, P., Watts, R.E., Choi, K., Jabri, B., Omary, M.B., and Khosla, C. (2008). Extracellular Transglutaminase 2 Is Catalytically Inactive, but Is Transiently Activated upon Tissue Injury. PLOS ONE *3*, e1861.

Slaughter, T.F., Achyuthan, K.E., Lai, T.S., and Greenberg, C.S. (1992). A microtiter plate transglutaminase assay utilizing 5-(biotinamido)pentylamine as substrate. Anal. Biochem. *205*, 166–171.

Smyth, G.K. (2004). Linear models and empirical bayes methods for assessing differential expression in microarray experiments. Stat Appl Genet Mol Biol *3*, Article3.

Sollid, L.M. (2002). Coeliac disease: dissecting a complex inflammatory disorder. Nature Reviews Immunology *2*, 647–655.

Sollid, L.M., and Jabri, B. (2011). Celiac disease and transglutaminase 2: a model for posttranslational modification of antigens and HLA association in the pathogenesis of autoimmune disorders. Curr. Opin. Immunol. *23*, 732–738.

Sollid, L.M., and Jabri, B. (2013). Triggers and drivers of autoimmunity: lessons from coeliac disease. Nat. Rev. Immunol. *13*, 294–302.

Sollid, L.M., Qiao, S.-W., Anderson, R.P., Gianfrani, C., and Koning, F. (2012). Nomenclature and listing of celiac disease relevant gluten T-cell epitopes restricted by HLA-DQ molecules. Immunogenetics *64*, 455–460.

Sospedra, M., and Martin, R. (2005). Immunology of multiple sclerosis. Annu. Rev. Immunol. *23*, 683–747.

Spencer, J., and Sollid, L.M. (2016). The human intestinal B-cell response. Mucosal Immunol *9*, 1113–1124.

Steel, J.C., Waldmann, T.A., and Morris, J.C. (2012). Interleukin-15 biology and its therapeutic implications in cancer. Trends in Pharmacological Sciences *33*, 35–41.

Stene, L.C., Honeyman, M.C., Hoffenberg, E.J., Haas, J.E., Sokol, R.J., Emery, L., Taki, I., Norris, J.M., Erlich, H.A., Eisenbarth, G.S., et al. (2006). Rotavirus infection frequency and risk of celiac disease autoimmunity in early childhood: a longitudinal study. Am. J. Gastroenterol. *101*, 2333–2340.

Sugahara, S., Shimizu, T., Yoshida, Y., Aiba, T., Yamagiwa, S., Asakura, H., and Abo, T. (1999). Extrathymic derivation of gut lymphocytes in parabiotic mice. Immunology *96*, 57–65.

Sun, C.-M., Hall, J.A., Blank, R.B., Bouladoux, N., Oukka, M., Mora, J.R., and Belkaid, Y. (2007). Small intestine lamina propria dendritic cells promote de novo generation of Foxp3 T reg cells via retinoic acid. J. Exp. Med. *204*, 1775–1785.

Tack, G.J., Verbeek, W.H.M., Schreurs, M.W.J., and Mulder, C.J.J. (2010). The spectrum of celiac disease: epidemiology, clinical aspects and treatment. Nat Rev Gastroenterol Hepatol *7*, 204–213.

Thomázy, V., and Fésüs, L. (1989). Differential expression of tissue transglutaminase in human cells. An immunohistochemical study. Cell Tissue Res. *255*, 215–224.

Tollefsen, S., Arentz-Hansen, H., Fleckenstein, B., Molberg, O., Ráki, M., Kwok, W.W., Jung, G., Lundin, K.E.A., and Sollid, L.M. (2006). HLA-DQ2 and -DQ8 signatures of gluten T cell epitopes in celiac disease. J. Clin. Invest. *116*, 2226–2236.

Trynka, G., Wijmenga, C., and van Heel, D.A. (2010). A genetic perspective on coeliac disease. Trends Mol Med *16*, 537–550.

Umesaki, Y., Setoyama, H., Matsumoto, S., and Okada, Y. (1993). Expansion of alpha beta T-cell receptor-bearing intestinal intraepithelial lymphocytes after microbial colonization in germ-free mice and its independence from thymus. Immunology *79*, 32–37.

Verdu, E.F., Huang, X., Natividad, J., Lu, J., Blennerhassett, P.A., David, C.S., McKay, D.M., and Murray, J.A. (2008). Gliadin-dependent neuromuscular and epithelial secretory responses in gluten-sensitive HLA-DQ8 transgenic mice. Am. J. Physiol. Gastrointest. Liver Physiol. *294*, G217-225.

van de Wal, Y., Kooy, Y., van Veelen, P., Peña, S., Mearin, L., Papadopoulos, G., and Koning, F. (1998). Selective deamidation by tissue transglutaminase strongly enhances gliadin-specific T cell reactivity. J. Immunol. *161*, 1585–1588.

Waldmann, T.A. (2006). The biology of interleukin-2 and interleukin-15: implications for cancer therapy and vaccine design. Nature Reviews Immunology *6*, 595–601.

Waldmann, T.A., and Tagaya, Y. (1999). The multifaceted regulation of interleukin-15 expression and the role of this cytokine in NK cell differentiation and host response to intracellular pathogens. Annu. Rev. Immunol. *17*, 19–49.

Watts, R.E., Siegel, M., and Khosla, C. (2006). Structure-activity relationship analysis of the selective inhibition of transglutaminase 2 by dihydroisoxazoles. J. Med. Chem. *49*, 7493–7501.

Yokoyama, S., Watanabe, N., Sato, N., Perera, P.-Y., Filkoski, L., Tanaka, T., Miyasaka, M., Waldmann, T.A., Hiroi, T., and Perera, L.P. (2009). Antibody-mediated blockade of IL-15 reverses the autoimmune intestinal damage in transgenic mice that overexpress IL-15 in enterocytes. Proc Natl Acad Sci U S A *106*, 15849–15854.

Yurkovetskiy, L., Pickard, J.M., and Chervonsky, A.V. (2015). Microbiota and Autoimmunity: exploring new avenues. Cell Host Microbe *17*, 548–552.

Zhang, X., Sun, S., Hwang, I., Tough, D.F., and Sprent, J. (1998). Potent and selective stimulation of memory-phenotype CD8+ T cells in vivo by IL-15. Immunity *8*, 591–599.

Zhou, R., Wei, H., Sun, R., Zhang, J., and Tian, Z. (2007). NKG2D recognition mediates Toll-like receptor 3 signaling-induced breakdown of epithelial homeostasis in the small intestines of mice. Proc Natl Acad Sci U S A *104*, 7512–7515.